# Assessing the extent of local assimilation within the Platreef, Northern Limb of the Bushveld Igneous Complex, using sulfur isotopes and trace element geochemistry

by

Evan Keir-Sage

A thesis submitted in partial fulfilment

of the requirements for the degree of

Master of Science (MSc) in Geology

The Faculty of Graduate Studies

Laurentian University

Sudbury Ontario, Canada

**THESIS DEFENCE COMMITTEE/COMITÉ DE SOUTENANCE DE THÈSE**
**Laurentian Université/Université Laurentienne**
Faculty of Graduate Studies/Faculté des études supérieures

| | |
|---|---|
| Title of Thesis<br>Titre de la thèse | Assessing the extent of local assimilation within the Platreef, Northern Limb of the Bushveld Igneous Complex, using sulfur isotopes and trace element geochemistry |
| Name of Candidate<br>Nom du candidat | Keir-Sage, Evan |
| Degree<br>Diplôme | Master of Science |
| Department/Program<br>Département/Programme | Geology |

Date of Defence
Date de la soutenance April 15, 2019

**APPROVED/APPROUVÉ**

Thesis Examiners/Examinateurs de thèse:

Dr. Matt Leybourne
(Co-Supervisor/Co-directeur de thèse)

Dr. Pedro Jugo
(Co-Supervisor/Co-directeur de thèse)

Dr. Denis Grobler
(Committee member/Membre du comité)

Dr. Sarah Penniston-Dorland
(External Examiner/Examinateur externe)

Approved for the Faculty of Graduate Studies
Approuvé pour la Faculté des études supérieures
Dr. David Lesbarrères
Monsieur David Lesbarrères
Dean, Faculty of Graduate Studies
Doyen, Faculté des études supérieures

Abstract

The proximity to metasedimentary footwall units in the Northern Limb of the Bushveld Igneous Complex (BIC) has resulted in a complex local contamination of in this mafic-ultramafic intrusive body, including the units containing platinum group element (PGE) mineralization. To assess the extent of incorporation of non-magmatic material and its effects on PGE mineralization, geochemical and isotopic data were collected from drill core UMT094 on the Turfspruit project, where core logging has shown a clear macroscopic division between mineralization and local footwall contamination. The S isotopic data combined with whole rock geochemistry data (including $CaO/Al_2O_3$, V/Ti, Ni/Cr, S/Se, LOI) present substantial evidence to assess the range of incorporation of local footwall material. A $\delta^{34}S_{VCDT}$ profile shows a steady decrease from the footwall assimilation zone ($\delta^{34}S$ = +8 ‰) to near constant $\delta^{34}S$ values ($\delta^{34}S$ < +4 ‰) below mineralization. Through PGE mineralization, the $\delta^{34}S$ data converge to the range that has been documented for the Merensky Reef in the Eastern and Western Limbs of the BIC ($\delta^{34}S$: ~ 0 to +3 ‰). Other geochemical parameters through mineralization, such as S/Se and $CaO/Al_2O_3$, also match the ranges documented for the Merensky Reef. In addition, parameters such as whole rock V/Ti are shown to be useful indicators of the type of contaminant (e.g. V/Ti > 2 for intervals assimilating shales and V/Ti < 1 for intervals assimilating carbonates; 1 < V/Ti < 2 for uncontaminated magmatic units). The results indicate that there is negligible local contamination through mineralization and that the primary mechanism of PGE mineralization in the Platreef was no different than the mechanism that generated the Merensky Reef in the Eastern and Western limbs of the BIC.

Co-Authorship Statement

Contributions from various collaborators have resulted in this thesis. Dr. Leybourne, Dr. Jugo and Dr. Grobler conceived the project and Dr. Jugo and Dr. Leybourne have contributed with feedback on this writing. Drill core logging was completed by the candidate and sampling was completed by the candidate and C. Mayer with the supervision of Dr. Jugo and Dr. Leybourne. Whole-rock geochemistry was partially completed by the candidate and finalized by ALS Geochemistry, Vancouver, Canada. Sample preparation for isotopic analyses were completed by the candidate and C. Mayer at Queen's Facilities for Isotope Research (QFIR), and analyses were outsourced to the members of QFIR. Microprobe analyses were completed by Dr. McDonald, and Raman spectroscopy was competed by C. Beckett-Brown. Interpretation of the data was initially completed by the candidate and feedback and assistance was provided by Dr. Leybourne, Dr. Jugo, Dr. Lesher and Dr. Grobler. Drafts of the thesis were completed by the candidate and edited by Dr. Jugo and Dr. Leybourne.

Table of Contents

List of Figures

List of Tables

# 1. Introduction

The Bushveld Igneous Complex (BIC; Figure 1) is a layered mafic to ultramafic igneous complex located in north-eastern South Africa and hosts the largest known accumulation of Pt-Pd deposits in the world (Mudd 2012). The BIC was intruded at 2055.91 ± 0.26 Ma based on cooling ages of zircons in Marginal Zone rocks, and the economically important Rustenburg Layered Suite (RLS) formed at 2054.89 ± 0.37 Ma, based on zircon ages from the central part of the RLS (Zeh et al., 2015). The RLS is a series of mafic and ultramafic layers that appear throughout the BIC in the Western, Eastern, and Northern limbs. Although PGE mineralization in the Eastern and Western limbs of the BIC are well studied and characterized, the origin of PGE mineralization in the Northern Limb and its correlation with the main parts of the BIC (E and W limbs) has proven difficult, mostly because well-exposed mineralization along the Northern Limb is typically in sections with strong interaction between BIC magmas and footwall lithologies (the Platreef; Kinnaird et al. 2005). PGE mineralization in the Eastern and Western limbs is primarily hosted within the Merensky Reef and Upper Group 2 (UG2) chromitite (Mudd 2012), both within the Upper Critical Zone of the BIC. In contrast, PGE mineralization in the Northern Limb is typically interfingered with a variety of basement lithologies including Archean gneisses, banded-iron formation, dolostones (marble), and (meta) shales (Buchanan et al. 1981, Kinnaird et al. 2005). The stratigraphic interval showing magma-footwall interaction (up to 400 m thickness) constitutes the Platreef. Within this interval of magma-footwall interaction, mineralized units (up to about 40 m in thickness) occur (e.g. Grobler et al. 2018).

Much of the research on the Platreef (e.g., Buchanan et al. 1981; Sharman-Harris et al. 2005; Holwell et al. 2007; Yudovskaya et al. 2017; Magalhaes et al. 2018) used samples in which magmatic units of the BIC have been variably affected by assimilation of Transvaal (TVL) metasedimentary rocks. This proximal contamination has prevented a clear understanding of the relative importance of assimilation of footwall lithologies on PGE mineralization in the Platreef. This study focuses on whole rock geochemistry and S isotopes ($\delta^{34}S$) of drill core samples from more distal portions of the Platreef (Ivanplats Ltd. Hole UMT094), in which there is a clear macroscopic separation between mineralization (i.e., without visible evidence of assimilation) and progressive evidence of assimilation with depth, as well as intersection of footwall lithologies. This study complements the work of Mayer et al. (2018), which focused on the Sr isotopic stratigraphy of the transition between the Upper Critical Zone and the Main Zone in the Northern Limb of the BIC. The results, which combine major and trace element geochemistry with $\delta^{34}S$, show extensive assimilation with the local footwall lithologies. However, in UMT094 the effect of assimilation decreases upwards and is largely insignificant across the main mineralization interval. The $\delta^{34}S$ values are comparable to those documented in the main sectors of the BIC (E and W limbs). If UMT094 is assumed to be representative of primary PGE mineralization in the Northern Limb, then it can be concluded that mineralization in the Northern Limb is mostly of magmatic origin.

## 2. Background geology

The Bushveld Igneous Complex is subdivided into six different zones: 1) Marginal Zone; 2) Lower Zone; 3) Lower Critical Zone; 4) Upper Critical Zone; 5) Main Zone; and 6) Upper Zone. Extensive descriptions of the BIC are well documented elsewhere (e.g., Zinetek et al. 2017) and will be only summarized here briefly. The Marginal Zone rests below all of the other zones, in contact with country rock and is made up of cyclic olivine melanorite and gabbronorite, mafic sills, and variably assimilated country rocks (Engelbrecht 1990). The Lower Zone lies on top of the Marginal Zone at the base of the BIC and is comprised of harzburgite and pyroxenite and associated subzones, including accessory chromite and minor plagioclase as an intercumulus phase (Cameron 1978). The Lower Critical Zone has a gradational basal contact, and primarily comprises pyroxenite, with minor amounts of harzburgite. The main characteristic of the Lower Critical Zone is the presence of laterally extensive chromitite seams, which occur throughout much of the zone. The Lower Critical Zone is the largest chromite resource in the world, and produces nearly 50% of the world's chromium (Papp 2014). The Upper Critical Zone is made up of orthopyroxenite, norite and anorthosite, and is where most of the PGE resources within the BIC occur, primarily within specific laterally correlative reefs, dominated by the UG2 chromitite and the Merensky Reef. The Merensky Reef is a laterally continuous cumulate layer of orthopyroxene, plagioclase, chromite, and rare olivine, which bears PGE and some sulfides, primarily pyrrhotite, pentlandite and chalcopyrite. Most PGE occur within or near (up to 1 m) the Merensky Reef pegmatite and chromite stringers (Naldrett et al. 2009). Above the Critical Zone are the Main Zone and the Upper Zone, which host little to no PGE or chromite. The Main Zone is comprised of norite and gabbronorite with some cyclical units of anorthosite and pyroxenite. The Main Zone is the thickest unit of the entire complex, and shows minimal laterally-extensive magmatic layering, but bears unique markers that can be correlated across the complex. In the uppermost section of the Main Zone is a cumulate pyroxene marker present in both the Western and Eastern limbs, which distinguishes the Lower Main Zone and Upper Main Zone. Above the

Main Zone lies the Upper Zone, which contains cumulate magnetite as laterally continuous layers, similar to the chromitite seams of the Lower Critical Zone.

## 2.1 Footwall geology

In the Northern Limb, much of the Lower and Critical Zones are not exposed; instead sections of the Upper Critical Zone are interfingering the various units of the Transvaal metasedimentary rocks as well as on top of the Archean gneisses of the Kapvaal Craton (Figure 1). The Transvaal metasedimentary rocks near Turfspruit include dolostones (now marbles) of the Malmani Subgroup, (meta) shales of the Duitschland Formation, and banded iron formation of the Penge Formation. To the north, the Transvaal metasedimentary rocks pinch out between the Archean gneisses and the BIC, nearest Overysel. Satellite bodies of the Lower Zone outcrop at various points within the metasedimentary rocks and seem associated with large scale faults (Yudovskaya et al. 2013). Substantial contact metamorphism of Transvaal rocks was documented by Armitage et al. (2002) and Eroglu et al. (2015). The interaction between the BIC and the metasedimentary rocks becomes more complicated both on local scales and at depth (Holwell et al. 2007).

## 2.2 The Platreef

The Platreef is situated in the Northern Limb of the BIC, and is stratigraphically comparable to the Merensky Reef in the other limbs (Wagner 1929; van der Merwe 1976), although the thickness of the mineralization in the Platreef (~20 – 100 m) is much greater than the thickness of the Merensky Reef in the Eastern and Western limbs (0.8 – 4 m) (Grobler et al. 2019). Substantial work has been undertaken to assess possible correlation between the Merensky Reef lithologies and mineralized units within the Platreef (Buchanan et al. 1981; Grobler et al. 2019), although there is no consensus, with some studies suggesting that the Platreef is stratigraphically higher than the Merensky Reef (Kinnaird 2005; Kruger 2005). A key difference between the Platreef in the Northern Limb to the Merensky Reef is the close relationship to the footwall granites, banded iron formations and dolostones. This proximity, in addition to subsequent fluid-rock interaction causing alteration, has changed the appearance of the Platreef in many places so that it is visually distinct from the Merensky Reef (Harris and Chaumba 2001; Armitage et al. 2002). In some locations of the Northern Limb, the Lower Zone is located beneath the footwall units of the RLS, intruding into footwall units (Yudovskaya et al. 2013). This is interpreted as indicators that the Northern Limb could have been intruded as a series of sills (Kinnaird 2005), separate from an earlier staging chamber, interfingering into the various footwall lithologies, or as a large chamber that had detached sections of the footwall lithologies as xenoliths and rafts. For consistency with previous work in Turfspruit, the nomenclature for the stratigraphic subdivisions of the Platreef (Grobler et al. 2018) will be used in this thesis.

# 3. Methods

## 3.1 Drill core and surface sampling

Most samples were collected from core (drilled by Ivanplats) in the Turfspruit area near Mokopane. Sampling focused on core from hole UMT094 (Figure 2), located in the deeper extension of the Platreef. This drill core was selected because Ivanplats' previous logging (as well was core logging performed on site) indicated a clear, macroscopic separation between relatively uncontaminated and mineralized igneous stratigraphy and evidence of increasing footwall assimilation with depth. Drill core samples ranged from 15 to 30 cm in length of NQ core sawed as half-core sections or quarter-core (if intervals were previously sampled). Sampling through some of the mineralized stratigraphy was limited to whole rock pulps because the core had been extensively sampled previously. Where possible, sampling avoided veins to ensure that only representative samples of the magmatic or assimilated stratigraphy were used for whole rock geochemistry. In addition to drill core samples, twelve samples (mostly Timeball Hill shales and quartzites, and Malmani dolostone) were collected at surface from the Dehoop farm (several km to the E of UMT094) to obtain reference geochemical and isotopic values of potential assimilated sedimentary material.

### 3.2 Petrography

Thin sections for 36 selected samples were prepared at the Harquail School of Earth Sciences (HES). Transmitted and reflected light microscopy were used for petrographic characterization (summary of thin section mineralogy in appendix, Table A1). Raman spectroscopy data was collected at Laurentian University using a HORIBA Jobin Yvon XploRA spectrometer with an Olympus BX-41 microscope. The excitation wavelength used was 532 nm and an approximate beam size of 2 μm. Spectra were obtained over the range of 100-1000 $cm^{-1}$ using a counting time of 120 s and a grating of 1200 $cm^{-1}$. Calibration was conducted using synthetic Si and the 521 $cm^{-1-}$ line as reference.

## 3.3 Whole-rock geochemistry

Samples for whole rock geochemistry were crushed and pulverized at HES with a steel hammer and a low-Cr-Mo steel disk mill. Samples were sent to at ALS Geochemistry, Vancouver, Canada for analysis by different methods: 1) ALS method ME-MS61L: four acid digestion ($HClO_4$, HF, $HNO_3$, HCl) with analysis by inductively-coupled plasma optical emission spectroscopy and mass spectrometry (ICP-OES and ICP-MS); 2) ALS method ME-MS81: lithium-metaborate fusion with analysis of major elements by ICP-OES and trace elements by ICP-MS; and 3) ALS method PGM-MS23L: ICP-MS following PbO fire assay for gold, platinum and palladium contents. In addition, Pt, Pd, Au, Rh, Ni, Cu, Cr and S data were provided by Ivanplats from their ~1 m sample assaying through most of the drill core.

## 3.4 Sulfur isotopes

Sulfur isotopic data were collected at the Queen's Facility for Isotope Research (QFIR), Queen's University, Kingston, Ontario. Sulfur isotope analyses were completed using both whole rock powders and by micro-drilling of sulfide minerals. Drill core samples with visible sulfides were selected for micro-drilling, and whole rock analyses were used on samples in which there were no visible sulfides or Ivanplats' assay pulps. Visible chalcopyrite and pyrrhotite were drilled using a diamond drill bit, cleaned with ultrasonic baths between samples. Sulfur isotope samples were weighed into tin capsules and analyzed using a Finnigan MAT 253 stable isotope ratio mass spectrometer system coupled to a Costech ECS 4010 elemental analyzer. The $\delta^{34}S$ values were calculated by normalizing the measured $^{34}S/^{32}S$ values in the sample to that in the Vienna Canyon Diablo Troilite (VCDT). Values are reported using the delta ($\delta$) notation in permil units (‰), and sample duplicate analyses were reproducible within 0.2 ‰. The certified reference material (CRM) used was NBS-127 (calibrated back through 4 analyses to 20.2, 20.3, 20.3 and 20.4 ‰) as well as an in-house standard from QFIR (M6801).

## 4. Results

### 4.1 Core logging and field relationships

Visual inspection of drill core cannot reliably distinguish between clino- and orthopyroxene, but can reliably distinguish between altered pyroxene, olivine, and plagioclase. The most common relationships between the major minerals within economic zones (BCU, 1230 to 1239 m; unmineralized Middling unit (MD1): 1239 to 1252 m; mineralized MCU: 1252 to 1292 m) are cumulate pyroxene with interstitial plagioclase (with variations in relative abundance of pyroxene and plagioclase), minor interstitial sulfides, and in some cases substantial olivine/serpentine content (~0 to ~15 modal %) at the base of cyclic units. Changes in grain size are common (up to and greater than ~3 cm pyroxene grains) within these stratigraphic units, as pegmatitic bands commonly occur on a local scale within MCU, between lengths of 10 cm and 3 m. Several quartz-feldspar veins (QFV) sharply cut sections of the BCU and MCU (three within 1228 to 1231 m, four within 1249 to 1253 m, one from 1270 to 1270.4 m) ranging between 5 and 40 cm in thickness. Within the footwall cyclic units (FCU, 1292 m to 1326 m), plagioclase is the dominant mineral with variable proportions of pyroxene. A general trend of more plagioclase at the top of a single cyclic unit exists, with pyroxene increasing towards the base of each unit and a minor chromite stringer at the base of a single cyclic unit. This trend is not consistent however, and bands of pyroxenite appear throughout plagioclase-rich sections of the FCU. The individual cyclic units are also not well defined, and commonly are not terminated by anorthosite at the top of a cycle and pyroxenite or chromitite on the base, instead are terminated by gabbronorite with variable proportions of pyroxene and plagioclase. Rare irregularities also occur within the FCU as either small xenoliths or local bands of veining and/or increased alteration. These xenoliths occur between 1294 and 1300 m, are smaller than those of the footwall assimilation zone (10 to 30 cm rather than ~1 m) and are commonly pyroxenite or serpentinite. The upper group 2 cyclic unit (UG2CU) lies below the FCU, beginning at 1326 m with a decrease in plagioclase content (< 5 modal %). In this drill core, the upper section of the UG2CU (1326 to 1347 m) is similar in appearance to the BCU and MCU, with only one pegmatoid, from 1333.3 to 1333.6 m. Between 1333.6 and 1336 m is a partially digested carbonaceous xenolith, containing serpentine, magnetite, calcite, pentlandite, pyrite, anhydrite and chalcopyrite. Within the base of the UG2CU and footwall assimilation zone (FAZ) (1347 to ~1380 m), chromite and magnetite content is substantially higher, and formed as both disseminated and solid bands up to 5 cm thick. Below the chromite-rich bands of the FAZ, atypical magmatic textures appear, primarily serpentine surrounding lenses of magnetite as well as sub-rounded relicts of pyroxene and calcite. Some hydrous minerals appear within the FAZ, and were not easily identified in hand sample, but were identified petrographically.

## 4.2 Petrography

Within the Main Zone of UMT094, anorthite makes up the bulk of the mineral composition, with minor amounts of orthopyroxene and clinopyroxene (Figure 3). Plagioclase grains are comparable in size and larger than pyroxenes through most of the Main zone, with rare bands, which show clumping and mottling of pyroxenes. These mottled textures are similar to those seen elsewhere in the BIC.

Magmatic sections of the MCU and BCU contain cumulate ortho- and clinopyroxene, with intercumulus plagioclase, with some alteration and fracturing throughout. Sulfides occur as blebs, primarily pentlandite and pyrrhotite with blebs of chalcopyrite at the edges (Figure 4). Alteration of plagioclase is prevalent, occurring along twinning and across larger grains, assumed to be alteration to clay minerals.

Pyrrhotite, pentlandite and chalcopyrite are all present within the BCU, although they show a distinction of chalcopyrite being more common within patches of silicate alteration, whereas pyrrhotite and pentlandite form in intercumulus textures, with some chalcopyrite towards the rims. Similarly, sulfides within the MCU are dominantly pyrrhotite-pentlandite blebs, with chalcopyrite at the edges, again with chalcopyrite being more abundant within altered patches, although this relationship is less evident within the MCU compared to the BCU. Chalcopyrite and pyrite become more common with depth, all four sulfides being present within the UG2CU, and pyrite content increasing towards and within the calc-silicates (CS).

One analyzed thin section at the base of the MCU contains calcite as optically continuous grains (Figure 5), with talc and tremolite appearing between and within optically continuous boundaries. The section of the MCU below this sample contains large increases in Ca (2.89 to 20.10 wt. % CaO) and other elements, such as Ti, and sulfur isotopic values, discussed within the following sections.

Figure 6 shows alteration of orthopyroxene by chlorite at the base of the MCU within its contaminated base. Moving away from pyroxene towards chalcopyrite, chlorite begins to deviate from the orientation within the orthopyroxene and curl, as well as increasing in overall grain size.

Serpentinization of olivine, alteration of plagioclase to white mica, and talc-tremolite alteration of pyroxenes is present in nearly every sample within the FAZ (Figure 7), with less alteration further towards the dolostone footwall rocks. Several contact metamorphic minerals were identified in other thin sections within the calc-silicate and dolostone footwall, by use of a combination of petrography, Raman spectroscopy, and microprobe analyses. These minerals include, and are not limited to, clinohumite, Mg-Fe-Al spinel, vesuvianite, calcite (Figure 5) and olivine-bearing dolomite (Figure 8). Although the origin of these minerals has not been established, they are assumed to be of contact-metamorphic origin.

## 4.3 Whole rock geochemistry, major elements

Major element data from whole rock geochemistry is presented in Table 1 and summarized in Figure 9. The variation between the relative abundances of plagioclase and pyroxene are the predominant change through most of the magmatic units, influencing the major element composition. Variations in major element content with stratigraphic level include: 1) increases in CaO and $Al_2O_3$ contents with increasing plagioclase content and decreasing pyroxene content; and 2) increases of CaO with depth, which is consistent with the observed appearance of calcite, dolomite or calc-silicate xenoliths.

The plagioclase-rich Main Zone and plagioclase-rich sections of the cyclic units have $CaO/Al_2O_3$ values averaging 0.6, whereas pyroxenite and feldspathic pyroxenite of the MCU have values that are closer to 1.0 (Figure 5). At the base of the MCU, between 1285 and 1292 m, the $CaO/Al_2O_3$ values increase and average 2.8, and distinguish it from the other sections of the MCU as MCU-Contaminated due to the presence of minor amounts of calcite (Figure 5). Within the Upper Group 2 cyclic group's (UG2CU) hanging wall (UG2HW), an entrained calc-silicate xenolith is observed in thin section from sample UMT094-1333, which is spatially related to an increased $CaO/Al_2O_3$ value of 2.6, higher than samples both above and within the UG2CU. Within the FAZ, $CaO/Al_2O_3$ values gradually increase from 0.7 to 1.8 and become more variable towards the calc-silicate footwall. Within the calc-silicate footwall $CaO/Al_2O_3$ values are highly variable (between 0.49 and 12.0), and 4 samples from the dolostone footwall from 1494 to 1601 m (end of hole) have an average $CaO/Al_2O_3$ value of 15.8, and a maximum value of 19.0.

Loss on ignition (LOI) values are low (generally < 1 wt. %) within unaltered, magmatic sections of the drill hole (MCU at 1232 to 1278 m and FCU at 1292 to 1332 m). Magmatic units with visible alteration or clay-rich bands show increasing LOI values (up to 2 to 5 wt. %), including increases within the MCU-Contaminated (1279 to 1292 m), with one sample at the base of the MCU-Contaminated reaching LOI = 5.66 wt. % (UMT094-1291A). Below the FCU and through the FAZ, the LOI values increase progressively with depth (from ~2 wt. % at 1334 m to 9 wt. % at 1405 m) similar to the increase in $CaO/Al_2O_3$ values; the LOI values increase from 9 wt. % up to 30 wt. % (average = 16.9 wt. %) within the calc-silicate and dolostone footwall.

### 4.4 Whole rock geochemistry, trace elements

Whole rock trace element geochemical data from UMT094 are summarized in Tables 2 and 3 and shown as spider diagrams in Figure 10 (with units grouped based on stratigraphy and lithology). Notable excursions in sulfur isotopic values have been labeled as separated sub-units to help identify potential assimilation. Samples from ATS 139, with more highly contaminated drill core, have also been included in geochemical interpretation to give insight to its contamination. The primary elements used in these interpretations to discern between magmatic contributions and sedimentary contributions are vanadium, titanium, nickel, chromium, and selenium.

The average V/Ti value within the MCU-Contaminated (1285 to 1292 m) is 1.23, which is lower than the rest of the mineralized MCU (1252 to 1285 m, V/Ti = 1.56), and closer to the values of the FAZ and footwall units (1338 to 1405 m). The FAZ has V/Ti values ranging from 0.2 to 3, both above and below those of the magmatic units. The calc-silicate footwall (1405 to 1494 m) contains V/Ti values as low as 0.054, due to very low vanadium contents (as low as 0.36% of primitive mantle values). Samples within a second analyzed drill hole, ATS 139, which is in the up-dip section of the Platreef, contains substantial hornfels shales proximal to the Merensky Reef equivalent and have V/Ti values that are generally greater than 3 within both its mineralized and assimilation dominant units.

Sulfur and selenium ratios were also calculated to attempt to constrain assimilation of other material (Figure 11). Samples with S concentrations less than 0.08% and Se concentrations less than the detection limit of 0.2 ppm have been excluded from the S/Se interpretation following methods of Barnes et al. (2009). This exclusion removes samples that are mostly within the Main Zone, and some small sections within the magmatic stratigraphy, primarily within the plagioclase-rich upper sections of the poorly-mineralized units. Within the BCU and MCU (1230 to 1292 m), S/Se values range between 1344 and 3400. Within the FCU and UG2CU (1292 to 1338 m), S concentrations show local decreases (to the lower detection limit. 0.01 wt.%), and S/Se values increase to 2578 to 4500. The calc-silicate xenolith within the UG2HW (1333.3 to 1333.6 m) has a S/Se value of 6050, distinct from values of 3444 to 3750 below it, within the UG2CU. Below the base of the UG2CU, S/Se values increase, and become more variable. Within the FAZ and CS/TVL footwall (1338 to 1601), the average S/Se value is 10766, but have a wide range, between 3000 and 24833.

### 4.5 PGE and gold

Gold, Pt, Pd, and Rh data (from ~1 m-long core samples) were provided by Ivanplats (Table 4). Additional PGE and Au content data generated for this study is summarized in Table 5. PGE and gold contents are close to or below detection limits through both the Main Zone (1096 to 1230 m) and the dolostone xenolith at the base of drill hole UMT094 (1494 to 1601 m). Within the mineralized zones, these economic metals are focused within three reefs, the Bastard Reef equivalent (1230 to 1239 m: average ~2000 ppb Pt+Pd+Au+Rh), the Merensky Reef equivalent (1252 to 1292 m: average ~3600 ppb Pt+Pd+Au+Rh) and the UG2CU (1335 to 1338 m: average ~4400 ppb Pt+Pd+Au+Rh). In the units between and below these reefs (FCU, FAZ) PGE and Au are much less abundant but are still elevated relative to the unmineralized hanging wall and footwall (1239 to 1252 m, 1292 to 1335 m and 1338 to 1405 m: average ~600 ppb Pt+Pd+Au+Rh).

## 4.6 Sulfur isotopic data

Sulfur data is summarized in Table 7. Data from all UMT094 samples range between 1.5 and 8.1 ‰ $\delta^{34}S$, with lower values higher in the stratigraphy (1233 to 1282 m, average = 2.6 ‰), and values increase towards a maximum value (1333 and 1335 m, 6‰), lower in the magmatic stratigraphy. The first visible magmatic sulfides downhole occur within the BCU, and three micro-drilled samples of pyrrhotite and chalcopyrite yielded $\delta^{34}S$ values between 2.4 to 2.8 ‰. The range of $\delta^{34}S$ values of whole rock powders within the Merensky Reef equivalent ranges between 1.5 ‰ and 3.8 ‰ (Figure 12). Within the contaminated base of the MCU, $\delta^{34}S$ values range from 3.3 to 3.8 ‰ $\delta^{34}S$. Sulfur isotope values increase through the FAZ (up to 8.1 ‰). Below the FAZ, in a calc-silicate footwall, whole rock $\delta^{34}S$ was used, and values range between 7.5 and 10 ‰ (0.1 to 0.7 wt. % S). Within the base of the drill core, in an olivine bearing dolostone (Figure 8), sulfides are not visible until the lowest section, within which one sample contained sufficient sulfur (within pyrite) to be analyzed with micro-drilling, as with other samples the whole rock methods used were ineffective. The $\delta^{34}S$ value for this drilled sample was 3.7‰, much lower when compared to the nearest calc-silicate value of 8.9‰ $\delta^{34}S$.

# 5. Discussion

## 5.1 Proximal footwall assimilation

There has been some debate in the literature as to the origin of the Platreef and whether or not it represents the lateral equivalence of the Critical Zone of the Eastern and Western limbs (Langa et al. submitted; Grobler et al. 2018; Kinnaird 2005; Sharman et al. 2013; Mayer et al.

submitted). Much of this debate has centred around differing interpretations regarding the extent of crustal assimilation into the Platreef magmas, in particular the role of the addition of crustal S into the atypical thickness of PGE mineralization in the Platreef compared to the rest of the BIC (Holwell et al. 2007; Sharman et al. 2013).

The magmatic sections of drill core UMT094 show large shifts in major element geochemistry over short ranges, caused mainly by changes in plagioclase content between units. In addition, one of the main contaminants in the section are footwall marbles (carbonate lithologies). Thus, $CaO/Al_2O_3$ is a very useful parameter to track carbonate assimilation (as assimilation of dolostone would produce an increase in CaO and MgO but not in $Al_2O_3$). Similarly, PGE and Au tenors help track association of PGE content with variations in local footwall assimilation. Loss on ignition and $\delta^{34}S$ (both of which also track footwall assimilation), are combined with $CaO/Al_2O_3$ and PGE tenors in Figure 12 to identify variation in contamination within UMT094 by depth.

Between 1285 and 1292 m the $CaO/Al_2O_3$ value increases from ~1 to ~2.6. The upper and lower bounds of this excursion are marked by sharp shifts. Increases in LOI (up to 5.66 wt.% at 1291 m) and decreases in PGE tenors (1254 to 1285 m = 263.8 ppm in 100% sulfides, and 1285 to 1292 m = 131.3 ppm in 100% sulfides) coincide with this band, along with a minor change in $\delta^{34}S$ (from 1282 to 1288 m =3.4 to 3.8 ‰). A similar trend (increased LOI, $CaO/Al_2O_3$, and decreased PGE tenor) occurs within the UG2CU between 1333.3 and 1333.6 m, with a larger increase in $\delta^{34}S$ (from 1329 to 1333 m = 5 to 6 ‰). Thin section petrography identified this segment as containing small calc-silicate xenoliths. Below the UG2CU, from 1350 m depth until the end of the drill core, these features remain similar: high $CaO/Al_2O_3$ and LOI, high $\delta^{34}S$ (~8

‰), and low PGE tenors. The sections which do not show these increases in $CaO/Al_2O_3$ and LOI are: the MZ, the BCU, MCU (above 1285 m), the FCU, and parts of the UG2CU. This is interpreted as evidence of minimal contamination by local footwall lithologies.

Figure 13 compares two element ratios (normalized to primitive mantle estimates), which are useful to distinguish magmatic units from those that show contamination with different types of sedimentary footwall. Values in V/Ti < 1 distinguish dolostone and calc-silicate samples from magmatic samples (V/Ti = 1 to 2) and from hornfels shale samples (V/Ti > 2). Several samples within the FAZ are below 1, between calc-silicate samples and magmatic samples. MCU and FAZ samples within UMT139 (proximal to Transvaal shales) extend above 2, between the uncontaminated samples and hornfels shale samples. Nickel and chromium ratios are also used to compare magmatic samples to sedimentary samples, as well as between the various units of the BIC. Cr content is the highest within chromite bearing units, highest within the UG2CU, moderate within chromite stringer bearing units (FCU, MCU), and nearly absent within footwall units. Ni content is related to pentlandite and olivine content.

Similar mixing trends are shown between an anhydrite-bearing, metasedimentary raft that had been intersected between the FAZ and LZ based on data from Yudovskaya et al. (2018) (Figure 8). The V/Ti values of the metasedimentary raft plot well below magmatic values at 0.17 and 0.21, and the values from the Lower Zone plot between 1.09 and 1.34. This part of the Lower Zone shows less of a contaminated signature than the feldspathic orthopyroxenite and olivine-bearing feldspathic pyroxenite above the raft (V/Ti = 1.09 to 1.34 vs 0.53, 0.71). We believe that this represents the same mixing trend shown in our data between sedimentary material and magmatic material resulting in intermediate V/Ti values. The data show a downward shift in the Ni/Cr values, which we attribute to higher overall Cr content within the LZ.

The contaminated signature within the FAZ in UMT094 extends upwards from the lower contact to dolostone footwall through over 50 m of the FAZ. The contaminated section of the UG2CU could also contribute to the large scale of this contamination, although the trend of the contamination appears constant from the footwall upwards through the base of the FCU and is absent within the upper half of the FCU. This large range of influence differs from the conclusions that have been presented elsewhere (e.g., Penniston-Dorland et al. 2012). For example, Sharman et al. (2013) used this limit of proximal contamination of ~ 5 meters to suggest that $\Delta^{33}S > 0.23$ ‰ must have been produced by distal contamination, most likely in a staging chamber prior to emplacement of the Platreef magmas. They also suggested that the large variability in both $\Delta^{33}S$ and $\delta^{34}S$ of proximal footwall lithologies could not have produced the range in values observed for Platreef sulfides. What we observe in UMT094 is evidence for both proximal and more distal controls on the $\delta^{34}S$ values of sulfide minerals in the Platreef at Turfspruit, and most significantly, that the effects of primal assimilation can be observed at a scale of > 100 m, rather than < 5 m. The key to this large extent of the influence of local assimilation can be seen in Figure 2; the extent to which local footwall lithologies extend upwards into the Lower Zone and Critical Zone along the Northern Limb. With the large scale of contamination seen in UMT094, it is likely that this contamination present within the FAZ is not simply an upward migration of contamination from the local footwall, but from assimilation during the magmas travel to its final location.

Holwell et al. (2007) performed conventional and laser ablation S isotope analyses of primary, secondary and late stage sulfide minerals from the Sandsloot, Zwartfontein, Overysel and Witrivier portions of the Platreef, to the north of Turfspruit. They found that what they considered to be primary sulfides had $\delta^{34}S \leq +2.6$ ‰, similar to the range for kimberlite diamonds from the Kapvaal craton (Westerlund et al. 2004) and to values for magmatic sulfides in the Eastern and Western limbs of the BIC (Penniston-Dorland et al. 2012). Secondary sulfides, however, were more variable and isotopically heavier, attributed to assimilation of variable lithologies along the Northern Limb, either by magmatic assimilation and/or leaching of S from sulfate minerals and incorporation into the secondary sulfides via hydrothermal fluids (Holwell et al. 2007). Conversely, Sharman et al. (2013) suggested that the large range in $\Delta^{33}S$ and $\delta^{34}S$ of Platreef rocks, but inconsistent variation compared to the range in the local footwall lithologies, indicated that the contamination was prior to the emplacement of the Platreef magmas. We have shown here with the $\delta^{34}S$, S/Se, $CaO/Al_2O_3$ and Ti/V values (Figs. 6, 7) and elsewhere with Sr isotopic values (Mayer et al. submitted) that UMT094 intersected Critical Zone magmatic rocks and associated PGE mineralization at the stratigraphic position of the Merensky Reef in which there is little to no evidence for proximal assimilation i.e., $\delta^{34}S$ and $^{87}Sr/^{86}Sr_i$ values overlap those of the Eastern and Western limbs of the BIC. Conversely, the lower part of the Platreef stratigraphy in UMT094, which includes the stratigraphic equivalent of the UG2, shows evidence for local assimilation in $\delta^{34}S$, S/Se, $CaO/Al_2O_3$, Ti/V (Figs. 6-10) and $^{87}Sr/^{86}Sr_i$ (Mayer et al. submitted). Our data do not obviate the need for contamination prior to emplacement of the Platreef; $\delta^{34}S$ presented in this study and $^{87}Sr/^{86}Sr_i$ values from Mayer et al. overlap those of the Eastern and Western limbs of the BIC, but as shown by Penniston-Dorland (2012), the slightly positive $\Delta^{33}S$ values of the Merensky Reef in the Eastern and Western limbs indicate that some surface S was incorporated into the BIC melts prior to emplacement of the Merensky Reef.

## 5.2 Contamination within the Merensky Cyclic Unit

Above the MCU mineralization (1230 to 1260 m), $\delta^{34}S$ values are relatively constant (roughly 2.5 ‰) and average 3.2 ‰ between the MCU mineralization and most of the FCU (1260 to 1310 m). The $\delta^{34}S$ values increase steadily below this level through the UG2CU and into the FAZ. The assimilation of sedimentary sulfur within the UG2CU is supported by higher values of S/Se presented in Figure 11, whereas S/Se values within the MCU is below and within primitive mantle S/Se ranges for all but a sample with small xenoliths.

Although the $\delta^{34}S$ values within the MCU (1.5 to 3.8 ‰) could be interpreted as indication of local footwall assimilation, such values are consistent with the $\delta^{34}S$ values documented in the Merensky and UG2 reef in the Eastern and Western limbs, which have been interpreted to indicate assimilation in the lower crust (i.e. not at the level of emplacement). For example, Penniston-Dorland et al. (2012) analyzed sulfur isotopes ($\delta^{34}S$ and $\Delta^{33}S$) within the Eastern and Western limbs and showed that $\delta^{34}S$ and $\Delta^{33}S$ within the Merensky Reef, UG2 and Main Zone in the Eastern and Western limbs ($\delta^{34}S$: BIC = 1.08 to 3.01 ‰; $\Delta^{33}S$: BIC = 0.09 to 0.15 ‰) were above what is widely considered as mantle values ($\delta^{34}S$: 0 ± 2 ‰; $\Delta^{33}S$: 0.0 ‰).

Figure 14 compares S/Se values with three other distinguishing characteristics that have been outlined above: V/Ti, PGE content and $CaO/Al_2O_3$. The contamination of the MCU shows a slight decrease in V/Ti, and increases in $CaO/Al_2O_3$, but little to no change in Pt+Pd content and no change in S/Se values. The change in V/Ti (Figure 14A) is attributed to the addition of minor amounts of Ti by assimilation of an unknown material. Because there is no change in S/Se, and only a small change in $\delta^{34}S$, the amount of sedimentary sulfur added to this unit must have been low. Figure 14C shows similar increases in $CaO/Al_2O_3$ values within the MCU-Contaminated and FAZ, but the influence of crustal sulfur appears to have had no effect on S/Se values and $\delta^{34}S$ values of the MCU, and a substantial impact on the S/Se values of the FAZ. Similar comparisons as Figure 14 are shown in Figure 15, comparing $\delta^{34}S$ to $CaO/Al_2O_3$ and S/Se. Blue fields show the estimates from the Eastern and Western limbs

## 6. Conclusions

The combined data obtained (whole rocks major and trace element chemistry, and $\delta^{34}S$) show that the extent of direct footwall assimilation within the drill core examined (UMT094) is limited to sections below the main mineralization and extend ~ 50 m upwards from the metasedimentary footwall. The combination of $CaO/Al_2O_3$, V/Ti, S/Se, LOI, and $\delta^{34}S$ show a gradual decreasing trend of local assimilation from the Footwall Assimilation Zone to the base of the Merensky Cyclic Unit. The overall trend is interrupted by local anomalies caused mainly by dolostone and calcite xenoliths near the base of the MCU; however, most of the mineralization is clearly contained within uncontaminated magmatic units. The $\delta^{34}S$ obtained in the mineralized interval of UMT094 are consistent with $\delta^{34}S$ values from the Merensky Reef in the Eastern and Western Limbs of the Bushveld, for which contamination at depth has been proposed but where no local contamination is seen. The results summarized here indicate that the primary mechanism of PGE mineralization in the Platreef is no different than the mechanism that operated in the rest of the BIC. However, footwall assimilation likely caused remobilization and redistribution of metals in sectors of the Platreef with strong intermingling of footwall rocks.

## 7. Acknowledgements

Special thanks to Ivanhoe Mines Ltd for support through the opportunity for this research, samples and financial support. Additional support for this project was provided by the Natural Sciences and Engineering Research Council of Canada, the Goodman's School of Mines, and the Queen's Elizabeth II Diamond Jubilee Scholarship. Thanks are also extended to Cedric Mayer for sampling, sample preparation and consultation, and to Chris Beckett-Brown for his work with Raman Spectroscopy. Additional thanks to the participants and presenters of the 13th International Platinum Symposium for their comments and insight.

## 8. References

Armitage PEB, McDonald I, Edwards SJ, Manby GM (2002) Platinum-group element mineralization in the Platreef and calc-silicate footwall at Sandsloot, Potgietersrus District, South Africa. Applied Earth Science 111:36–45. doi: 10.1179/aes.2002.111.1.36

Barnes S-J, Savard D, Bédard LP, Maier WD (2009) Selenium and sulfur concentrations in the Bushveld Complex of South Africa and implications for formation of the platinum-group element deposits. Mineralium Deposita 44:647. doi: 10.1007/s00126-009-0237-3

Buchanan DL, Nolan J, Suddaby P, et al (1981) The genesis of sulfide mineralization in a portion of the Potgietersrus Limb of the Bushveld Complex. Economic Geology 76:568–579. doi: 10.2113/gsecongeo.76.3.568

Cameron EN (1978) The Lower Zone of the Eastern Bushveld Complex in the Olifants River Trough. Journal of Petrology 19:437–462. doi: 10.1093/petrology/19.3.437

Engelbrecht JP (1990) The Marico Hypabyssal Suite, and the marginal zone of the Bushveld Complex in the Marico District, western Transvaal, South Africa. 11

Eroglu S, Schoenberg R, Wille M, et al (2015) Geochemical stratigraphy, sedimentology, and Mo isotope systematics of the ca. 2.58–2.50 Ga-old Transvaal Supergroup carbonate platform, South Africa. Precambrian Research 266:27–46. doi: 10.1016/j.precamres.2015.04.014

Grobler DF, Brits JAN, Maier WD, Crossingham A (2019) Litho- and chemostratigraphy of the Flatreef PGE deposit, northern Bushveld Complex. Mineralium Deposita. doi: 10.1007/s00126-018-0800-x

Harris C, Chaumba JB (2001) Crustal Contamination and Fluid–Rock Interaction during the Formation of the Platreef, Northern Limb of the Bushveld Complex, South Africa. Journal of Petrology 42:1321–1347. doi: 10.1093/petrology/42.7.1321

Holwell DA, Boyce AJ, McDonald I (2007) Sulfur Isotope Variations within the Platreef Ni-Cu-PGE Deposit: Genetic Implications for the Origin of Sulfide Mineralization. Economic Geology 102:1091–1110. doi: 10.2113/gsecongeo.102.6.1091

Kinnaird JA (2005) Geochemical evidence for multiphase emplacement in the southern Platreef. Applied Earth Science 114:225–242. doi: 10.1179/037174505X82152

Kruger FJ (2005) Filling the Bushveld Complex magma chamber: lateral expansion, roof and floor interaction, magmatic unconformities, and the formation of giant chromitite, PGE and Ti-V-magnetitite deposits. Mineralium Deposita 40:451–472. doi: 10.1007/s00126-005-0016-8

McDonough WF, Sun S -s. (1995) The composition of the Earth. Chemical Geology 120:223–253. doi: 10.1016/0009-2541(94)00140-4

Mudd GM (2012) Key trends in the resource sustainability of platinum group elements. Ore Geology Reviews 46:106–117. doi: 10.1016/j.oregeorev.2012.02.005

Naldrett AJ, Wilson A, Kinnaird J, Chunnett G (2009) PGE Tenor and Metal Ratios within and below the Merensky Reef, Bushveld Complex: Implications for its Genesis. Journal of Petrology 50:625–659. doi: 10.1093/petrology/egp015

Papp J (2014) Chromium 2014 Minerals Yearbook Report. USGS 2014 Minerals

Penniston-Dorland SC, Mathez EA, Wing BA, et al (2012) Multiple sulfur isotope evidence for surface-derived sulfur in the Bushveld Complex. Earth and Planetary Science Letters 337–338:236–242. doi: 10.1016/j.epsl.2012.05.013

van der Merwe MJ (1976) The layered sequence of the Potgietersrus Limb of the Bushveld Complex. Economic Geology 71:1337–1351. doi: 10.2113/gsecongeo.71.7.1337

Wagner (1929) The Platinum Deposits and Mines of South Africa. By P. A. Wagner. pp. xv + 326, with 38 plates and 37 text-figures. Edinburgh: Oliver and Boyd. 1929. Price 21s. Geological Magazine 67:40. doi: 10.1017/S0016756800002703

Wilson A, Chunnett G (2006) Trace Element and Platinum Group Element Distributions and the Genesis of the Merensky Reef, Western Bushveld Complex, South Africa. Journal of Petrology 47:2369–2403. doi: 10.1093/petrology/egl048

Yudovskaya MA, Kinnaird JA, Sobolev AV, et al (2013) Petrogenesis of the Lower Zone Olivine-Rich Cumulates Beneath the Platreef and Their Correlation with Recognized Occurrences in the Bushveld Complex. Economic Geology 108:1923–1952. doi: 10.2113/econgeo.108.8.1923

9. Figures

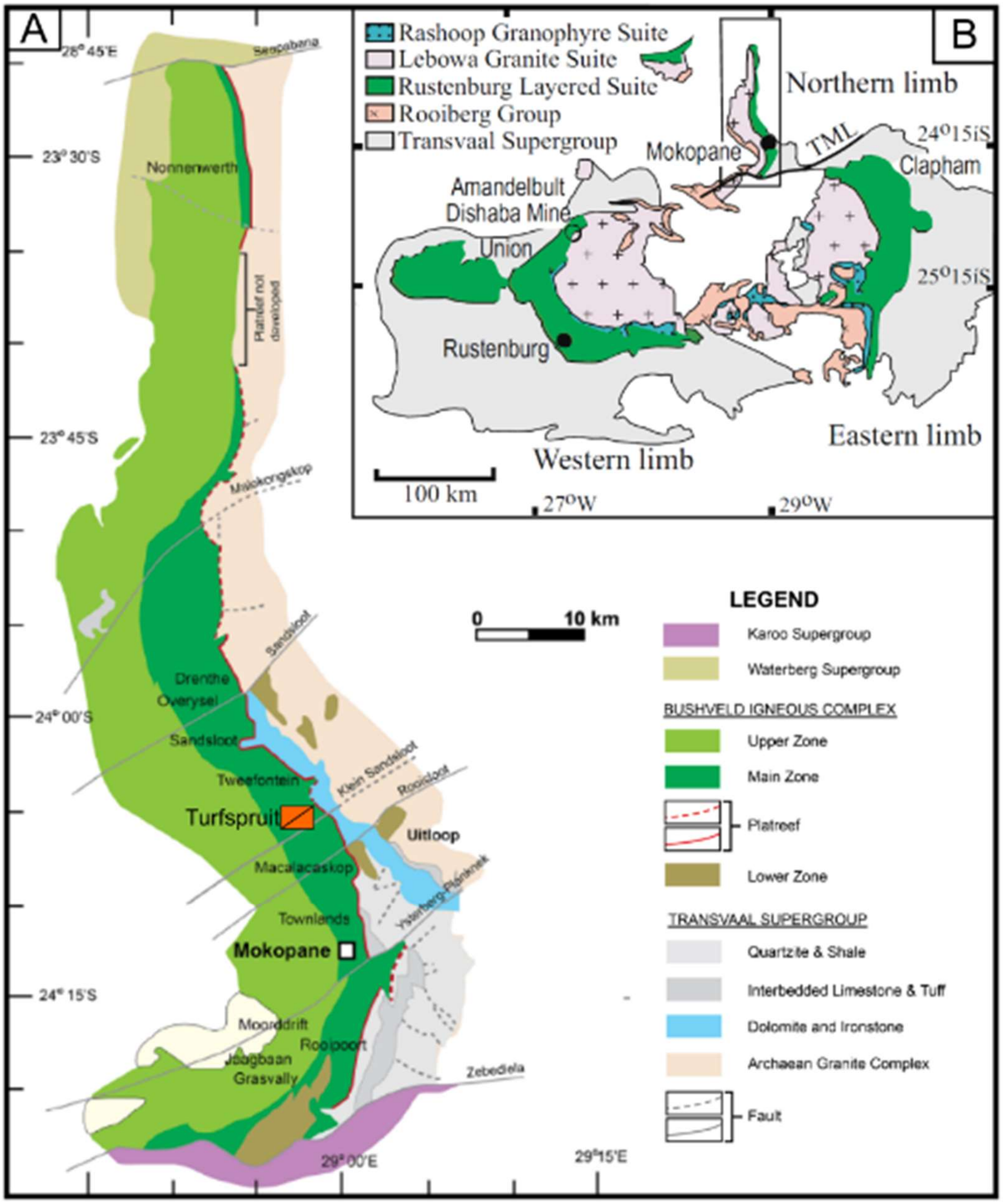


Figure 1. A) Map of the Northern Limb of the BIC, showing the area of study. Location of Figure 2 cross section shown within orange box on Turfspruit farm. B) Map of the Bushveld Igneous Complex, showing location of the Northern Limb within the BIC. 1A Modified from Grobler et al., 2018, 1B Modified from Yudovskaya et al., 2017

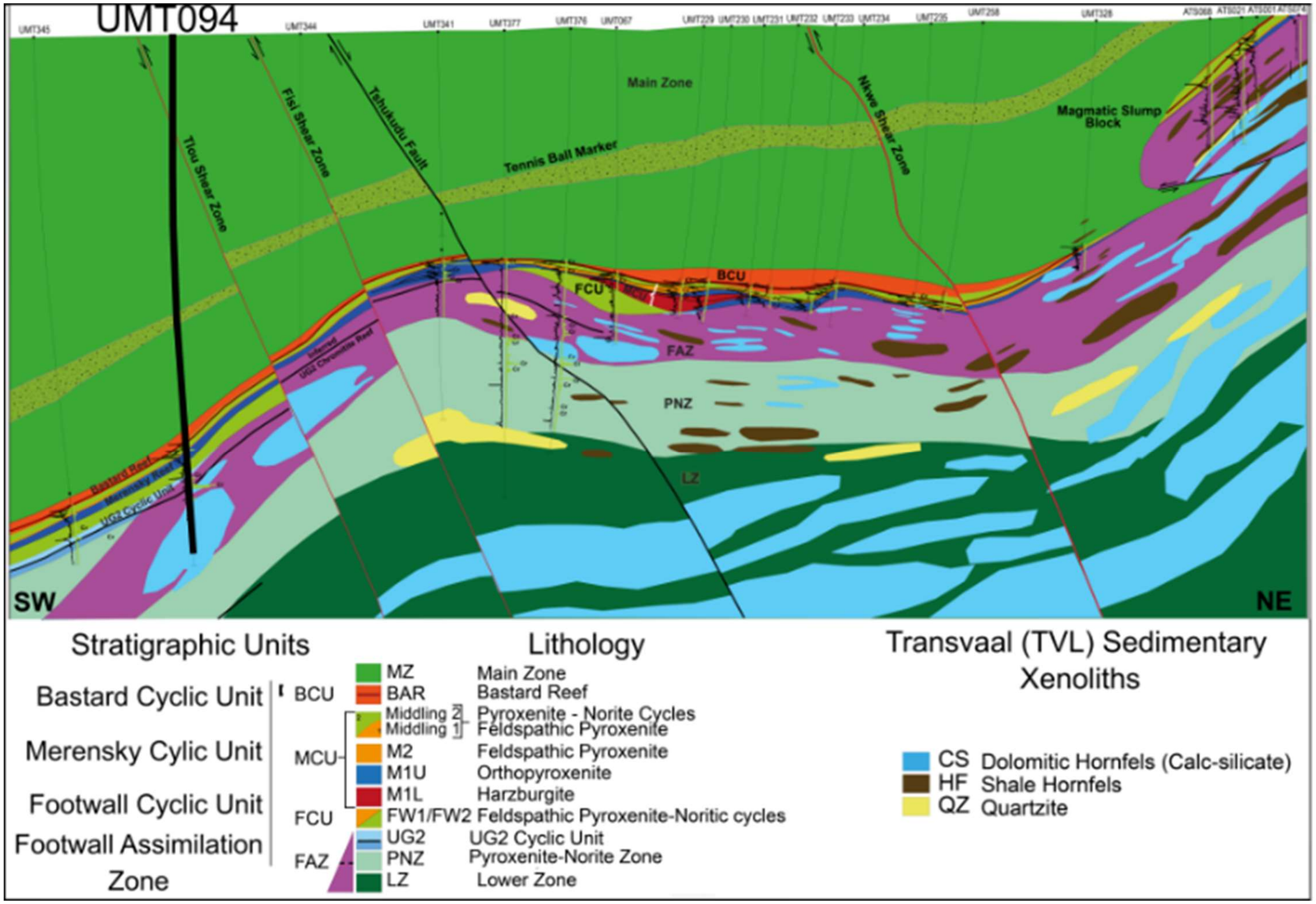


Figure 2. Cross section on Turfspruit farm. Location of UMT094 shown in bold. The up-dip drill holes (NE) show more incorporation of metasedimentary material compared to the Flatreef with even less assimilation within the down-dip extension. Units below the base of drill holes are inferred. Modified from Grobler et al., 2018

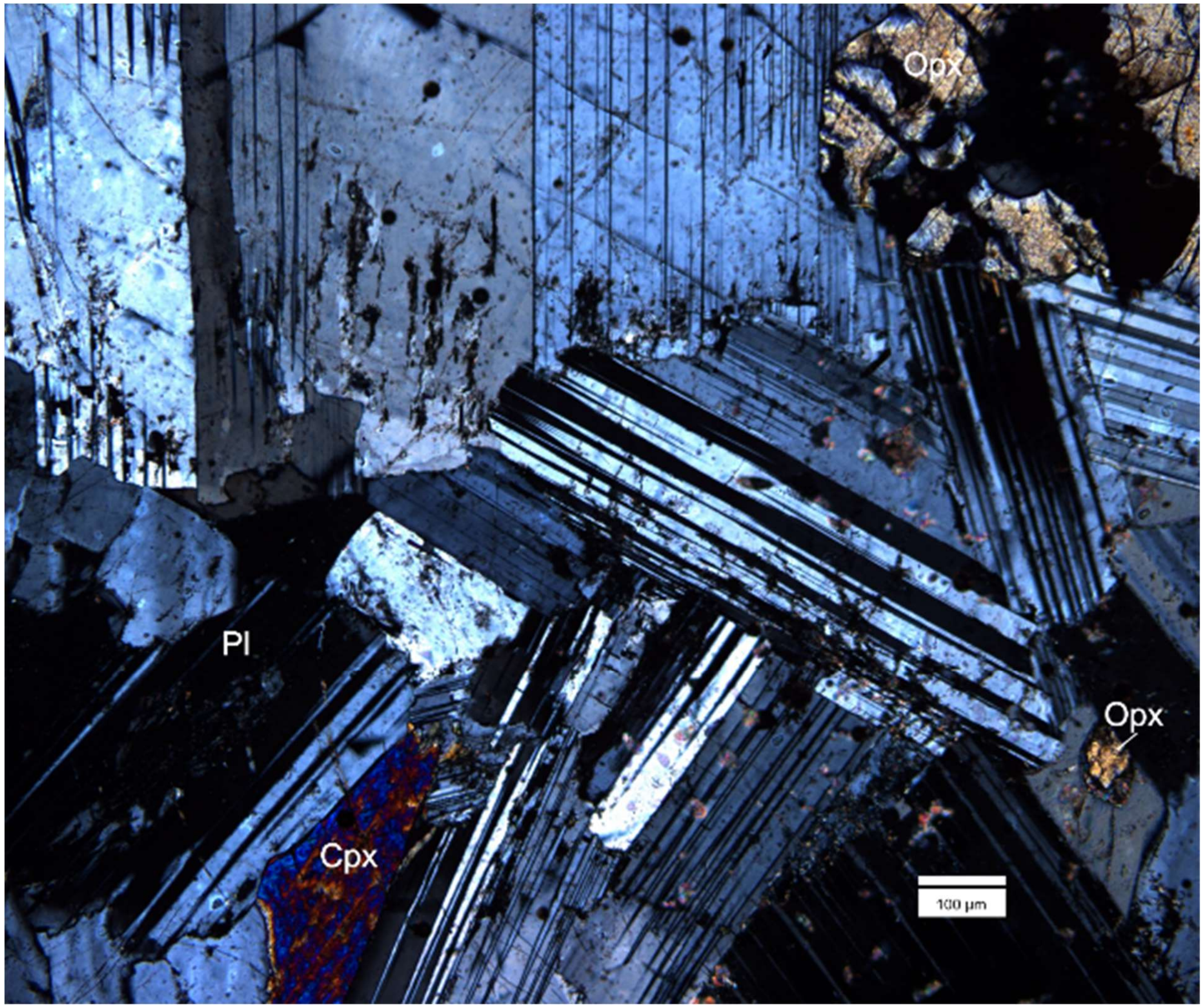

Figure 3. Main zone (anorthite-rich) gabbronorite (sample UMT094-1096). Large percentage of Pl with some Opx and Cpx. Some spots of alteration throughout. Most Pl unlabeled. Cpx = clinopyroxene, Opx = orthopyroxene, Pl = plagioclase

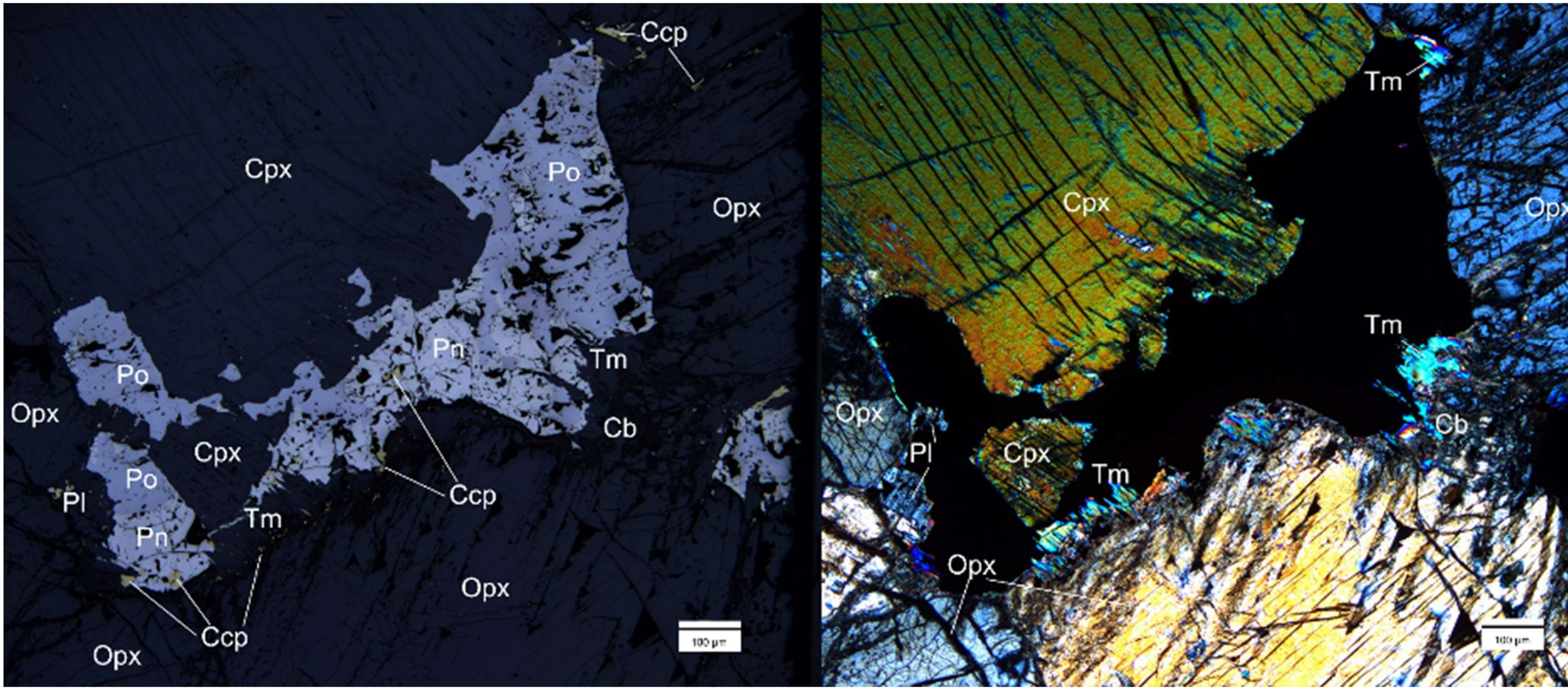


Figure 4. Sulfides within MCU (sample UMT094-1260, RL and XPL). Po and Pn are the dominant sulfides, Ccp is minor. Some carbonate and tremolite occur along contacts of silicates and sulfides. Cb = carbonaceous material, Ccp = chalcopyrite, Cpx = clinopyroxene, Opx = orthopyroxene, Pl = plagioclase, Pn = pentlandite, Po = pyrrhotite, Tm = tremolite

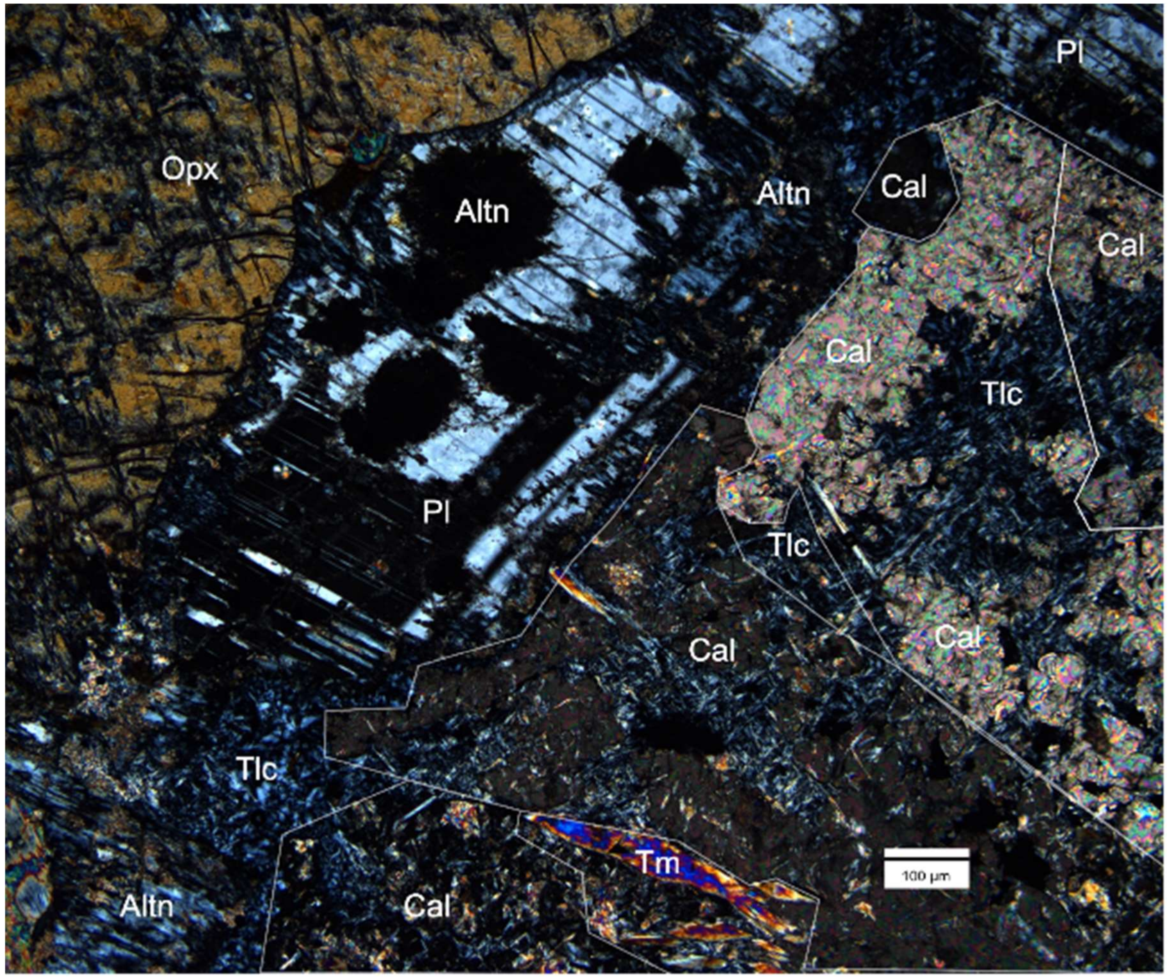


Figure 5. Calcite xenolith within MCU (sample UMT094-1285). Optically continuous calcite relicts with patches of Tlc and Tm. Optically continuous zones are outlined in white. Plagioclase grains show some alteration. Contacts between Pl and Cal are sharp where present. Altn = alteration, Cal = calcite, Opx = orthopyroxene, Pl = plagioclase, Tlc = talc, Tm = tremolite

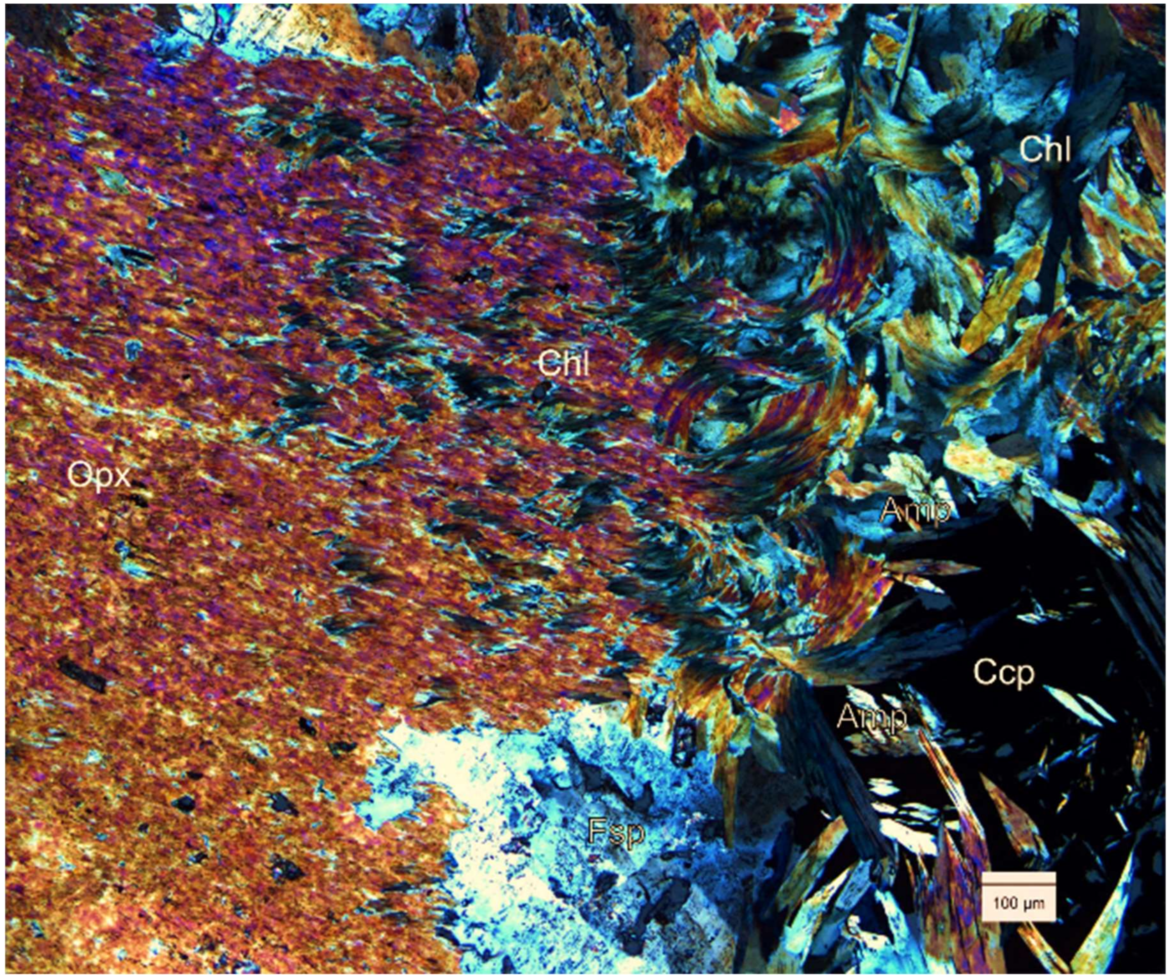


Figure 6. Alteration of orthopyroxene (sample UMT094-1291). Alteration of pyroxene, starting in line with pyroxene orientation to the left and curving towards Ccp to the right. The increased curving of amphibole and chlorite is interpreted as alteration. Amp = unidentified amphibole Ccp = chalcopyrite, Chl = chlorite, Fsp = altered feldspar, Opx = orthorpyroxene.

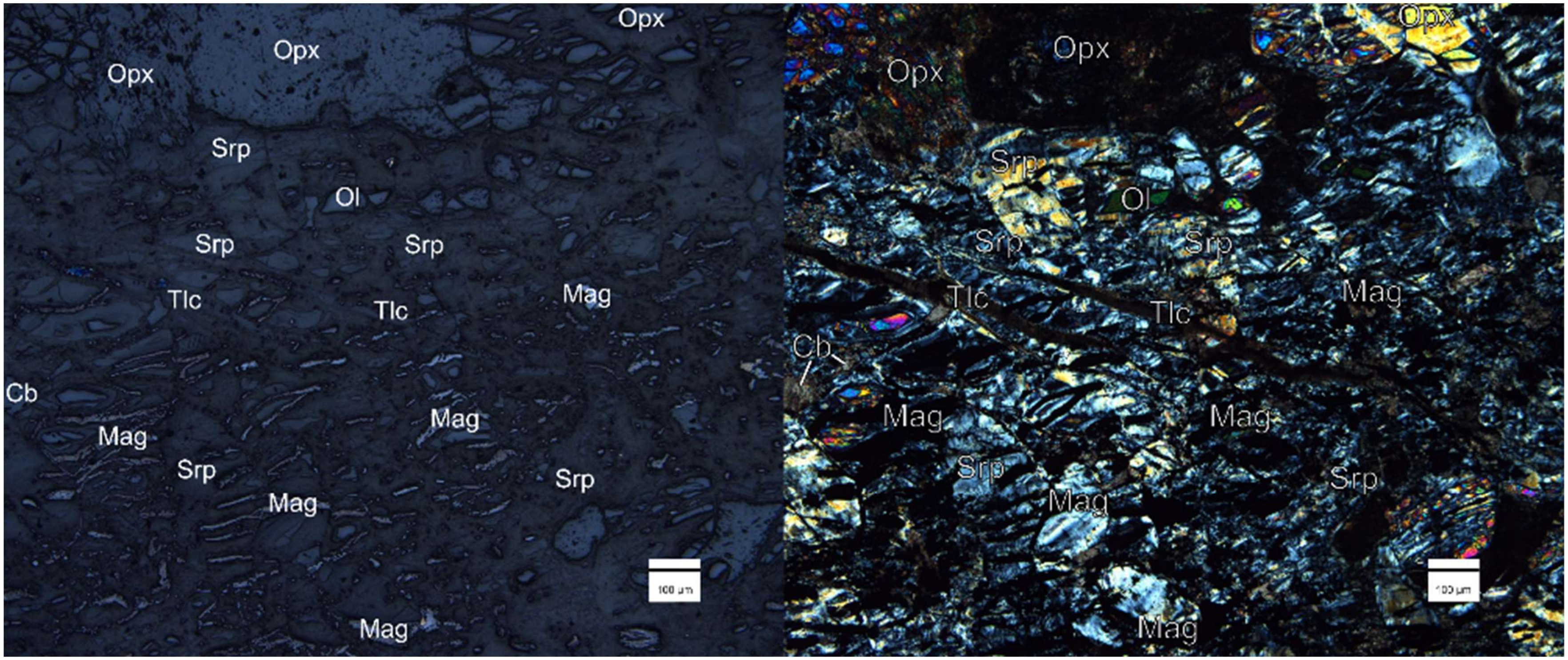


Figure 7. Serpentine and magnetite alteration within footwall assimilation zone (sample UMT094-1390-1). Lenses of magnetite oriented in similar directions within bands of serpentine. Relicts of carbonaceous material, olivine and orthopyroxene rarely appeared scattered through serpentine bands. Cb = carbonaceous material, Mag = magnetite. Ol = olivine, Opx = orthopyroxene, Srp = serpentine, Tlc = talc.

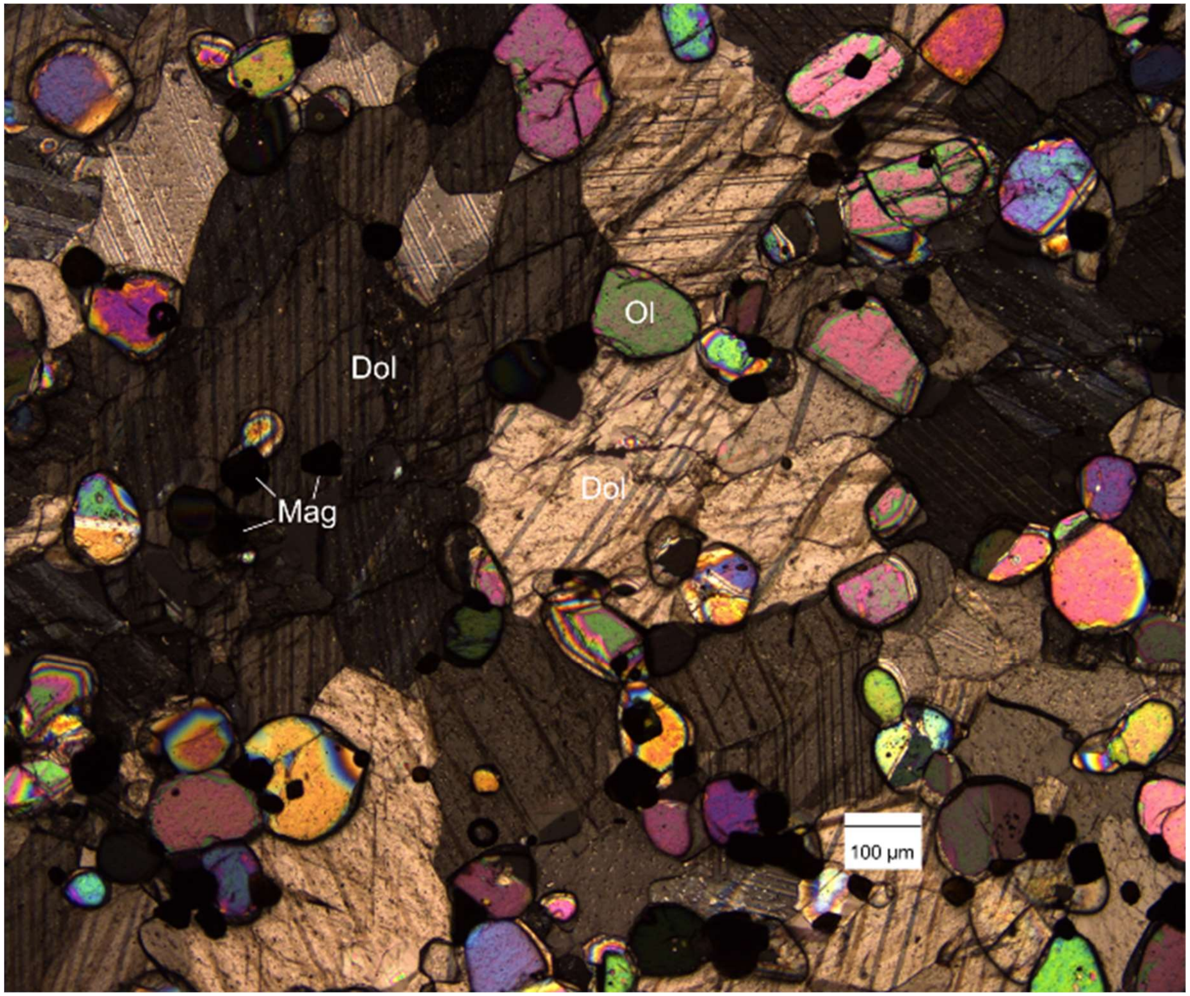

Figure 8. Siliceous dolostone (sample 094-1601). Ol and Mag spread homogenously throughout. Ol interpreted to be contact metamorphic in origin. Dol shows some granoblastic recrystallization textures. Dol = dolomite, Mag = magnetite, Ol = olivine.

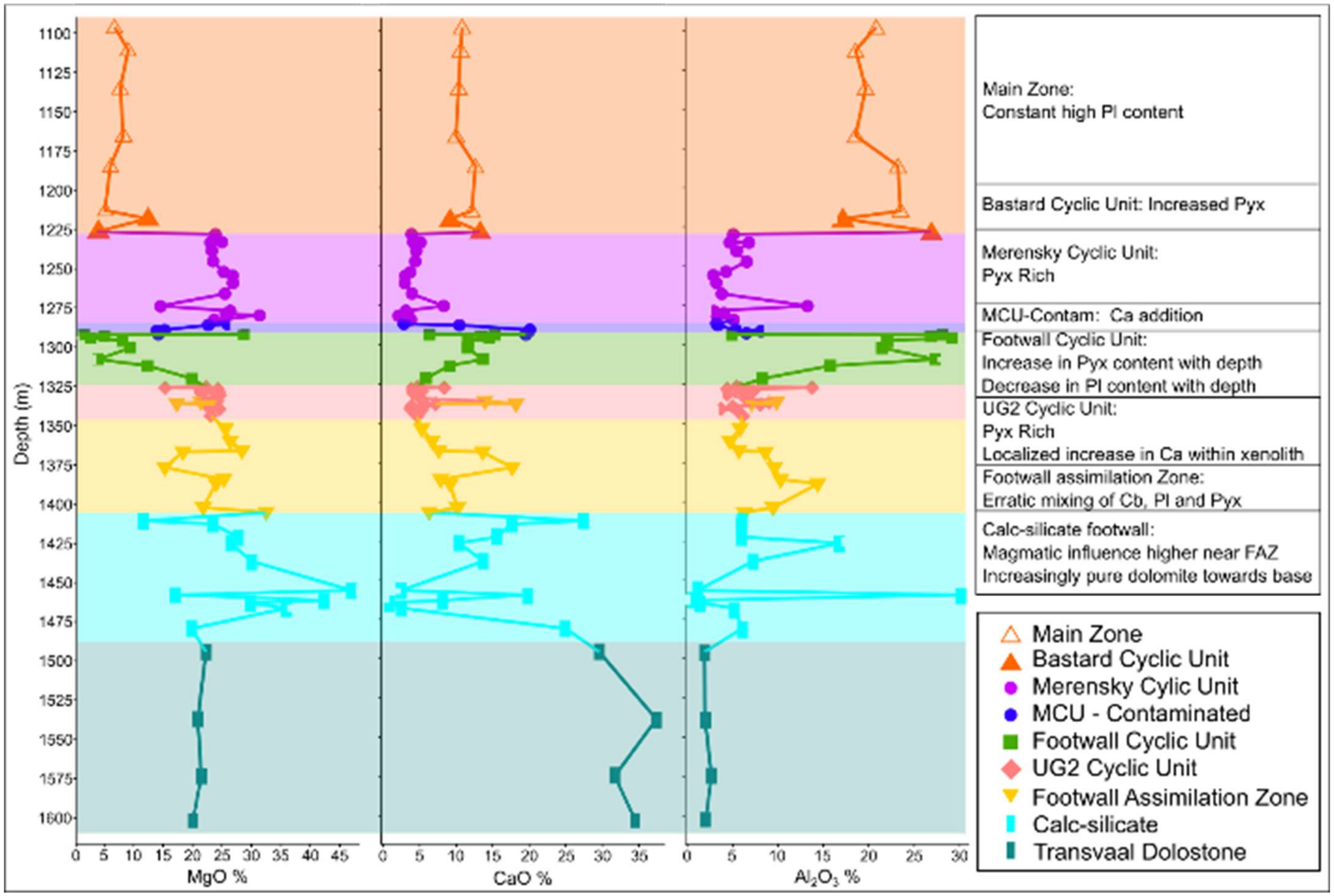


Figure 9. Major element variations with stratigraphy. Variations in pyroxene and plagioclase content seems to be the primary control. Samples with high Pl content have high Al, and moderate Ca, whereas high Pyx shows higher Mg, and lower Ca and Al. Contamination by carbonaceous material increases Ca without large increases in Al. Contamination within UG2CU is shown as part of the FAZ. Irregular bands within CS are due to local variations within metasedimentary units. Less metasomatised dolostone near base, though substantial olivine (~10 modal %) still present.

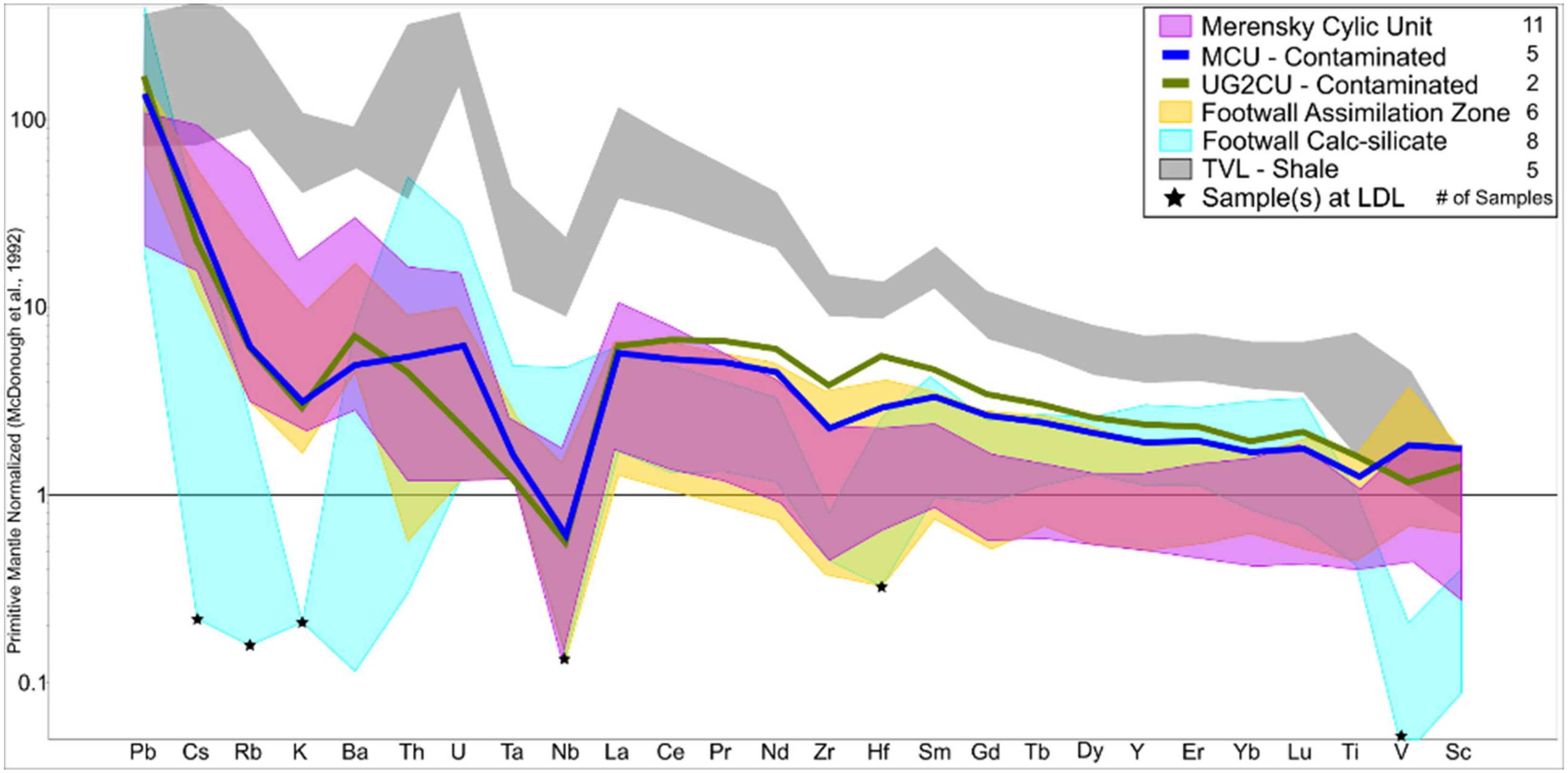


Figure 10. Trace Element Spider Plot. Contaminated samples of the MCU and UG2CU are isolated and show more HREE enrichment than the uncontaminated MCU samples. Samples plotting at or below detection limit are marked by stars. Mineral identification samples that were non-representative are not shown and data for them are available in Table 3. Sr, Eu and Al presented within McDonough et al 1992 are not shown due to their strong dependence on plagioclase content.

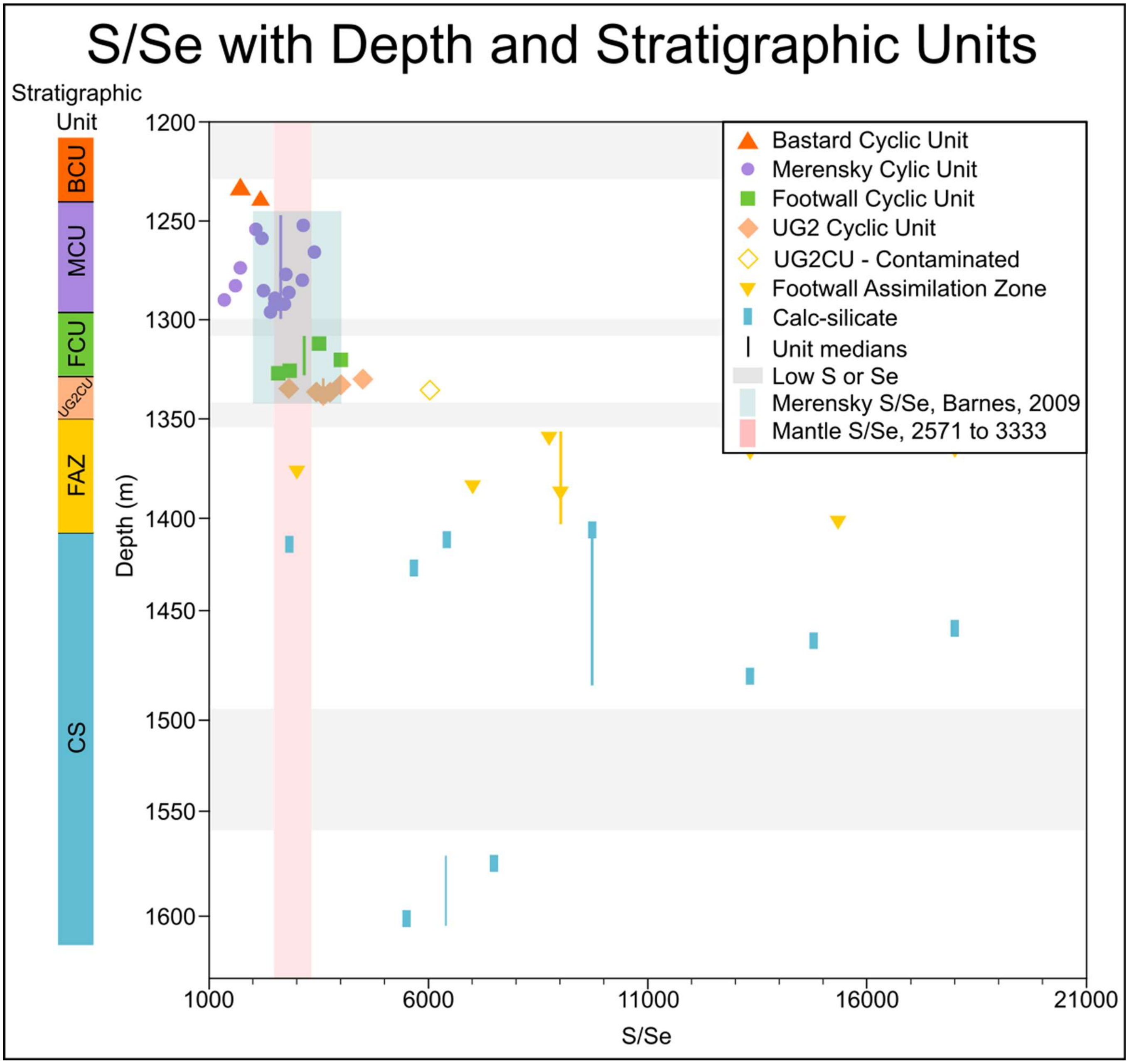


Figure 11. S/Se with depth separated by stratigraphic units. Mantle S/Se values calculated using McDonough and Sun 1995. MCU contaminated unit contains values of S/Se consistent with mantle values, as opposed to showing contributions of S from Se poor country rock. Local contamination present within the UG2CU does not appear to influence the base of the MCU.

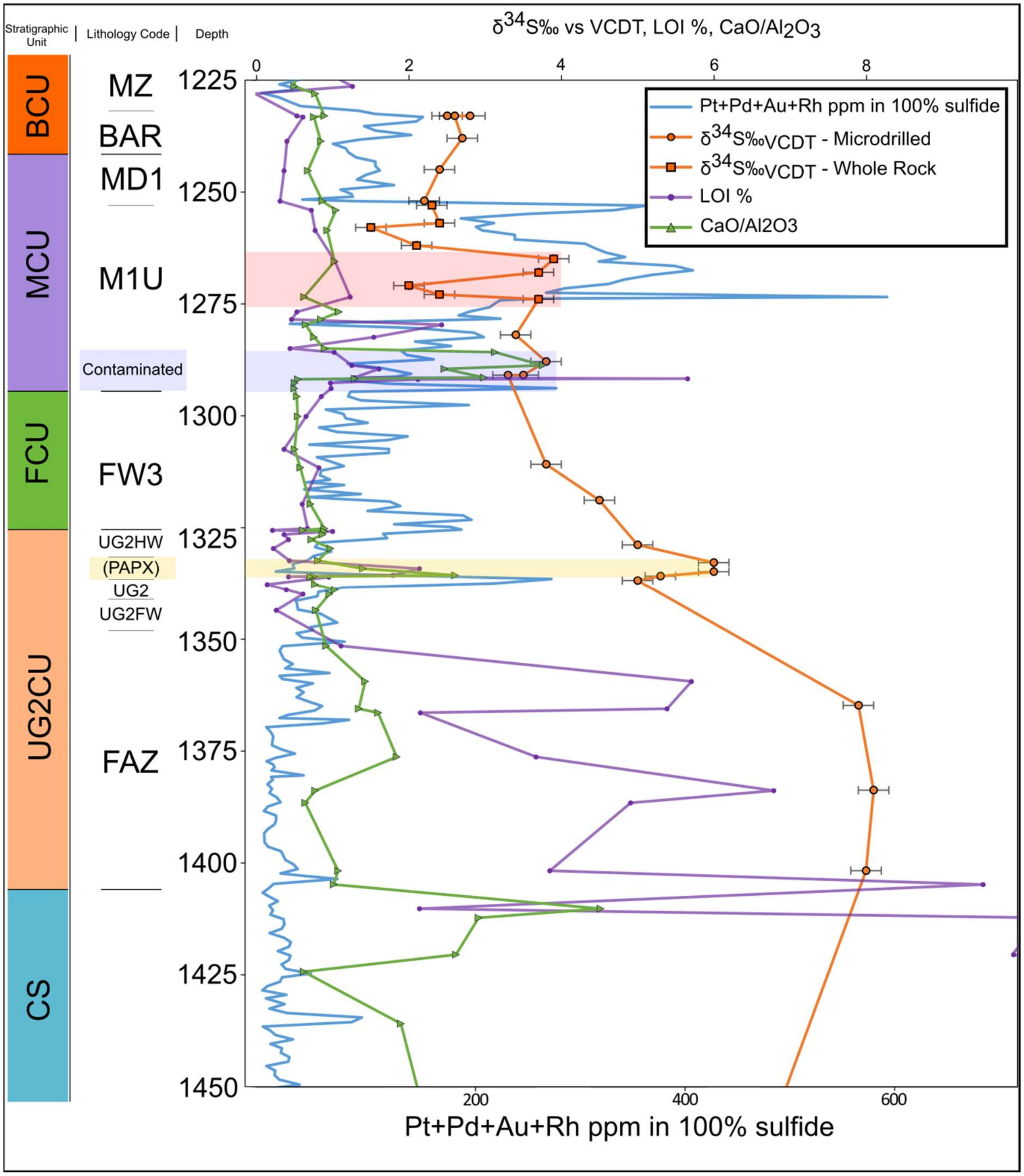


Figure 12. Variations in $\delta^{34}S$, Loss on ignition, $CaO/Al_2O_3$ and PGE tenor with depth (scale on top for all values except PGE/S, which is shown at the bottom). The three coloured boxes (orange, purple, yellow, at 1265 to 1274 m, 1285 to 1291 m, and 1333 to 1335 m depth, respectively) show anomalies in the $\delta^{34}S$ trends. $\delta^{34}S$ values decrease to a plateau before the base of the MCU, showing the limit of incorporation of local footwall sulfur into the main mineralization. Local increases in $CaO/Al_2O_3$ and LOI show potential zones of local contamination by assimilated xenoliths. $\delta^{34}S$ values extend to 3.7 ‰ at 1601 m depth (not shown). Loss on ignition values increase to 20 % at 1450 m and 30% at 1601 m.

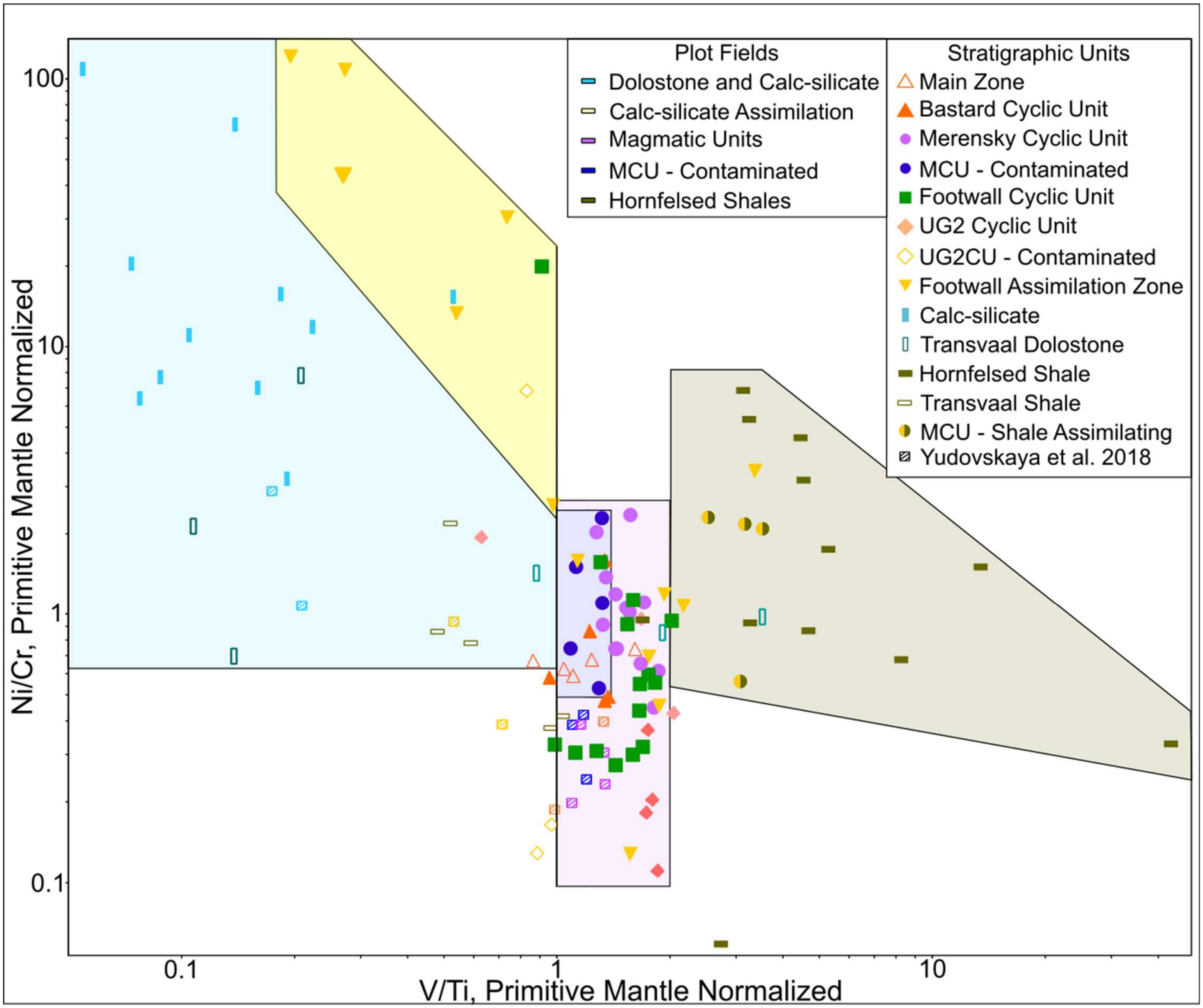


Figure 13. Primitive Mantle normalized plot of V/Ti and Ni/Cr showing magmatic trends and footwall lithology trends. Note that contaminated sections of the MCU have lower V/Ti values, potentially due to addition of Ti by sedimentary assimilation. UG2 values of Cr are highly elevated and most samples, contaminated or otherwise, show lower values of Ni/Cr than other magmatic units. Samples normalized to primitive mantle data from McDonough and Sun 1995.

This is 8pt font

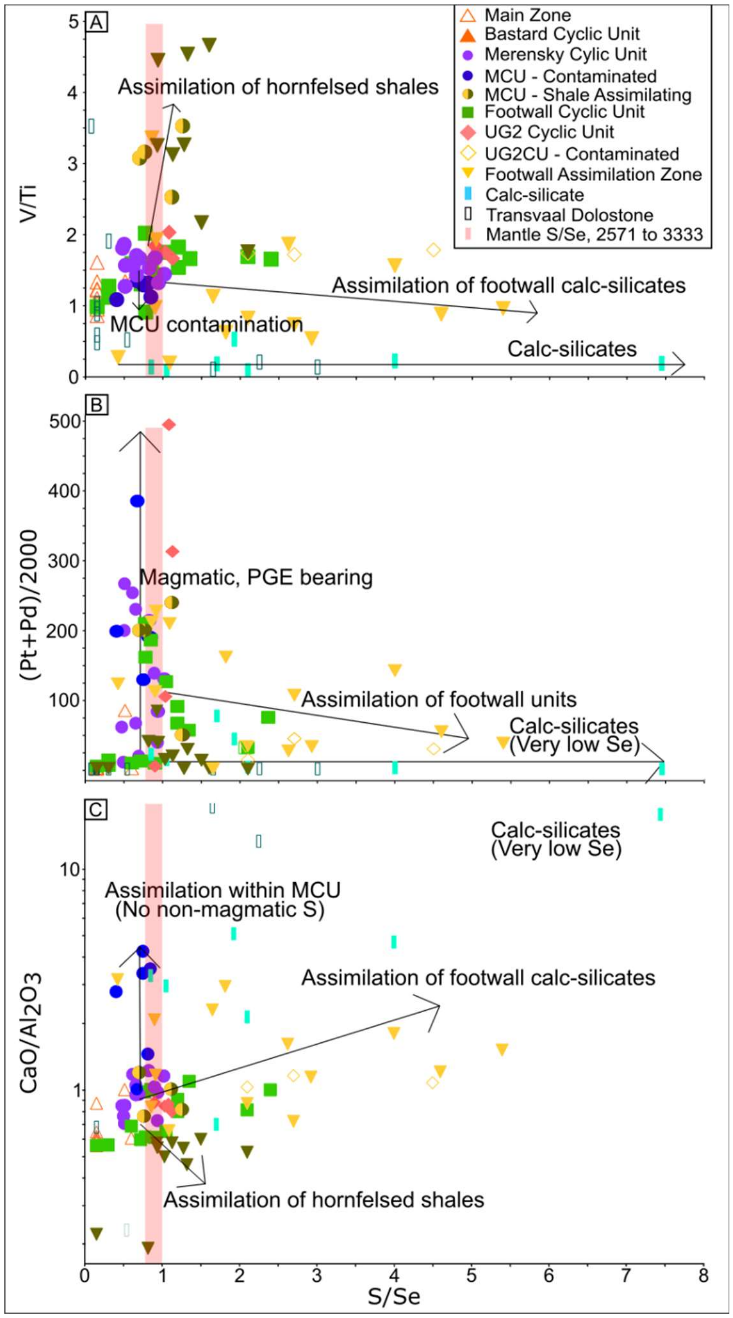


Figure 14. Comparison of S/Se values with other elemental trends. All values are normalized to Primitive Mantle values. A) V/Ti, B) Pt+Pd and C) $CaO/Al_2O_3$ are used to discriminate magmatic and non-magmatic sources. A) Assimilation within the MCU shows decreases in V/Ti but no change in S/Se. Assimilation of Shales increases both V/Ti and S/Se values B) Pt+Pd and S/Se trends showing a strong anti correlation between PGE bearing magmatic units and assimilated footwall units C) MCU assimilation in UMT 094 showing increased Ca/Al2O3, but no S/Se increase related to the footwall assimilation, interpreted to show no significant addition of crustal S. Shale assimilation is only present within ATS 139 and UMT 365.

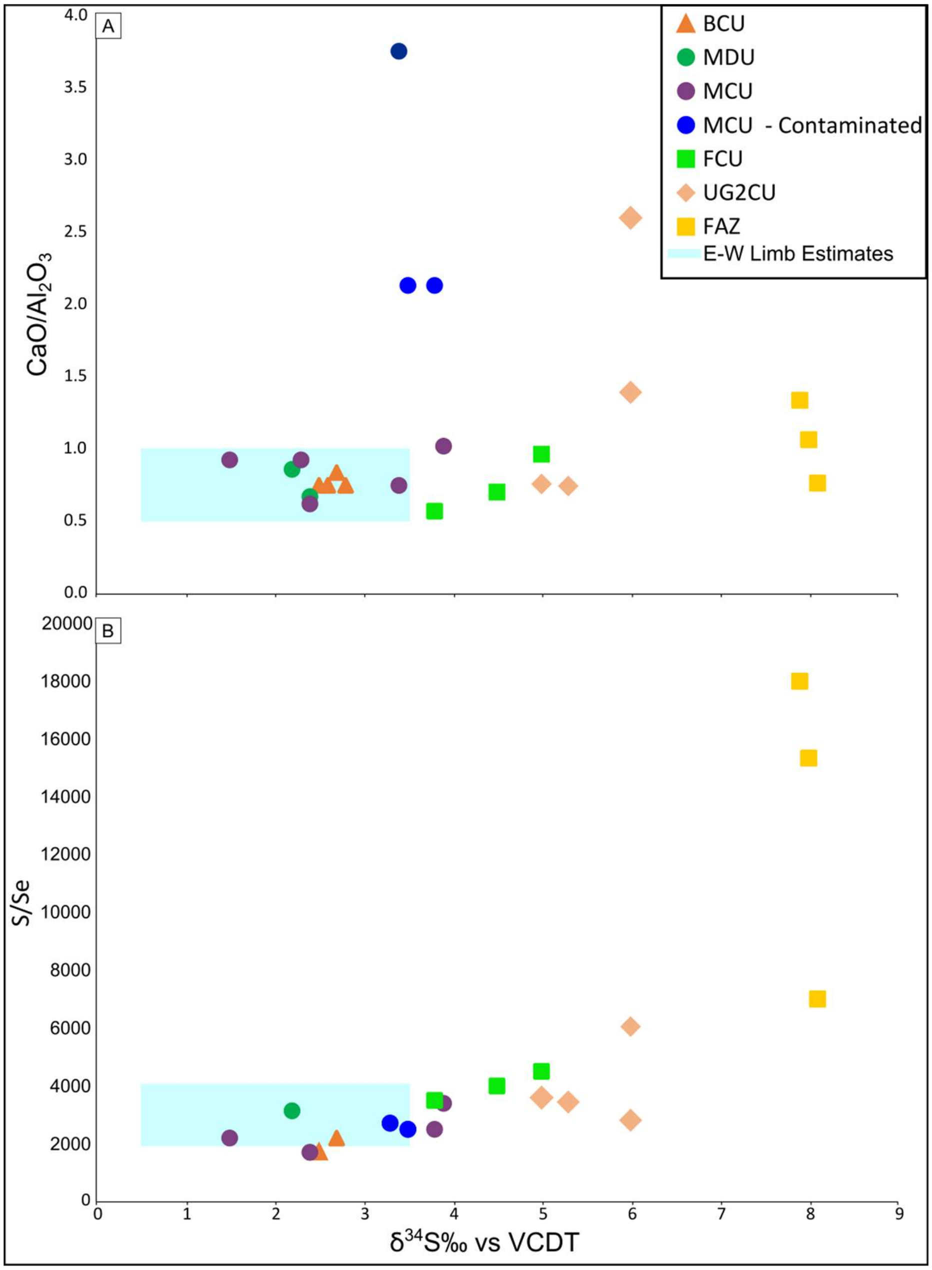


Figure 15. Comparison of $\delta^{34}S$ values with A) $CaO/Al_2O_3$ and B) S/Se, blue fields are estimates of the Eastern and Western limbs: S/Se from Barnes et al. (2009), CaO/Al2O3 from Wilson and Chunnett (2006), and $\delta^{34}S$ from Penniston-Dorland et al. (2012). Local scale contamination within the MCU shows an increase in $Ca/Al_2O_3$ but not an increase in $\delta^{34}S$ or S/Se trends within the FAZ, UG2CU and FAZ show increases in all values, reflecting local footwall assimilation.

## 10. Tables

Table 1. Major Element Data for UMT094 and De Hoop farm sedimentary samples (ALS method ME-ICP06)

| | Analyte | $SiO_2$ | $Al_2O_3$ | $Fe_2O_3$ | CaO | MgO | $Na_2O$ | $K_2O$ | $Cr_2O_3$ | $TiO_2$ | MnO | LOI | Total |
|---|---|---|---|---|---|---|---|---|---|---|---|---|---|
| | Units | % | % | % | % | % | % | % | % | % | % | % | % |
| | LDL | 0.01 | 0.01 | 0.01 | 0.01 | 0.01 | 0.01 | 0.01 | 0.01 | 0.01 | 0.01 | 0.01 | 0.01 |
| Sample | Stratigraphy | | | | | | | | | | | | |
| UMT094-1096 | MZ | 51.4 | 20.80 | 6.16 | 10.85 | 6.8 | 2.28 | 0.43 | 0.07 | 0.22 | 0.10 | 0.22 | 99.39 |
| UMT094-1111 | MZ | 52.0 | 18.55 | 7.38 | 10.60 | 9.06 | 2.08 | 0.34 | 0.09 | 0.23 | 0.12 | 0.15 | 100.65 |
| UMT094-1135 | MZ | 52.3 | 19.65 | 6.86 | 10.35 | 7.74 | 2.36 | 0.42 | 0.07 | 0.29 | 0.11 | 0.65 | 100.85 |
| UMT094-1165 | MZ | 50.0 | 18.55 | 7.24 | 9.99 | 8.23 | 1.96 | 0.36 | 0.08 | 0.20 | 0.13 | 1.62 | 98.42 |
| UMT094-1184 | MZ | 49.7 | 23.20 | 5.27 | 12.65 | 6.04 | 2.07 | 0.21 | 0.05 | 0.12 | 0.09 | 0.21 | 99.66 |
| UMT094-1213 | BCU | 50.3 | 23.50 | 5.34 | 12.15 | 5.13 | 2.41 | 0.30 | 0.04 | 0.14 | 0.09 | 0.32 | 99.79 |
| UMT094-1218 | BCU | 51.0 | 17.15 | 7.49 | 9.18 | 12.35 | 1.60 | 0.18 | 0.16 | 0.15 | 0.13 | 0.33 | 99.77 |
| UMT094-1226 | BCU | 47.9 | 26.90 | 2.69 | 13.30 | 3.79 | 2.18 | 0.77 | 0.05 | 0.08 | 0.05 | 1.26 | 99.04 |
| UMT094-1228 | BCU | 52.4 | 5.09 | 12.20 | 3.92 | 23.9 | 0.61 | 0.07 | 0.32 | 0.20 | 0.22 | <0.01 | 98.94 |
| UMT094-1232 | BCU | 53.3 | 4.66 | 12.80 | 4.14 | 25 | 0.46 | 0.07 | 0.40 | 0.21 | 0.23 | 0.53 | 101.80 |
| UMT094-1233 | MCU | 52.8 | 6.79 | 11.95 | 5.11 | 23.1 | 0.70 | 0.15 | 0.41 | 0.15 | 0.20 | 0.61 | 101.99 |
| UMT094-1238 | MCU | 52.1 | 5.42 | 11.50 | 4.56 | 23.3 | 0.62 | 0.19 | 0.40 | 0.18 | 0.20 | 0.40 | 98.90 |
| UMT094-1245 | MCU | 52.5 | 6.56 | 10.90 | 4.42 | 23.5 | 0.60 | 0.24 | 0.38 | 0.13 | 0.21 | 0.36 | 99.83 |
| UMT094-1252 | MCU | 53.3 | 4.30 | 12.20 | 3.71 | 25.3 | 0.50 | 0.16 | 0.40 | 0.19 | 0.22 | 0.31 | 100.61 |
| UMT094-1254 | MCU | 53.8 | 2.95 | 13.05 | 3.07 | 26.8 | 0.35 | 0.13 | 0.45 | 0.17 | 0.23 | 0.72 | 101.73 |
| UMT094-1258 | MCU | 52.7 | 3.19 | 12.35 | 2.96 | 26.9 | 0.27 | 0.09 | 0.52 | 0.15 | 0.22 | 0.77 | 100.12 |
| UMT094-1265 | MCU | 52.6 | 3.84 | 11.75 | 3.93 | 25.5 | 0.36 | 0.19 | 0.46 | 0.18 | 0.21 | 1.03 | 100.07 |
| UMT094-1273 | MCU | 52.2 | 13.25 | 8.180 | 8.27 | 14.6 | 1.79 | 0.59 | 0.25 | 0.15 | 0.15 | 1.23 | 100.80 |
| UMT094-1277 | MCU | 53.0 | 2.92 | 13.85 | 3.16 | 26.4 | 0.29 | 0.09 | 0.41 | 0.17 | 0.23 | 0.53 | 101.06 |
| UMT094-1278 | MCU | 54.5 | 4.03 | 12.35 | 3.41 | 25.7 | 0.38 | 0.10 | 0.42 | 0.15 | 0.23 | 0.46 | 101.74 |

Table 1. (Cont.)

| | Analyte | $SiO_2$ | $Al_2O_3$ | $Fe_2O_3$ | CaO | MgO | $Na_2O$ | $K_2O$ | $Cr_2O_3$ | $TiO_2$ | MnO | LOI | Total |
|---|---|---|---|---|---|---|---|---|---|---|---|---|---|
| | Units | % | % | % | % | % | % | % | % | % | % | % | % |
| | LDL | 0.01 | 0.01 | 0.01 | 0.01 | 0.01 | 0.01 | 0.01 | 0.01 | 0.01 | 0.01 | 0.01 | 0.01 |
| Sample | Stratigraphy | | | | | | | | | | | | |
| UMT094-1279 | MCU | 46.3 | 3.22 | 14.20 | 2.07 | 31.4 | 0.12 | 0.23 | 0.67 | 0.11 | 0.21 | 2.43 | 100.98 |
| UMT094-1282 | MCU | 50.3 | 5.10 | 12.35 | 3.83 | 23.7 | 0.56 | 0.07 | 0.86 | 0.17 | 0.21 | 1.54 | 98.71 |
| UMT094-1289 | MCU | 47.6 | 8.09 | 8.05 | 19.95 | 13.9 | 0.62 | 0.19 | 0.86 | 0.36 | 0.15 | 1.61 | 101.43 |
| UMT094-1291A | MCU | 47.9 | 6.55 | 7.29 | 19.55 | 14.15 | 0.72 | 0.08 | 0.51 | 0.26 | 0.13 | 1.28 | 98.43 |
| UMT094-1291B | MCU | 38.0 | 4.85 | 15.10 | 6.24 | 28.7 | 0.26 | 0.04 | 0.45 | 0.09 | 0.15 | 5.66 | 99.56 |
| UMT094-1292A | FCU | 44.5 | 28.10 | 4.04 | 15.25 | 1.58 | 2.17 | 0.62 | 0.05 | 0.04 | 0.03 | 2.12 | 98.59 |
| UMT094-1292B | FCU | 49.3 | 26.80 | 2.91 | 13.35 | 5.04 | 2.21 | 0.50 | 0.13 | 0.05 | 0.05 | 0.97 | 101.39 |
| UMT094-1294 | FCU | 48.7 | 29.10 | 1.97 | 14.45 | 2.7 | 2.39 | 0.44 | 0.07 | 0.04 | 0.03 | 0.98 | 100.93 |
| UMT094-1296 | FCU | 48.2 | 22.00 | 5.00 | 11.60 | 8.12 | 1.89 | 0.25 | 0.19 | 0.07 | 0.08 | 0.85 | 98.30 |
| UMT094-1300 | FCU | 50.0 | 21.40 | 5.05 | 11.55 | 9.44 | 1.84 | 0.19 | 0.27 | 0.09 | 0.09 | 0.65 | 100.62 |
| UMT094-1308 | FCU | 49.4 | 27.30 | 2.63 | 13.60 | 3.96 | 2.18 | 0.14 | 0.12 | 0.05 | 0.04 | 0.36 | 99.86 |
| UMT094-1311 | FCU | 48.7 | 15.75 | 8.62 | 9.04 | 12.4 | 1.64 | 0.28 | 0.90 | 0.17 | 0.13 | 0.82 | 98.50 |
| UMT094-1319 | FCU | 51.0 | 8.30 | 11.25 | 5.86 | 19.85 | 0.78 | 0.15 | 0.56 | 0.16 | 0.20 | 0.60 | 98.74 |
| UMT094-1325A | FCU | 51.1 | 5.46 | 13.00 | 4.86 | 22.3 | 0.55 | 0.10 | 0.40 | 0.17 | 0.22 | 0.67 | 98.87 |
| UMT094-1325B | FCU | 51.0 | 13.80 | 8.66 | 8.37 | 15.3 | 1.29 | 0.16 | 0.43 | 0.15 | 0.16 | 0.21 | 99.57 |
| UMT094-1326A | FCU | 52.2 | 5.87 | 12.65 | 5.20 | 22.3 | 0.54 | 0.10 | 0.63 | 0.20 | 0.22 | 1.00 | 100.94 |
| UMT094-1326B | FCU | 51.9 | 4.43 | 12.45 | 3.84 | 24.3 | 0.32 | 0.03 | 0.56 | 0.12 | 0.22 | 0.36 | 98.54 |
| UMT094-1327 | FCU | 51.0 | 7.26 | 11.45 | 5.22 | 21.1 | 0.72 | 0.13 | 0.62 | 0.18 | 0.21 | 0.42 | 98.34 |
| UMT094-1329 | FCU | 52.2 | 4.36 | 12.45 | 4.22 | 24.8 | 0.41 | 0.05 | 0.47 | 0.14 | 0.22 | 0.22 | 99.55 |
| UMT094-1332 | FCU | 51.3 | 6.39 | 11.95 | 5.13 | 21.8 | 0.67 | 0.11 | 0.40 | 0.15 | 0.21 | 0.43 | 98.57 |
| UMT094-1334 * | UG2HW | 38.7 | 9.95 | 11.05 | 13.90 | 24.2 | 0.06 | 0.02 | 0.01 | 0.62 | 0.16 | 2.14 | 100.81 |
| UMT094-1335 | UG2HW | 44.6 | 6.97 | 9.90 | 18.15 | 17.35 | 0.34 | 0.09 | 0.31 | 0.33 | 0.14 | 1.79 | 100.00 |

Table 1. (Cont.)

| | Analyte | $SiO_2$ | $Al_2O_3$ | $Fe_2O_3$ | CaO | MgO | $Na_2O$ | $K_2O$ | $Cr_2O_3$ | $TiO_2$ | MnO | LOI | Total |
|---|---|---|---|---|---|---|---|---|---|---|---|---|---|
| | Units | % | % | % | % | % | % | % | % | % | % | % | % |
| | LDL | 0.01 | 0.01 | 0.01 | 0.01 | 0.01 | 0.01 | 0.01 | 0.01 | 0.01 | 0.01 | 0.01 | 0.01 |
| Sample | Stratigraphy | | | | | | | | | | | | |
| UMT094-1336A | UG2HW | 46.7 | 9.64 | 11.05 | 7.21 | 21.3 | 0.96 | 0.12 | 0.56 | 0.09 | 0.16 | 0.42 | 98.23 |
| UMT094-1365 | UG2FW | 34.2 | 5.68 | 15.10 | 7.62 | 28.4 | 0.16 | 0.01 | 2.87 | 0.19 | 0.19 | 5.39 | 99.82 |
| UMT094-1366 | FAZ | 34.4 | 8.53 | 13.85 | 13.60 | 18.35 | 0.31 | 0.07 | 6.59 | 0.40 | 0.24 | 2.15 | 98.50 |
| UMT094-1376 | FAZ | 46.4 | 9.60 | 6.17 | 17.65 | 15.3 | 0.37 | 0.25 | 0.14 | 0.27 | 0.16 | 3.67 | 100.04 |
| UMT094-1384 | UG2FW | 36.2 | 10.25 | 10.60 | 7.87 | 25.3 | 0.50 | 0.13 | 0.02 | 0.22 | 0.15 | 6.79 | 98.07 |
| UMT094-1386 | FAZ | 34.1 | 14.40 | 12.45 | 9.18 | 24 | 0.28 | 0.05 | 0.01 | 0.30 | 0.14 | 4.91 | 99.86 |
| UMT094-1402 | UG2FW | 32.4 | 9.50 | 15.55 | 10.15 | 21.8 | 0.25 | 0.17 | 3.80 | 0.36 | 0.17 | 3.85 | 98.01 |
| UMT094-1405 | FAZ | 38.1 | 6.28 | 7.46 | 6.35 | 32.5 | 0.05 | 0.06 | 0.02 | 0.23 | 0.06 | 9.54 | 100.67 |
| UMT094-1410 * | FW2A | 41.2 | 6.07 | 8.00 | 27.40 | 11.7 | 0.09 | <0.01 | 0.02 | 0.64 | 0.14 | 2.14 | 97.54 |
| UMT094-1412 | FW2A | 34.2 | 6.02 | 7.51 | 17.55 | 23.4 | 0.02 | <0.01 | <0.01 | 0.12 | 0.24 | 10.30 | 99.37 |
| UMT094-1421 | FW2A | 36.5 | 5.94 | 3.28 | 15.55 | 27.8 | 0.03 | 0.01 | <0.01 | 0.09 | 0.08 | 9.92 | 99.20 |
| UMT094-1424 | FW2A | 28.3 | 16.75 | 4.49 | 10.35 | 26.5 | 0.05 | 0.01 | 0.01 | 0.14 | 0.06 | 12.70 | 99.38 |
| UMT094-1436 | FW2A | 32.4 | 7.26 | 4.39 | 13.75 | 30 | 0.01 | <0.01 | 0.01 | 0.11 | 0.19 | 13.10 | 101.23 |
| UMT094-1454 * | FW2A | 19.05 | 1.15 | 8.28 | 2.50 | 47 | <0.01 | 0.02 | 0.01 | 0.15 | 0.22 | 18.80 | 97.18 |
| UMT094-1457 | FW2A | 3.43 | 30.10 | 8.35 | 19.8 | 17.1 | 0.03 | 0.01 | 0.01 | 0.26 | 0.28 | 19.10 | 98.49 |
| UMT094-1461 * | FW2A | 27.8 | 0.68 | 9.05 | 8.20 | 42.4 | 0.02 | 0.05 | <0.01 | 0.62 | 0.24 | 8.56 | 97.63 |
| UMT094-1463 * | FW2A | 23.9 | 1.26 | 35.90 | 0.85 | 29.8 | 0.02 | 0.02 | <0.01 | 0.12 | 0.15 | 9.11 | 101.13 |
| UMT094-1466 * | FW2A | 22.3 | 5.21 | 12.25 | 2.58 | 35.9 | 0.01 | <0.01 | 0.01 | 0.09 | 0.12 | 21.20 | 99.72 |
| UMT094-1479 | FW2A | 25.8 | 6.04 | 7.21 | 25.00 | 19.9 | 0.02 | <0.01 | <0.01 | 0.09 | 0.38 | 13.55 | 98.02 |
| UMT094-1494 | TVL - DS | 8.1 | 1.89 | 5.20 | 29.6 | 22.3 | 0.02 | <0.01 | <0.01 | 0.11 | 0.19 | 29.70 | 97.20 |
| UMT094-1537 | TVL - DS | 9.35 | 1.97 | 1.81 | 37.4 | 20.9 | 0.04 | 0.01 | <0.01 | 0.11 | 0.11 | 30.00 | 101.72 |
| UMT094-1573 | TVL - DS | 11.7 | 2.68 | 2.94 | 31.7 | 21.5 | 0.01 | <0.01 | <0.01 | 0.18 | 0.12 | 28.20 | 99.07 |

Table 1. (Cont.)

| | Analyte | $SiO_2$ | $Al_2O_3$ | $Fe_2O_3$ | CaO | MgO | $Na_2O$ | $K_2O$ | $Cr_2O_3$ | $TiO_2$ | MnO | LOI | Total |
|---|---|---|---|---|---|---|---|---|---|---|---|---|---|
| | Units | % | % | % | % | % | % | % | % | % | % | % | % |
| | LDL | 0.01 | 0.01 | 0.01 | 0.01 | 0.01 | 0.01 | 0.01 | 0.01 | 0.01 | 0.01 | 0.01 | 0.01 |
| Sample | Stratigraphy | | | | | | | | | | | | |
| UMT094-1601 | TVL - DS | 13.8 | 2.04 | 1.37 | 34.5 | 20.1 | <0.01 | <0.01 | <0.01 | 0.09 | 0.08 | 27.5 | 99.51 |
| LUD001 | TVL - Shale | 55.8 | 25.3 | 8.98 | 0.14 | 1.17 | 0.76 | 3.1 | 0.03 | 0.69 | 0.03 | 4.39 | 100.56 |
| LUD002 | TVL - Shale | 56.1 | 24.9 | 8.41 | 0.12 | 1.2 | 0.75 | 3.19 | 0.03 | 0.73 | 0.03 | 4.18 | 99.85 |
| LUD003 | TVL | 32.1 | 5.19 | 3.62 | 16.75 | 13.65 | 0.05 | 0.95 | 0.01 | 0.19 | 0.08 | 26.10 | 98.81 |
| LUD004 | TVL - Qtz | 80.2 | 2.58 | 2.08 | 4.79 | 3.23 | 0.02 | 0.77 | 0.01 | 0.08 | 0.04 | 7.28 | 101.15 |
| LUD005 | TVL - Shale | 58.9 | 12.90 | 8.34 | 2.65 | 7.01 | 0.38 | 1.17 | <0.01 | 1.58 | 0.04 | 6.37 | 99.69 |
| LUD006 | TVL - DS | 1.60 | 0.71 | 0.92 | 29.40 | 20.9 | 0.02 | 0.03 | <0.01 | 0.02 | 0.19 | 45.60 | 99.44 |
| LUD007 | TVL | 45.5 | 12.95 | 8.33 | 7.76 | 8.22 | 0.55 | 2.17 | 0.02 | 0.48 | 0.23 | 12.75 | 99.15 |
| LUD008 | TVL - Qtz | 83.4 | 0.11 | 0.92 | 4.94 | 3.29 | 0.02 | 0.02 | <0.01 | <0.01 | 0.04 | 7.96 | 100.72 |
| LUD009 | TVL - Shale | 55.4 | 19.50 | 11.4 | 0.15 | 3.68 | 0.82 | 3.00 | 0.04 | 0.80 | 0.07 | 4.46 | 99.51 |
| LUD010A | TVL - Qtz | 89.5 | 0.06 | 0.48 | 3.37 | 2.4 | <0.01 | 0.01 | <0.01 | <0.01 | 0.06 | 5.35 | 101.24 |
| LUD010B | TVL - DS | 5.22 | 0.08 | 1.02 | 28.4 | 19.80 | 0.01 | <0.01 | <0.01 | <0.01 | 0.48 | 44.30 | 99.31 |
| LUD011 | TVL - DS | 22.2 | 0.08 | 0.44 | 23.2 | 16.25 | 0.02 | 0.02 | <0.01 | <0.01 | 0.25 | 36.20 | 98.67 |

Notes: $P_2O_5$, SrO, BaO not shown (at or below LDL). Data for these elements are available in Tables 2 and 3. Stratigraphy Codes: MZ =Main Zone, BCU= Bastard Cyclic Unit, MCU = Merensky Cyclic Unit, FCU = Footwall Cyclic Unit, UG2CU = Upper Group 2 Cyclic Unit, FAZ = Footwall Assimilation Zone, FW2A = Calc-silicate footwall, TVL = Transvaal, DS = Dolostone, Qtz = quartzite
* Sample was for mineral identification, was non-representative and excluded from geochemical interpretation.

Table 2. Trace Element Data for UMT094 and De Hoop farm sedimentary samples (ALS method ME-MS81)

| | Analyte | Ba | Ce | Cr | Cs | Dy | Er | Eu | Ga | Gd | Hf | Ho | La | Lu | Nb |
|---|---|---|---|---|---|---|---|---|---|---|---|---|---|---|---|
| | Units | ppm | ppm | ppm | ppm | ppm | ppm | ppm | ppm | ppm | ppm | ppm | ppm | ppm | ppm |
| | LDL | 0.5 | 0.5 | 10 | 0.01 | 0.05 | 0.03 | 0.03 | 0.1 | 0.05 | 0.2 | 0.01 | 0.5 | 0.01 | 0.2 |
| Sample | Stratigraphy | | | | | | | | | | | | | | |
| UMT094-1096 | MZ | 134.5 | 13.6 | 480 | 0.39 | 1.14 | 0.74 | 0.64 | 16.3 | 1.09 | 1.0 | 0.25 | 7.2 | 0.10 | 1.6 |
| UMT094-1111 | MZ | 123.0 | 14.0 | 670 | 0.38 | 1.38 | 0.87 | 0.71 | 15.1 | 1.43 | 0.6 | 0.30 | 7.3 | 0.12 | 1.1 |
| UMT094-1135 | MZ | 113.5 | 13.5 | 570 | 0.80 | 1.20 | 0.84 | 0.58 | 16.4 | 1.16 | 1.0 | 0.27 | 7.0 | 0.13 | 2.2 |
| UMT094-1165 | MZ | 120.5 | 10.0 | 580 | 0.92 | 0.97 | 0.64 | 0.53 | 14.3 | 0.93 | 0.6 | 0.20 | 5.3 | 0.10 | 1.0 |
| UMT094-1184 | MZ | 81.0 | 5.7 | 390 | 0.12 | 0.64 | 0.40 | 0.51 | 16.7 | 0.52 | 0.3 | 0.14 | 3.0 | 0.07 | 0.3 |
| UMT094-1213 | BCU | 93.0 | 8.1 | 250 | 0.36 | 0.65 | 0.46 | 0.53 | 16.7 | 0.77 | 0.4 | 0.16 | 4.3 | 0.07 | 0.7 |
| UMT094-1218 | BCU | 69.9 | 6.7 | 1200 | 0.47 | 0.64 | 0.49 | 0.39 | 13.5 | 0.46 | 0.3 | 0.16 | 3.6 | 0.10 | 0.4 |
| UMT094-1226 | BCU | 196.0 | 6.3 | 380 | 1.26 | 0.40 | 0.23 | 0.43 | 18.4 | 0.43 | 0.2 | 0.09 | 3.6 | 0.03 | 0.3 |
| UMT094-1228 | BCU | 28.0 | 4.7 | 2330 | 0.45 | 0.96 | 0.70 | 0.19 | 6.2 | 0.66 | 0.4 | 0.20 | 2.3 | 0.13 | 0.6 |
| UMT094-1232 | BCU | 26.5 | 3.2 | 2850 | 0.97 | 0.83 | 0.58 | 0.16 | 5.5 | 0.67 | 0.3 | 0.20 | 1.5 | 0.09 | 0.2 |
| UMT094-1233 | MCU | 57.8 | 4.0 | 2840 | 0.58 | 0.62 | 0.48 | 0.18 | 6.6 | 0.59 | 0.3 | 0.14 | 2.0 | 0.08 | <0.2 |
| UMT094-1238 | MCU | 45.0 | 6.0 | 2830 | 0.74 | 0.88 | 0.56 | 0.23 | 6.3 | 0.73 | 0.3 | 0.18 | 2.9 | 0.10 | 1.2 |
| UMT094-1245 | MCU | 69.5 | 2.9 | 2720 | 0.95 | 0.53 | 0.35 | 0.19 | 6.2 | 0.40 | 0.2 | 0.12 | 1.5 | 0.07 | <0.2 |
| UMT094-1252 | MCU | 39.1 | 5.0 | 2910 | 0.55 | 0.86 | 0.59 | 0.16 | 5.7 | 0.72 | 0.4 | 0.19 | 2.4 | 0.10 | 0.6 |
| UMT094-1254 | MCU | 29.2 | 4.1 | 3230 | 0.98 | 0.76 | 0.54 | 0.15 | 4.6 | 0.63 | 0.3 | 0.18 | 1.9 | 0.10 | 0.5 |
| UMT094-1258 | MCU | 30.9 | 3.5 | 3770 | 0.76 | 0.65 | 0.53 | 0.13 | 5.0 | 0.48 | 0.3 | 0.15 | 1.7 | 0.09 | 0.2 |
| UMT094-1265 | MCU | 47.5 | 5.6 | 3400 | 1.14 | 0.89 | 0.56 | 0.21 | 5.4 | 0.75 | 0.4 | 0.19 | 2.6 | 0.10 | 0.6 |
| UMT094-1273 | MCU | 210.0 | 14.1 | 1860 | 1.27 | 0.89 | 0.61 | 0.35 | 11.0 | 0.93 | 0.7 | 0.19 | 7.5 | 0.09 | 1.3 |
| UMT094-1277 | MCU | 29.5 | 2.9 | 2970 | 1.04 | 0.81 | 0.53 | 0.12 | 4.8 | 0.54 | 0.3 | 0.19 | 1.3 | 0.11 | 0.2 |
| UMT094-1278 | MCU | 38.2 | 2.5 | 3110 | 1.40 | 0.60 | 0.53 | 0.13 | 5.4 | 0.41 | 0.2 | 0.15 | 1.3 | 0.10 | <0.2 |
| UMT094-1279 | MCU | 111.5 | 3.2 | 4900 | 2.03 | 0.49 | 0.33 | 0.09 | 4.3 | 0.34 | 0.3 | 0.08 | 1.5 | 0.04 | 0.2 |
| UMT094-1282 | MCU | 19.8 | 3.6 | 6280 | 2.15 | 0.48 | 0.43 | 0.13 | 6.4 | 0.41 | 0.3 | 0.14 | 1.9 | 0.09 | 0.3 |

Table 2. (Cont.)

| | Analyte | Ba | Ce | Cr | Cs | Dy | Er | Eu | Ga | Gd | Hf | Ho | La | Lu | Nb |
|---|---|---|---|---|---|---|---|---|---|---|---|---|---|---|---|
| | Units | ppm | ppm | ppm | ppm | ppm | ppm | ppm | ppm | ppm | ppm | ppm | ppm | ppm | ppm |
| | LDL | 0.5 | 0.5 | 10 | 0.01 | 0.05 | 0.03 | 0.03 | 0.1 | 0.05 | 0.2 | 0.01 | 0.5 | 0.01 | 0.2 |
| Sample | Stratigraphy | | | | | | | | | | | | | | |
| UMT094-1285 | MCU | 35.9 | 5.6 | 5660 | 1.08 | 0.75 | 0.53 | 0.15 | 5.8 | 0.60 | 0.5 | 0.17 | 2.9 | 0.10 | 0.9 |
| UMT094-1286 | MCU | 39.3 | 9.7 | 3730 | 0.69 | 1.87 | 1.07 | 0.47 | 5.3 | 1.92 | 0.8 | 0.39 | 3.3 | 0.15 | 0.2 |
| UMT094-1288 | MCU | 15.7 | 16.2 | 7310 | 0.37 | 2.42 | 1.34 | 0.65 | 7.8 | 2.42 | 1.5 | 0.50 | 6.5 | 0.17 | 0.4 |
| UMT094-1289 | MCU | 69.4 | 17.9 | 6020 | 0.70 | 2.34 | 1.37 | 0.66 | 8.6 | 2.52 | 1.6 | 0.51 | 7.3 | 0.16 | 0.7 |
| UMT094-1291A | MCU | 33.8 | 8.5 | 3690 | 0.52 | 1.60 | 0.96 | 0.42 | 7.1 | 1.49 | 0.7 | 0.37 | 3.3 | 0.13 | 0.3 |
| UMT094-1291B | MCU | 12.2 | 2.1 | 3230 | 0.75 | 0.48 | 0.30 | 0.12 | 4.4 | 0.49 | 0.3 | 0.11 | 0.9 | 0.05 | <0.2 |
| UMT094-1292A | FCU | 148.0 | 2.7 | 390 | 0.92 | 0.19 | 0.11 | 0.28 | 16.9 | 0.17 | <0.2 | 0.03 | 1.5 | 0.01 | <0.2 |
| UMT094-1292B | FCU | 123.0 | 2.9 | 920 | 1.04 | 0.18 | 0.14 | 0.25 | 16.4 | 0.20 | <0.2 | 0.05 | 1.6 | 0.02 | 0.2 |
| UMT094-1294 | FCU | 97.5 | 2.7 | 480 | 0.88 | 0.20 | 0.13 | 0.27 | 17.8 | 0.15 | <0.2 | 0.04 | 1.6 | 0.01 | 0.2 |
| UMT094-1296 | FCU | 74.5 | 3.5 | 1430 | 0.76 | 0.27 | 0.20 | 0.28 | 15.1 | 0.26 | 0.2 | 0.07 | 1.9 | 0.03 | 0.2 |
| UMT094-1300 | FCU | 62.9 | 3.4 | 1960 | 0.52 | 0.33 | 0.26 | 0.26 | 14.3 | 0.26 | 0.2 | 0.08 | 1.9 | 0.03 | 0.2 |
| UMT094-1308 | FCU | 61.0 | 3.1 | 860 | 0.19 | 0.19 | 0.13 | 0.27 | 17.1 | 0.18 | <0.2 | 0.05 | 1.7 | 0.02 | <0.2 |
| UMT094-1311 | FCU | 89.2 | 6.8 | 6630 | 0.61 | 0.57 | 0.33 | 0.36 | 13.3 | 0.55 | 0.3 | 0.13 | 3.7 | 0.06 | 0.6 |
| UMT094-1319 | FCU | 49.4 | 4.5 | 4070 | 0.62 | 0.58 | 0.46 | 0.26 | 8.2 | 0.54 | 0.3 | 0.13 | 2.4 | 0.08 | 0.4 |
| UMT094-1325A | FCU | 50.0 | 4.1 | 2880 | 0.65 | 0.71 | 0.48 | 0.17 | 6.1 | 0.57 | 0.3 | 0.15 | 1.9 | 0.10 | 0.6 |
| UMT094-1325B | FCU | 60.1 | 4.1 | 3120 | 0.24 | 0.49 | 0.40 | 0.30 | 10.8 | 0.50 | 0.3 | 0.12 | 2.2 | 0.08 | 0.2 |
| UMT094-1326A | FCU | 34.0 | 4.9 | 4460 | 1.07 | 0.76 | 0.58 | 0.19 | 6.9 | 0.61 | 0.4 | 0.18 | 2.3 | 0.09 | 0.7 |
| UMT094-1326B | FCU | 13.9 | 3.5 | 4030 | 0.15 | 0.37 | 0.28 | 0.12 | 5.0 | 0.31 | <0.2 | 0.08 | 1.5 | 0.07 | 1.7 |
| UMT094-1327 | FCU | 53.4 | 4.7 | 4130 | 0.24 | 0.65 | 0.45 | 0.23 | 7.5 | 0.52 | 0.3 | 0.16 | 2.5 | 0.09 | 0.4 |
| UMT094-1329 | FCU | 21.0 | 2.0 | 3500 | 0.12 | 0.56 | 0.41 | 0.12 | 5.2 | 0.34 | 0.2 | 0.11 | 1.0 | 0.06 | 0.2 |
| UMT094-1332 | FCU | 50.8 | 4.1 | 2950 | 0.20 | 0.64 | 0.41 | 0.17 | 6.8 | 0.43 | 0.3 | 0.14 | 2.1 | 0.08 | 0.5 |
| UMT094-1334 * | UG2HW | 16.5 | 18.6 | 50 | 0.06 | 5.44 | 2.69 | 0.69 | 11.5 | 4.87 | 14.5 | 1.03 | 6.3 | 0.34 | 1.3 |

Table 2. (Cont.)

| | Analyte | Ba | Ce | Cr | Cs | Dy | Er | Eu | Ga | Gd | Hf | Ho | La | Lu | Nb |
|---|---|---|---|---|---|---|---|---|---|---|---|---|---|---|---|
| | Units | ppm | ppm | ppm | ppm | ppm | ppm | ppm | ppm | ppm | ppm | ppm | ppm | ppm | ppm |
| | LDL | 0.5 | 0.5 | 10 | 0.01 | 0.05 | 0.03 | 0.03 | 0.1 | 0.05 | 0.2 | 0.01 | 0.5 | 0.01 | 0.2 |
| Sample | Stratigraphy | | | | | | | | | | | | | | |
| UMT094-1335 | UG2HW | 49.1 | 12.3 | 2190 | 0.52 | 1.91 | 1.11 | 0.59 | 8.1 | 2.05 | 1.7 | 0.41 | 4.4 | 0.16 | 0.4 |
| UMT094-1336A | UG2HW | 33.4 | 1.9 | 4090 | 0.38 | 0.40 | 0.25 | 0.16 | 7.4 | 0.29 | <0.2 | 0.10 | 0.9 | 0.04 | <0.2 |
| UMT094-1336B | UG2HW | 34.0 | 2.2 | 3790 | 0.85 | 0.38 | 0.29 | 0.15 | 7.2 | 0.27 | 0.2 | 0.08 | 1.2 | 0.05 | <0.2 |
| UMT094-1337 | UG2HW | 30.9 | 4.5 | >10000 | 0.27 | 0.57 | 0.43 | 0.17 | 8.1 | 0.46 | 0.2 | 0.13 | 2.2 | 0.09 | 0.4 |
| UMT094-1339 | UG2HW | 26.1 | 2.9 | 8700 | 0.36 | 0.60 | 0.53 | 0.13 | 6.9 | 0.49 | 0.3 | 0.15 | 1.3 | 0.11 | 0.3 |
| UMT094-1340 | UG2HW | 30.7 | 3.0 | 8010 | 0.45 | 0.65 | 0.47 | 0.15 | 7.1 | 0.50 | 0.3 | 0.14 | 1.3 | 0.09 | 0.2 |
| UMT094-1343 | UG2HW | 30.0 | 2.5 | 9700 | 0.24 | 0.54 | 0.34 | 0.13 | 7.9 | 0.39 | 0.2 | 0.12 | 1.2 | 0.08 | 0.2 |
| UMT094-1351 | UG2HW | 32.4 | 3.0 | 5810 | 0.08 | 0.55 | 0.35 | 0.17 | 6.3 | 0.45 | 0.2 | 0.11 | 1.4 | 0.06 | 0.2 |
| UMT094-1359 | FAZ | 54.7 | 4.7 | 7260 | 0.28 | 0.80 | 0.51 | 0.23 | 6.1 | 0.72 | 0.3 | 0.17 | 2.1 | 0.07 | 0.4 |
| UMT094-1365 | UG2FW | 9.3 | 6.9 | >10000 | 0.14 | 0.76 | 0.42 | 0.22 | 8.4 | 0.82 | 0.6 | 0.17 | 3.0 | 0.06 | 0.5 |
| UMT094-1366 | FAZ | 45.4 | 11.4 | >10000 | 0.30 | 1.49 | 0.82 | 0.42 | 16.5 | 1.51 | 1.2 | 0.30 | 4.4 | 0.12 | 0.8 |
| UMT094-1376 | FAZ | 119.5 | 8.5 | 1020 | 1.32 | 1.64 | 0.90 | 0.48 | 9.2 | 1.59 | 0.8 | 0.34 | 3.7 | 0.14 | 0.5 |
| UMT094-1384 | UG2FW | 65.9 | 7.3 | 170 | 0.77 | 1.12 | 0.67 | 0.28 | 12.8 | 1.08 | 1.0 | 0.24 | 3.3 | 0.12 | 0.4 |
| UMT094-1386 | FAZ | 41.2 | 8.9 | 100 | 0.66 | 1.46 | 0.74 | 0.32 | 23.5 | 1.38 | 1.1 | 0.30 | 3.7 | 0.11 | 0.5 |
| UMT094-1402 | UG2FW | 32.4 | 9.3 | >10000 | 1.05 | 1.57 | 0.90 | 0.37 | 23.9 | 1.58 | 1.2 | 0.31 | 3.4 | 0.12 | 0.4 |
| UMT094-1405 | FAZ | 51.6 | 10.0 | 110 | 0.43 | 1.14 | 0.66 | 0.29 | 8.3 | 1.06 | 0.8 | 0.26 | 4.4 | 0.12 | 1.0 |
| UMT094-1410 * | FW2A | 8.3 | 30.4 | 170 | 0.03 | 3.69 | 2.20 | 0.89 | 9.8 | 3.77 | 3.2 | 0.77 | 13.7 | 0.30 | 1.9 |
| UMT094-1412 | FW2A | 2.0 | 8.9 | 20 | 0.01 | 1.91 | 1.40 | 0.29 | 8.3 | 1.48 | 0.3 | 0.46 | 4.3 | 0.23 | 0.6 |
| UMT094-1421 | FW2A | 1.1 | 8.4 | 30 | 0.03 | 1.38 | 1.14 | 0.17 | 9.3 | 1.11 | 0.5 | 0.35 | 3.4 | 0.24 | 1.1 |
| UMT094-1424 | FW2A | 0.8 | 2.4 | 80 | 0.01 | 1.58 | 1.35 | 0.18 | 12.4 | 0.98 | 0.2 | 0.39 | 1.2 | 0.24 | <0.2 |
| UMT094-1436 | FW2A | 1.2 | 6.4 | 60 | <0.01 | 1.01 | 0.96 | 0.14 | 10.6 | 0.74 | 0.3 | 0.26 | 2.4 | 0.18 | 0.8 |
| UMT094-1454 * | FW2A | 1.3 | 2.0 | 10 | 0.02 | 0.17 | 0.29 | 0.03 | 2.3 | 0.12 | 4.4 | 0.06 | 1.0 | 0.08 | 0.2 |

Table 2. (Cont.)

| | Analyte | Ba | Ce | Cr | Cs | Dy | Er | Eu | Ga | Gd | Hf | Ho | La | Lu | Nb |
|---|---|---|---|---|---|---|---|---|---|---|---|---|---|---|---|
| | Units | ppm | ppm | ppm | ppm | ppm | ppm | ppm | ppm | ppm | ppm | ppm | ppm | ppm | ppm |
| | LDL | 0.5 | 0.5 | 10 | 0.01 | 0.05 | 0.03 | 0.03 | 0.1 | 0.05 | 0.2 | 0.01 | 0.5 | 0.01 | 0.2 |
| Sample | Stratigraphy | | | | | | | | | | | | | | |
| UMT094-1457 | FW2A | 31.6 | 34.9 | 90 | 0.02 | 1.04 | 0.54 | 0.40 | 36.8 | 1.35 | 0.8 | 0.19 | 21.4 | 0.05 | <0.2 |
| UMT094-1461 * | FW2A | 6.3 | 1.6 | 30 | 0.16 | 0.51 | 0.46 | 0.04 | 1.1 | 0.44 | 4.6 | 0.13 | 0.5 | 0.26 | 69.8 |
| UMT094-1463 * | FW2A | 4.8 | 1.3 | 20 | 0.31 | 0.50 | 0.45 | 0.06 | 9.5 | 0.35 | 0.5 | 0.12 | <0.5 | 0.34 | 2.1 |
| UMT094-1466 * | FW2A | 3.3 | 0.7 | 50 | 0.03 | 0.32 | 0.41 | 0.03 | 6.3 | 0.24 | <0.2 | 0.09 | <0.5 | 0.34 | 1.5 |
| UMT094-1479 | FW2A | 56.6 | 3.1 | 30 | 0.02 | 0.95 | 0.78 | 0.10 | 9.4 | 0.54 | <0.2 | 0.22 | 1.4 | 0.14 | 3.4 |
| UMT094-1537 | TVL - DS | 86.5 | 12.2 | 20 | 0.07 | 0.67 | 0.42 | 0.17 | 2.8 | 0.79 | 1.7 | 0.16 | 6.3 | 0.06 | 0.6 |
| UMT094-1573 | TVL - DS | 112.0 | 11.6 | 20 | 0.04 | 0.80 | 0.45 | 0.15 | 4.0 | 0.77 | 0.8 | 0.15 | 5.9 | 0.05 | 0.5 |
| UMT094-1601 | TVL - DS | 66.8 | 13.7 | 10 | 0.08 | 0.80 | 0.56 | 0.21 | 2.8 | 0.84 | 0.9 | 0.18 | 7.1 | 0.07 | 0.3 |
| LUD001 | TVL - Shale | 532.0 | 101 | 170 | 8.36 | 4.41 | 2.75 | 1.31 | 30.9 | 5.06 | 4.0 | 0.95 | 54.2 | 0.39 | 15.4 |
| LUD002 | TVL - Shale | 606.0 | 153 | 190 | 9.13 | 5.77 | 3.29 | 1.81 | 33.7 | 6.92 | 3.9 | 1.22 | 82.1 | 0.42 | 16.7 |
| LUD003 | TVL | 297.0 | 23.7 | 70 | 1.12 | 1.32 | 0.86 | 0.35 | 7.7 | 1.41 | 1.2 | 0.29 | 12.6 | 0.12 | 3.2 |
| LUD004 | TVL - Qtz | 175.0 | 8.5 | 40 | 1.86 | 0.41 | 0.28 | 0.10 | 4.0 | 0.45 | 0.4 | 0.09 | 3.7 | 0.04 | 0.8 |
| LUD005 | TVL - Shale | 495.0 | 59.6 | 10 | 1.69 | 5.01 | 2.99 | 1.22 | 21.2 | 5.28 | 4.2 | 1.08 | 27.1 | 0.42 | 6.4 |
| LUD006 | TVL - DS | 8.8 | 5.4 | 10 | 0.12 | 0.63 | 0.30 | 0.18 | 1.1 | 0.67 | <0.2 | 0.11 | 2.5 | 0.04 | 0.2 |
| LUD007 | TVL | 407.0 | 74.3 | 160 | 6.58 | 3.39 | 1.95 | 1.07 | 18.9 | 4.25 | 2.7 | 0.69 | 39.7 | 0.26 | 10.1 |
| LUD008 | TVL - Qtz | 7.8 | 1.5 | 30 | 0.13 | 0.07 | <0.03 | 0.03 | 0.3 | 0.08 | <0.2 | 0.01 | 0.6 | <0.01 | 0.4 |
| LUD009 | TVL - Shale | 517.0 | 114 | 290 | 12.0 | 5.91 | 3.28 | 1.60 | 29.2 | 6.43 | 3.9 | 1.19 | 59.9 | 0.48 | 16.7 |
| LUD010A | TVL - Qtz | 1.9 | 3.5 | 30 | 0.01 | 0.13 | 0.05 | 0.08 | 0.1 | 0.17 | <0.2 | 0.02 | 1.4 | <0.01 | 2.1 |
| LUD010B | TVL - DS | 4.0 | 1.5 | 10 | 0.03 | 0.21 | 0.12 | 0.09 | 0.5 | 0.24 | <0.2 | 0.05 | 0.7 | 0.01 | <0.2 |
| LUD011 | TVL - DS | 2.2 | 2.8 | 10 | 0.02 | 0.06 | <0.03 | 0.06 | 0.5 | 0.14 | <0.2 | 0.01 | 1.3 | 0.01 | 0.4 |

Notes: Sn, Ta, and W not shown (consistently at or below LDL). Data for these elements are available in Table 3. Stratigraphy Codes: MZ =Main Zone, BCU= Bastard Cyclic Unit, MCU = Merensky Cyclic Unit, FCU = Footwall Cyclic Unit, UG2CU = Upper Group 2 Cyclic Unit, FAZ = Footwall Assimilation Zone, FW2A = Calc-silicate footwall, TVL = Transvaal, DS = Dolostone, Qtz = quartzite.
Average RSD of standards for ME-MS81: 2.608
* Sample was for mineral identification, was non-representative and excluded from geochemical interpretation.

Table 2. (Cont.)

| | Analyte | Nd | Pr | Rb | Sm | Sr | Tb | Th | Tm | U | V | Y | Yb | Zr |
|---|---|---|---|---|---|---|---|---|---|---|---|---|---|---|
| | Units | ppm | ppm | ppm | ppm | ppm | ppm | ppm | ppm | ppm | ppm | ppm | ppm | ppm |
| | LDL | 0.1 | 0.03 | 0.2 | 0.03 | 0.1 | 0.01 | 0.05 | 0.01 | 0.05 | 5 | 0.5 | 0.03 | 2 |
| Sample | Stratigraphy | | | | | | | | | | | | | |
| UMT094-1096 | MZ | 5.7 | 1.55 | 10.9 | 1.12 | 279 | 0.18 | 1.71 | 0.11 | 0.35 | 99 | 6.4 | 0.80 | 31 |
| UMT094-1111 | MZ | 6.2 | 1.63 | 7.8 | 1.41 | 247 | 0.22 | 1.34 | 0.13 | 0.12 | 124 | 7.7 | 0.83 | 19 |
| UMT094-1135 | MZ | 5.8 | 1.51 | 18.1 | 1.23 | 279 | 0.19 | 1.46 | 0.12 | 0.37 | 124 | 7.2 | 0.87 | 38 |
| UMT094-1165 | MZ | 4.4 | 1.11 | 12.2 | 0.85 | 243 | 0.16 | 0.86 | 0.11 | 0.19 | 111 | 5.6 | 0.62 | 21 |
| UMT094-1184 | MZ | 2.5 | 0.67 | 2.4 | 0.54 | 302 | 0.11 | 0.30 | 0.06 | <0.05 | 91 | 3.5 | 0.42 | 9 |
| UMT094-1213 | BCU | 3.6 | 0.92 | 6.9 | 0.78 | 307 | 0.12 | 0.58 | 0.07 | 0.15 | 80 | 4.3 | 0.40 | 15 |
| UMT094-1218 | BCU | 2.7 | 0.72 | 4.4 | 0.63 | 246 | 0.10 | 0.35 | 0.09 | 0.10 | 87 | 4.0 | 0.55 | 10 |
| UMT094-1226 | BCU | 2.5 | 0.72 | 34.7 | 0.48 | 337 | 0.08 | 0.18 | 0.03 | <0.05 | 38 | 2.2 | 0.19 | 6 |
| UMT094-1228 | BCU | 2.4 | 0.58 | 2.1 | 0.62 | 56.4 | 0.12 | 0.50 | 0.09 | 0.19 | 139 | 5.6 | 0.75 | 11 |
| UMT094-1232 | BCU | 2.0 | 0.41 | 2.0 | 0.55 | 53.8 | 0.12 | 0.10 | 0.09 | <0.05 | 129 | 5.2 | 0.63 | 6 |
| UMT094-1233 | MCU | 1.9 | 0.49 | 5.2 | 0.43 | 111 | 0.10 | 0.15 | 0.08 | <0.05 | 113 | 4.1 | 0.45 | 7 |
| UMT094-1238 | MCU | 3.0 | 0.72 | 7.5 | 0.57 | 61.9 | 0.14 | 0.41 | 0.09 | <0.05 | 123 | 5.1 | 0.62 | 10 |
| UMT094-1245 | MCU | 1.3 | 0.33 | 10.9 | 0.38 | 78.4 | 0.08 | 0.13 | 0.08 | <0.05 | 104 | 3.2 | 0.49 | 5 |
| UMT094-1252 | MCU | 2.6 | 0.56 | 6.1 | 0.60 | 44.4 | 0.14 | 0.70 | 0.09 | <0.05 | 121 | 5.1 | 0.64 | 11 |
| UMT094-1254 | MCU | 2.1 | 0.52 | 6.0 | 0.49 | 22.4 | 0.11 | 0.43 | 0.08 | 0.07 | 126 | 4.8 | 0.61 | 8 |
| UMT094-1258 | MCU | 1.8 | 0.44 | 4.4 | 0.42 | 30.5 | 0.09 | 0.24 | 0.08 | <0.05 | 121 | 3.9 | 0.47 | 8 |
| UMT094-1265 | MCU | 3.0 | 0.69 | 9.1 | 0.70 | 33.8 | 0.13 | 0.66 | 0.08 | 0.33 | 118 | 5.1 | 0.65 | 16 |
| UMT094-1273 | MCU | 5.6 | 1.54 | 25.6 | 1.06 | 194 | 0.15 | 1.38 | 0.08 | 0.32 | 82 | 5.3 | 0.45 | 26 |
| UMT094-1277 | MCU | 1.6 | 0.39 | 3.6 | 0.45 | 25.9 | 0.10 | 0.23 | 0.10 | <0.05 | 123 | 5.1 | 0.70 | 8 |
| UMT094-1278 | MCU | 1.4 | 0.33 | 4.3 | 0.39 | 48.2 | 0.08 | 0.10 | 0.08 | <0.05 | 124 | 4.1 | 0.56 | 6 |
| UMT094-1279 | MCU | 1.4 | 0.39 | 8.0 | 0.39 | 28.0 | 0.06 | 0.48 | 0.05 | 0.08 | 91 | 2.4 | 0.32 | 10 |
| UMT094-1282 | MCU | 1.8 | 0.46 | 4.2 | 0.37 | 64.3 | 0.08 | 0.29 | 0.07 | 0.09 | 140 | 3.6 | 0.48 | 12 |

Table 2. (Cont.)

| | Analyte | Nd | Pr | Rb | Sm | Sr | Tb | Th | Tm | U | V | Y | Yb | Zr |
|---|---|---|---|---|---|---|---|---|---|---|---|---|---|---|
| | Units | ppm | ppm | ppm | ppm | ppm | ppm | ppm | ppm | ppm | ppm | ppm | ppm | ppm |
| | LDL | 0.1 | 0.03 | 0.2 | 0.03 | 0.1 | 0.01 | 0.05 | 0.01 | 0.05 | 5 | 0.5 | 0.03 | 2 |
| Sample | Stratigraphy | | | | | | | | | | | | | |
| UMT094-1285 | MCU | 2.4 | 0.63 | 6.8 | 0.65 | 30.6 | 0.11 | 0.80 | 0.10 | 0.22 | 141 | 4.7 | 0.58 | 16 |
| UMT094-1286 | MCU | 7.1 | 1.48 | 3.3 | 1.81 | 42.4 | 0.29 | 0.24 | 0.15 | <0.05 | 146 | 10.1 | 0.95 | 21 |
| UMT094-1288 | MCU | 9.7 | 2.36 | 1.5 | 2.36 | 109.5 | 0.43 | 0.72 | 0.20 | 0.37 | 215 | 12.8 | 1.18 | 48 |
| UMT094-1289 | MCU | 10.7 | 2.48 | 7.9 | 2.35 | 178 | 0.41 | 0.62 | 0.20 | 0.12 | 178 | 12.9 | 1.13 | 43 |
| UMT094-1291A | MCU | 5.6 | 1.18 | 2.5 | 1.35 | 108.5 | 0.26 | 0.19 | 0.12 | <0.05 | 163 | 8.6 | 0.76 | 17 |
| UMT094-1291B | MCU | 1.4 | 0.35 | 1.6 | 0.35 | 67.4 | 0.08 | 0.17 | 0.05 | <0.05 | 63 | 2.7 | 0.27 | 7 |
| UMT094-1292A | FCU | 1.2 | 0.31 | 31.7 | 0.20 | 513 | 0.03 | 0.11 | 0.02 | <0.05 | 19 | 0.9 | 0.09 | 3 |
| UMT094-1292B | FCU | 1.2 | 0.31 | 23.5 | 0.25 | 423 | 0.03 | 0.12 | 0.02 | <0.05 | 29 | 1.0 | 0.10 | 4 |
| UMT094-1294 | FCU | 1.1 | 0.29 | 19.0 | 0.17 | 440 | 0.03 | 0.14 | 0.01 | <0.05 | 22 | 0.9 | 0.11 | 3 |
| UMT094-1296 | FCU | 1.4 | 0.40 | 10.2 | 0.27 | 374 | 0.04 | 0.19 | 0.03 | <0.05 | 47 | 1.6 | 0.22 | 5 |
| UMT094-1300 | FCU | 1.5 | 0.43 | 6.4 | 0.26 | 328 | 0.06 | 0.18 | 0.04 | <0.05 | 58 | 2.0 | 0.22 | 6 |
| UMT094-1308 | FCU | 1.1 | 0.35 | 2.9 | 0.20 | 416 | 0.02 | 0.16 | 0.02 | 0.05 | 25 | 1.1 | 0.18 | 5 |
| UMT094-1311 | FCU | 2.9 | 0.79 | 13.2 | 0.57 | 280 | 0.10 | 0.41 | 0.04 | 0.08 | 142 | 3.1 | 0.35 | 11 |
| UMT094-1319 | FCU | 2.3 | 0.54 | 6.1 | 0.47 | 114 | 0.10 | 0.23 | 0.08 | 0.07 | 131 | 3.8 | 0.43 | 10 |
| UMT094-1325A | FCU | 2.0 | 0.50 | 5.3 | 0.52 | 74.8 | 0.10 | 0.52 | 0.09 | 0.07 | 124 | 4.2 | 0.56 | 11 |
| UMT094-1325B | FCU | 2.1 | 0.48 | 2.7 | 0.36 | 206 | 0.08 | 0.16 | 0.06 | 0.05 | 105 | 3.3 | 0.38 | 8 |
| UMT094-1326A | FCU | 2.4 | 0.60 | 5.2 | 0.56 | 63.3 | 0.13 | 0.55 | 0.09 | 0.12 | 153 | 4.8 | 0.61 | 15 |
| UMT094-1326B | FCU | 1.8 | 0.42 | 0.5 | 0.32 | 49.7 | 0.06 | 0.17 | 0.04 | <0.05 | 112 | 2.2 | 0.33 | 3 |
| UMT094-1327 | FCU | 2.4 | 0.55 | 3.1 | 0.53 | 103.5 | 0.09 | 0.34 | 0.08 | 0.10 | 126 | 3.9 | 0.48 | 11 |
| UMT094-1329 | FCU | 1.2 | 0.29 | 1.2 | 0.29 | 50.6 | 0.06 | 0.11 | 0.05 | <0.05 | 107 | 2.9 | 0.44 | 6 |
| UMT094-1332 | FCU | 2.0 | 0.50 | 2.8 | 0.54 | 93.6 | 0.10 | 0.24 | 0.07 | 0.06 | 105 | 3.7 | 0.46 | 8 |
| UMT094-1334 * | UG2HW | 14.8 | 2.87 | 0.8 | 4.19 | 14.4 | 0.88 | 2.54 | 0.36 | 0.17 | 85 | 26.4 | 2.16 | 417 |

Table 2. (Cont.)

| | Analyte | Nd | Pr | Rb | Sm | Sr | Tb | Th | Tm | U | V | Y | Yb | Zr |
|---|---|---|---|---|---|---|---|---|---|---|---|---|---|---|
| | Units | ppm | ppm | ppm | ppm | ppm | ppm | ppm | ppm | ppm | ppm | ppm | ppm | ppm |
| | LDL | 0.1 | 0.03 | 0.2 | 0.03 | 0.1 | 0.01 | 0.05 | 0.01 | 0.05 | 5 | 0.5 | 0.03 | 2 |
| Sample | Stratigraphy | | | | | | | | | | | | | |
| UMT094-1335 | UG2HW | 8.2 | 1.84 | 3.9 | 2.07 | 74.5 | 0.33 | 0.38 | 0.17 | 0.05 | 96 | 10.8 | 0.93 | 43 |
| UMT094-1336A | UG2HW | 1.0 | 0.24 | 3.6 | 0.33 | 148.5 | 0.07 | 0.05 | 0.04 | <0.05 | 80 | 2.3 | 0.30 | 4 |
| UMT094-1336B | UG2HW | 1.1 | 0.26 | 4.9 | 0.24 | 122.5 | 0.05 | 0.11 | 0.04 | <0.05 | 90 | 2.3 | 0.25 | 5 |
| UMT094-1337 | UG2HW | 2.2 | 0.50 | 1.8 | 0.48 | 59.3 | 0.09 | 0.61 | 0.08 | 0.06 | 198 | 3.6 | 0.54 | 6 |
| UMT094-1339 | UG2HW | 1.7 | 0.38 | 2.7 | 0.50 | 40.2 | 0.10 | 0.27 | 0.08 | 0.07 | 164 | 4.1 | 0.56 | 9 |
| UMT094-1340 | UG2HW | 1.8 | 0.37 | 3.3 | 0.43 | 71.6 | 0.08 | 0.14 | 0.07 | <0.05 | 150 | 3.9 | 0.48 | 7 |
| UMT094-1343 | UG2HW | 1.3 | 0.33 | 2.0 | 0.36 | 78.7 | 0.08 | 0.14 | 0.05 | <0.05 | 160 | 3.2 | 0.47 | 5 |
| UMT094-1351 | UG2HW | 1.6 | 0.37 | 1.7 | 0.41 | 91.9 | 0.09 | 0.24 | 0.05 | <0.05 | 110 | 3.1 | 0.38 | 7 |
| UMT094-1359 | FAZ | 2.8 | 0.62 | 3.8 | 0.67 | 90.8 | 0.11 | 0.25 | 0.07 | 0.07 | 137 | 4.3 | 0.45 | 9 |
| UMT094-1365 | UG2FW | 3.6 | 0.89 | 0.8 | 0.82 | 34.4 | 0.13 | 0.51 | 0.08 | 0.07 | 121 | 3.9 | 0.42 | 23 |
| UMT094-1366 | FAZ | 6.6 | 1.51 | 2.7 | 1.51 | 46.6 | 0.27 | 0.59 | 0.11 | 0.07 | 306 | 7.9 | 0.77 | 37 |
| UMT094-1376 | FAZ | 5.4 | 1.26 | 14.0 | 1.48 | 107.5 | 0.25 | 0.73 | 0.13 | 0.20 | 126 | 8.3 | 0.71 | 22 |
| UMT094-1384 | UG2FW | 4.4 | 0.98 | 4.9 | 0.93 | 121.5 | 0.17 | 0.34 | 0.11 | 0.05 | 89 | 6.3 | 0.62 | 25 |
| UMT094-1386 | FAZ | 5.4 | 1.21 | 2.0 | 1.49 | 59.8 | 0.22 | 0.76 | 0.10 | 0.10 | 126 | 7.5 | 0.78 | 38 |
| UMT094-1402 | UG2FW | 6.4 | 1.37 | 12.7 | 1.43 | 36.7 | 0.26 | 0.31 | 0.13 | <0.05 | 220 | 8.5 | 0.90 | 29 |
| UMT094-1405 | FAZ | 5.0 | 1.23 | 4.4 | 1.19 | 24.8 | 0.19 | 0.68 | 0.09 | 0.09 | 59 | 6.3 | 0.73 | 23 |
| UMT094-1410 * | FW2A | 16.6 | 3.98 | 0.2 | 3.89 | 30.3 | 0.54 | 2.96 | 0.33 | 0.70 | 161 | 20.6 | 1.95 | 94 |
| UMT094-1412 | FW2A | 4.5 | 1.11 | 0.2 | 1.23 | 2.8 | 0.29 | 1.62 | 0.23 | 0.27 | 8 | 13.7 | 1.48 | 9 |
| UMT094-1421 | FW2A | 4.0 | 1.03 | <0.2 | 1.00 | 7.7 | 0.21 | 4.14 | 0.20 | 0.59 | <5 | 10.0 | 1.29 | 9 |
| UMT094-1424 | FW2A | 1.8 | 0.37 | <0.2 | 0.66 | 1.9 | 0.24 | 0.27 | 0.22 | 0.05 | 12 | 12.3 | 1.52 | 5 |
| UMT094-1436 | FW2A | 3.0 | 0.77 | <0.2 | 0.68 | 5.4 | 0.14 | 1.78 | 0.17 | 0.17 | <5 | 7.5 | 1.03 | 9 |
| UMT094-1454 * | FW2A | 0.9 | 0.22 | <0.2 | 0.19 | 4.3 | 0.03 | 0.28 | 0.05 | <0.05 | <5 | 1.8 | 0.49 | 177 |

Table 2. (Cont.)

| | Analyte | Nd | Pr | Rb | Sm | Sr | Tb | Th | Tm | U | V | Y | Yb | Zr |
|---|---|---|---|---|---|---|---|---|---|---|---|---|---|---|
| | Units | ppm | ppm | ppm | ppm | ppm | ppm | ppm | ppm | ppm | ppm | ppm | ppm | ppm |
| | LDL | 0.1 | 0.03 | 0.2 | 0.03 | 0.1 | 0.01 | 0.05 | 0.01 | 0.05 | 5 | 0.5 | 0.03 | 2 |
| Sample | Stratigraphy | | | | | | | | | | | | | |
| UMT094-1457 | FW2A | 11.5 | 3.46 | 0.2 | 1.89 | 126 | 0.19 | <0.05 | 0.06 | <0.05 | 17 | 5.1 | 0.40 | 18 |
| UMT094-1461 * | FW2A | 1.0 | 0.24 | 0.8 | 0.39 | 30.0 | 0.08 | 4.12 | 0.09 | 10.9 | <5 | 3.7 | 0.95 | 147 |
| UMT094-1463 * | FW2A | 1.1 | 0.24 | 2.8 | 0.30 | 4.9 | 0.07 | 0.94 | 0.11 | 3.53 | <5 | 3.8 | 1.31 | 13 |
| UMT094-1466 * | FW2A | 0.5 | 0.12 | 0.2 | 0.25 | 14.5 | 0.05 | 0.16 | 0.13 | 0.38 | 7 | 2.8 | 1.33 | <2 |
| UMT094-1479 | FW2A | 1.6 | 0.44 | <0.2 | 0.43 | 16.4 | 0.12 | 1.31 | 0.12 | 0.55 | 8 | 5.9 | 0.90 | 5 |
| UMT094-1537 | TVL - DS | 5.0 | 1.36 | 0.2 | 0.96 | 64.6 | 0.11 | 0.29 | 0.07 | <0.05 | 8 | 4.2 | 0.40 | 57 |
| UMT094-1573 | TVL - DS | 4.6 | 1.30 | <0.2 | 0.94 | 58.4 | 0.11 | 0.32 | 0.07 | <0.05 | 19 | 4.3 | 0.44 | 16 |
| UMT094-1601 | TVL - DS | 5.6 | 1.54 | 0.2 | 1.11 | 100.5 | 0.13 | 0.72 | 0.08 | 0.06 | 7 | 4.6 | 0.46 | 33 |
| LUD001 | TVL - Shale | 36.1 | 10.60 | 162 | 6.49 | 108 | 0.78 | 24 | 0.39 | 5.56 | 152 | 24.4 | 2.78 | 125 |
| LUD002 | TVL - Shale | 55.8 | 15.95 | 177.5 | 9.79 | 108.5 | 1.03 | 27 | 0.47 | 6.51 | 165 | 31 | 2.98 | 141 |
| LUD003 | TVL | 9.1 | 2.50 | 44.3 | 1.74 | 23.0 | 0.21 | 6.0 | 0.12 | 1.24 | 44 | 8.0 | 0.77 | 37 |
| LUD004 | TVL - Qtz | 3.6 | 0.98 | 41.6 | 0.60 | 9.7 | 0.05 | 2.4 | 0.04 | 0.73 | 27 | 2.5 | 0.35 | 16 |
| LUD005 | TVL - Shale | 28.3 | 7.16 | 56.7 | 6.03 | 17.2 | 0.86 | 3.2 | 0.43 | 7.45 | 358 | 28.2 | 2.95 | 166 |
| LUD006 | TVL - DS | 2.8 | 0.67 | 1.5 | 0.76 | 32.9 | 0.11 | 0.59 | 0.04 | 0.60 | 9 | 3.5 | 0.22 | 5 |
| LUD007 | TVL | 28.9 | 8.13 | 124 | 5.63 | 47.9 | 0.61 | 16.1 | 0.28 | 3.39 | 95 | 19.0 | 1.78 | 101 |
| LUD008 | TVL - Qtz | 0.7 | 0.18 | 0.6 | 0.14 | 10.3 | 0.02 | 0.10 | <0.01 | 0.34 | <5 | <0.5 | 0.04 | <2 |
| LUD009 | TVL - Shale | 42.7 | 12.20 | 188 | 8.07 | 108.5 | 0.99 | 24.5 | 0.47 | 4.74 | 151 | 30.4 | 3.18 | 147 |
| LUD010A | TVL - Qtz | 1.6 | 0.45 | 0.2 | 0.27 | 8.1 | 0.02 | 0.31 | 0.01 | <0.05 | <5 | <0.5 | <0.03 | <2 |
| LUD010B | TVL - DS | 0.8 | 0.20 | 0.2 | 0.26 | 46.4 | 0.06 | 1.18 | 0.01 | 0.23 | <5 | 1.2 | 0.06 | <2 |
| LUD011 | TVL - DS | 1.2 | 0.32 | 0.8 | 0.18 | 13.3 | 0.02 | 0.17 | 0.01 | 0.06 | <5 | <0.5 | 0.05 | <2 |

Notes: Sn, Ta, and W not shown (consistently at or below LDL). Data for these elements are available in Table 3. Stratigraphy Codes: MZ =Main Zone, BCU= Bastard Cyclic Unit, MCU = Merensky Cyclic Unit, FCU = Footwall Cyclic Unit, UG2CU = Upper Group 2 Cyclic Unit, FAZ = Footwall Assimilation Zone, FW2A = Calc-silicate footwall, TVL = Transvaal, DS = Dolostone, Qtz = quartzite.
Average RSD of standards for ME-MS81: 2.608
* Sample was for mineral identification, was non-representative and excluded from geochemical interpretation.

Table 3. Major and Trace Element Data for UMT094 and De Hoop farm sedimentary samples (ALS method ME-MS61L)

| | Analyte | Ag | Al | As | Ba | Be | Bi | Ca | Cd | Ce | Co | Cr | Cs |
|---|---|---|---|---|---|---|---|---|---|---|---|---|---|
| | Units | ppm | % | ppm | ppm | ppm | ppm | % | ppm | ppm | ppm | ppm | ppm |
| | LDL | 0.002 | 0.01 | 0.05 | 1 | 0.02 | 0.005 | 0.01 | 0.005 | 0.01 | 0.005 | 0.3 | 0.01 |
| Sample | Stratigraphy | | | | | | | | | | | | |
| UMT094-1096 | MZ | 0.021 | 8.35 | 0.45 | 126 | 0.37 | 0.009 | 7.29 | 0.032 | 9.17 | 32.4 | 323 | 0.22 |
| UMT094-1111 | MZ | 0.034 | 9.08 | 0.46 | 117 | 0.42 | 0.006 | 6.81 | 0.042 | 11.05 | 39.6 | 447 | 0.26 |
| UMT094-1135 | MZ | 0.028 | 8.37 | 0.53 | 98 | 0.46 | 0.011 | 6.96 | 0.042 | 10.05 | 40.7 | 352 | 0.53 |
| UMT094-1165 | MZ | 0.064 | 8.90 | 1.34 | 111 | 0.38 | 0.083 | 6.94 | 0.117 | 9.16 | 42.8 | 402 | 0.67 |
| UMT094-1184 | MZ | 0.018 | 9.77 | 0.20 | 78 | 0.26 | <0.005 | 8.29 | 0.028 | 3.85 | 29.8 | 241 | 0.05 |
| UMT094-1213 | BCU | 0.029 | 8.92 | 0.50 | 79 | 0.29 | 0.006 | 8.26 | 0.043 | 4.74 | 28.9 | 188.5 | 0.13 |
| UMT094-1218 | BCU | 0.025 | 7.49 | 0.19 | 58 | 0.29 | 0.011 | 6.00 | 0.035 | 4.99 | 44.9 | 747 | 0.30 |
| UMT094-1226 | BCU | 0.014 | 10.2 | 0.34 | 177 | 0.25 | 0.012 | 8.83 | 0.026 | 2.76 | 15.95 | 211 | 0.42 |
| UMT094-1228 | BCU | 0.021 | 2.88 | 0.35 | 29 | 0.20 | 0.014 | 2.82 | 0.061 | 5.03 | 89.4 | 1630 | 0.43 |
| UMT094-1232 | BCU | 0.455 | 2.50 | 0.10 | 24 | 0.11 | 0.201 | 2.88 | 0.125 | 2.93 | 115 | 2060 | 0.84 |
| UMT094-1233 | MCU | 0.603 | 3.46 | 0.20 | 59 | 0.16 | 0.885 | 3.33 | 0.169 | 4.02 | 123 | 1960 | 0.57 |
| UMT094-1238 | MCU | 0.340 | 2.92 | 0.36 | 46 | 0.22 | 0.235 | 3.15 | 0.116 | 6.25 | 101 | 2030 | 0.74 |
| UMT094-1245 | MCU | 0.111 | 3.30 | 0.24 | 66 | 0.13 | 0.039 | 2.98 | 0.069 | 2.72 | 84.7 | 1880 | 0.88 |
| UMT094-1252 | MCU | 0.155 | 2.28 | 0.24 | 39 | 0.16 | 0.092 | 2.48 | 0.087 | 5.01 | 96.7 | 1910 | 0.55 |
| UMT094-1254 | MCU | 0.185 | 1.58 | 0.88 | 30 | 0.14 | 0.199 | 2.07 | 0.126 | 4.12 | 112 | 2370 | 1.05 |
| UMT094-1258 | MCU | 0.261 | 1.75 | 0.43 | 28 | 0.09 | 0.179 | 2.10 | 0.132 | 3.00 | 114 | 2640 | 0.81 |
| UMT094-1265 | MCU | 0.139 | 2.00 | 0.44 | 42 | 0.14 | 0.089 | 2.58 | 0.106 | 4.96 | 96 | 2300 | 1.02 |
| UMT094-1273 | MCU | 0.277 | 6.57 | 2.10 | 189 | 0.29 | 0.455 | 5.38 | 0.113 | 13.15 | 74.9 | 1110 | 1.15 |
| UMT094-1277 | MCU | 0.255 | 1.50 | 0.33 | 29 | 0.12 | 0.214 | 2.11 | 0.165 | 2.82 | 107.5 | 2150 | 1.07 |
| UMT094-1278 | MCU | 0.097 | 2.20 | 0.20 | 36 | 0.12 | 0.089 | 2.41 | 0.119 | 2.62 | 94 | 2100 | 1.46 |
| UMT094-1279 | MCU | 0.259 | 1.67 | 0.54 | 110 | 0.07 | 0.432 | 1.45 | 0.508 | 3.03 | 143 | 3260 | 1.97 |
| UMT094-1282 | MCU | 0.200 | 2.73 | 0.23 | 17 | 0.15 | 0.079 | 2.63 | 0.117 | 3.50 | 101 | 4840 | 1.88 |

Table 3. (Cont.)

| | Analyte | Ag | Al | As | Ba | Be | Bi | Ca | Cd | Ce | Co | Cr | Cs |
|---|---|---|---|---|---|---|---|---|---|---|---|---|---|
| | Units | ppm | % | ppm | ppm | ppm | ppm | % | ppm | ppm | ppm | ppm | ppm |
| | LDL | 0.002 | 0.01 | 0.05 | 1 | 0.02 | 0.005 | 0.01 | 0.005 | 0.01 | 0.005 | 0.3 | 0.01 |
| Sample | Stratigraphy | | | | | | | | | | | | |
| UMT094-1285 | MCU | 0.716 | 1.67 | 0.56 | 34 | 0.12 | 0.738 | 1.92 | 0.244 | 5.44 | 146 | 3840 | 1.04 |
| UMT094-1286 | MCU | 0.479 | 1.79 | 0.32 | 41 | 0.13 | 0.346 | 6.98 | 0.172 | 9.91 | 123.5 | 2450 | 0.72 |
| UMT094-1288 | MCU | 0.492 | 2.90 | 0.62 | 16 | 0.25 | 0.313 | 12.9 | 0.290 | 15.30 | 80.9 | 5440 | 0.36 |
| UMT094-1289 | MCU | 0.512 | 4.15 | 0.67 | 57 | 0.33 | 0.351 | 12.6 | 0.265 | 17.15 | 69.9 | 4140 | 0.66 |
| UMT094-1291A | MCU | 0.525 | 3.58 | 0.51 | 35 | 0.15 | 0.323 | 13.05 | 0.229 | 8.72 | 66.9 | 2580 | 0.55 |
| UMT094-1291B | MCU | 0.456 | 2.65 | 0.31 | 12 | 0.04 | 0.371 | 4.21 | 0.122 | 2.16 | 173.5 | 2090 | 0.75 |
| UMT094-1292A | FCU | 1.330 | 11.80 | 0.28 | 144 | 0.15 | 1.015 | 10.00 | 0.296 | 1.64 | 79.7 | 261 | 0.42 |
| UMT094-1292B | FCU | 0.031 | 10.85 | 0.20 | 114 | 0.13 | 0.015 | 8.84 | 0.037 | 1.49 | 19.35 | 488 | 0.31 |
| UMT094-1294 | FCU | 0.030 | 11.35 | 0.48 | 94 | 0.16 | 0.008 | 9.35 | 0.029 | 1.43 | 11.2 | 271 | 0.31 |
| UMT094-1296 | FCU | 0.318 | 10.40 | 0.30 | 73 | 0.17 | 0.154 | 7.84 | 0.090 | 2.69 | 50.2 | 881 | 0.41 |
| UMT094-1300 | FCU | 0.035 | 9.99 | 0.21 | 61 | 0.17 | 0.020 | 7.61 | 0.039 | 2.68 | 35.2 | 1155 | 0.27 |
| UMT094-1308 | FCU | 0.030 | 10.35 | 0.23 | 55 | 0.15 | 0.019 | 9.38 | 0.026 | 1.46 | 16.4 | 498 | 0.03 |
| UMT094-1311 | FCU | 0.691 | 8.17 | 0.56 | 86 | 0.27 | 0.552 | 6.07 | 0.198 | 6.97 | 83.6 | 4140 | 0.53 |
| UMT094-1319 | FCU | 0.209 | 4.44 | 0.39 | 44 | 0.15 | 0.218 | 4.01 | 0.115 | 4.42 | 89 | 2750 | 0.60 |
| UMT094-1325A | FCU | 0.337 | 3.00 | 0.38 | 50 | 0.13 | 0.413 | 3.35 | 0.178 | 3.87 | 105 | 2070 | 0.65 |
| UMT094-1325B | FCU | 0.030 | 6.39 | 0.18 | 56 | 0.19 | 0.040 | 5.34 | 0.051 | 3.85 | 63.2 | 1955 | 0.16 |
| UMT094-1326A | FCU | 0.129 | 3.03 | 0.40 | 32 | 0.15 | 0.227 | 3.42 | 0.103 | 4.86 | 102.5 | 3040 | 1.04 |
| UMT094-1326B | FCU | 0.504 | 2.50 | 0.15 | 13 | 0.04 | 0.402 | 2.78 | 0.165 | 0.97 | 117 | 2880 | 0.15 |
| UMT094-1327 | FCU | 0.133 | 3.81 | 0.15 | 48 | 0.18 | 0.074 | 3.63 | 0.079 | 4.64 | 87.9 | 3050 | 0.20 |
| UMT094-1329 | FCU | 0.190 | 2.46 | 0.18 | 21 | 0.07 | 0.225 | 3.03 | 0.116 | 2.09 | 103.5 | 2440 | 0.12 |
| UMT094-1332 | FCU | 0.257 | 3.31 | 0.47 | 47 | 0.15 | 0.296 | 3.47 | 0.116 | 3.76 | 96.6 | 1930 | 0.19 |
| UMT094-1334 * | UG2HW | 0.459 | 3.87 | 0.73 | 15 | 0.25 | 0.303 | 9.24 | 0.214 | 18.65 | 72.4 | 27.5 | 0.04 |

Table 3. (Cont.)

| | Analyte | Ag | Al | As | Ba | Be | Bi | Ca | Cd | Ce | Co | Cr | Cs |
|---|---|---|---|---|---|---|---|---|---|---|---|---|---|
| | Units | ppm | % | ppm | ppm | ppm | ppm | % | ppm | ppm | ppm | ppm | ppm |
| | LDL | 0.002 | 0.01 | 0.05 | 1 | 0.02 | 0.005 | 0.01 | 0.005 | 0.01 | 0.005 | 0.3 | 0.01 |
| Sample | Stratigraphy | | | | | | | | | | | | |
| UMT094-1335 | UG2HW | 0.598 | 3.55 | 0.59 | 48 | 0.11 | 0.582 | 11.45 | 0.287 | 11.85 | 90.5 | 1440 | 0.53 |
| UMT094-1336A | UG2HW | 0.271 | 5.18 | 0.36 | 31 | 0.09 | 0.213 | 5.05 | 0.130 | 1.84 | 114 | 2660 | 0.37 |
| UMT094-1336B | UG2HW | 1.325 | 4.07 | 0.26 | 31 | 0.11 | 0.625 | 3.73 | 0.181 | 1.95 | 126 | 2360 | 0.71 |
| UMT094-1337 | UG2HW | 0.776 | 2.65 | 0.27 | 24 | 0.09 | 0.730 | 2.61 | 0.287 | 2.10 | 145 | 8770 | 0.25 |
| UMT094-1339 | UG2HW | 0.171 | 1.92 | 0.19 | 24 | 0.10 | 0.166 | 2.55 | 0.132 | 2.76 | 105 | 6010 | 0.37 |
| UMT094-1340 | UG2HW | 0.149 | 2.89 | 0.14 | 30 | 0.11 | 0.144 | 3.46 | 0.123 | 2.64 | 89.4 | 5140 | 0.46 |
| UMT094-1343 | UG2HW | 0.083 | 3.14 | 0.14 | 27 | 0.09 | 0.058 | 3.15 | 0.071 | 2.34 | 91.1 | 6320 | 0.27 |
| UMT094-1351 | UG2HW | 0.115 | 3.10 | 0.33 | 33 | 0.11 | 0.057 | 3.64 | 0.084 | 2.98 | 111.5 | 3970 | 0.08 |
| UMT094-1359 | FAZ | 0.287 | 2.57 | 0.37 | 50 | 0.11 | 0.353 | 4.63 | 0.156 | 4.74 | 122.5 | 5300 | 0.27 |
| UMT094-1365 | UG2FW | 0.180 | 1.59 | 0.28 | 9 | 0.13 | 0.214 | 5.18 | 0.135 | 6.68 | 97.4 | 6940 | 0.14 |
| UMT094-1366 | FAZ | 0.437 | 3.67 | 1.66 | 47 | 0.13 | 0.889 | 8.95 | 0.386 | 11.25 | 94.3 | >10000 | 0.30 |
| UMT094-1376 | FAZ | 1.410 | 5.10 | 1.20 | 112 | 0.16 | 0.715 | 12.05 | 0.313 | 8.30 | 70.1 | 628 | 1.13 |
| UMT094-1384 | UG2FW | 0.247 | 4.01 | 0.73 | 54 | 0.14 | 0.495 | 5.04 | 0.226 | 6.60 | 71.6 | 111.5 | 0.45 |
| UMT094-1386 | FAZ | 0.555 | 4.85 | 1.60 | 39 | 0.14 | 0.445 | 6.29 | 0.200 | 8.72 | 95.9 | 47.8 | 0.58 |
| UMT094-1402 | UG2FW | 0.172 | 2.44 | 0.67 | 29 | 0.11 | 0.240 | 6.67 | 0.090 | 9.51 | 79.7 | 7900 | 1.11 |
| UMT094-1405 | FAZ | 0.228 | 3.41 | 0.70 | 48 | 0.13 | 0.590 | 4.46 | 0.149 | 10.10 | 46.3 | 78.8 | 0.36 |
| UMT094-1410 * | FW2A | 0.720 | 3.35 | 2.46 | 9 | 0.31 | 0.610 | 18.75 | 0.613 | 32.20 | 85.6 | 126 | 0.04 |
| UMT094-1412 | FW2A | 0.258 | 3.26 | 0.24 | 1 | 0.60 | 0.397 | 11.85 | 0.315 | 7.99 | 80.3 | 16.0 | 0.01 |
| UMT094-1421 | FW2A | 0.038 | 3.23 | 9.98 | 1 | 1.26 | 0.491 | 10.70 | 0.266 | 8.36 | 32.1 | 25.0 | 0.02 |
| UMT094-1424 | FW2A | 2.620 | 6.67 | 1.05 | <1 | 0.33 | 1.955 | 6.07 | 0.764 | 2.21 | 27.4 | 60.3 | <0.01 |
| UMT094-1436 | FW2A | 0.122 | 3.74 | 1.14 | 1 | 0.17 | 0.119 | 9.12 | 0.346 | 5.66 | 24.2 | 39.0 | 0.01 |
| UMT094-1454 * | FW2A | 0.175 | 0.62 | 3.57 | 1 | 0.02 | 0.508 | 1.73 | 0.078 | 2.05 | 109.5 | 12.3 | 0.01 |

Table 3. (Cont.)

| | Analyte | Ag | Al | As | Ba | Be | Bi | Ca | Cd | Ce | Co | Cr | Cs |
|---|---|---|---|---|---|---|---|---|---|---|---|---|---|
| | Units | ppm | % | ppm | ppm | ppm | ppm | % | ppm | ppm | ppm | ppm | ppm |
| | LDL | 0.002 | 0.01 | 0.05 | 1 | 0.02 | 0.005 | 0.01 | 0.005 | 0.01 | 0.005 | 0.3 | 0.01 |
| Sample | Stratigraphy | | | | | | | | | | | | |
| UMT094-1457 | FW2A | 0.053 | 8.00 | 0.57 | 31 | 0.07 | 0.174 | 13.40 | 0.031 | 33.40 | 42.5 | 50.2 | 0.01 |
| UMT094-1461 * | FW2A | 0.100 | 0.34 | 1.83 | 5 | 0.02 | 2.450 | 5.42 | <0.005 | 0.88 | 156.0 | 19.8 | 0.14 |
| UMT094-1463 * | FW2A | 0.033 | 0.66 | 1.15 | 4 | 0.03 | 0.039 | 0.58 | 0.037 | 1.34 | 32.1 | 14.7 | 0.30 |
| UMT094-1466 * | FW2A | 0.017 | 2.60 | 18.75 | 1 | 0.03 | 0.927 | 1.77 | 0.255 | 0.66 | 88.7 | 35.6 | 0.02 |
| UMT094-1479 | FW2A | 0.902 | 3.30 | 6.30 | 54 | 0.28 | 0.432 | 16.95 | 0.715 | 2.76 | 30.4 | 19.4 | 0.01 |
| UMT094-1494 | TVL - DS | 0.147 | 0.96 | 2.26 | 610 | 0.06 | 0.152 | 20.70 | 2.80 | 11.2 | 6.36 | 9.6 | 0.03 |
| UMT094-1537 | TVL - DS | 0.094 | 0.46 | 1.47 | 81 | 0.04 | 0.015 | 23.30 | 0.395 | 11.9 | 2.05 | 22.3 | 0.06 |
| UMT094-1573 | TVL - DS | 0.063 | 0.69 | 2.42 | 111 | 0.09 | 0.017 | 22.00 | 0.419 | 11.95 | 6.67 | 11.3 | 0.03 |
| UMT094-1601 | TVL - DS | 0.088 | 0.37 | 3.33 | 68 | 0.06 | 0.018 | 24.30 | 0.214 | 13.75 | 1.76 | 6.3 | 0.09 |
| LUD001 | TVL - Shale | 0.141 | 12.70 | 23.8 | 550 | 3.89 | 0.447 | 0.12 | <0.005 | 54.20 | 7.31 | 149.5 | 8.57 |
| LUD002 | TVL - Shale | 0.152 | 12.25 | 22.1 | 550 | 4.01 | 0.948 | 0.11 | <0.005 | 72.70 | 8.13 | 154.5 | 8.32 |
| LUD003 | TVL | 0.007 | 2.79 | 3.93 | 290 | 1.20 | 0.035 | 10.80 | 0.005 | 21.90 | 7.25 | 47.9 | 1.25 |
| LUD004 | TVL - Qtz | 0.009 | 1.31 | 2.47 | 157 | 0.44 | 0.073 | 3.44 | 0.006 | 7.54 | 1.15 | 27.4 | 1.62 |
| LUD005 | TVL - Shale | 1.875 | 6.73 | 4.42 | 500 | 1.26 | 4.010 | 1.87 | 0.006 | 57.50 | 52.80 | 7.2 | 1.58 |
| LUD006 | TVL - DS | <0.002 | 0.39 | 0.95 | 8 | 0.33 | 0.010 | 19.85 | <0.005 | 5.21 | 4.46 | 6.8 | 0.12 |
| LUD007 | TVL | 0.002 | 6.50 | 3.40 | 388 | 2.15 | 0.311 | 5.39 | <0.005 | 66.20 | 23.10 | 113 | 5.90 |
| LUD008 | TVL - Qtz | 0.013 | 0.06 | 3.98 | 7 | 0.05 | 0.028 | 3.78 | 0.017 | 0.56 | 4.57 | 31.9 | 0.12 |
| LUD009 | TVL - Shale | <0.002 | 9.73 | 1.62 | 480 | 4.35 | 0.571 | 0.14 | <0.005 | 71.90 | 35.10 | 238 | 10.3 |
| LUD010A | TVL - Qtz | 0.014 | 0.03 | 0.79 | 1 | 0.04 | 0.190 | 2.63 | <0.005 | 0.17 | 0.568 | 24.9 | 0.01 |
| LUD010B | TVL - DS | 0.005 | 0.05 | 1.45 | 4 | 0.12 | 0.111 | 20.10 | 0.011 | 1.40 | 1.310 | 3.6 | 0.03 |
| LUD011 | TVL - DS | 0.009 | 0.05 | 1.43 | 2 | 0.07 | 0.292 | 15.40 | 0.006 | 1.07 | 0.905 | 5.8 | 0.05 |

Notes: Re not shown (consistently at or below LDL). Stratigraphy Codes: MZ = Main Zone, BCU = Bastard Cyclic Unit, MCU = Merensky Cyclic Unit, FCU = Footwall Cyclic Unit, UG2CU = Upper Group 2 Cyclic Unit, FAZ = Footwall Assimilation Zone, FW2A = Calc-silicate footwall, TVL = Transvaal, DS = Dolostone, Qtz = quartzite. Average RSD of standards for ME-MS61L: 4.372
* Sample was for mineral identification, was non-representative and excluded from geochemical interpretation.

Table 3. (Cont.)

| | Analyte | Cu | Fe | Ga | Ge | Hf | In | K | La | Li | Mg | Mn | Mo |
|---|---|---|---|---|---|---|---|---|---|---|---|---|---|
| | Units | ppm | % | ppm | ppm | ppm | ppm | % | ppm | ppm | % | ppm | ppm |
| | LDL | 0.02 | 0.002 | 0.05 | 0.05 | 0.004 | 0.005 | 0.01 | 0.005 | 0.2 | 0.01 | 0.2 | 0.02 |
| Sample | Stratigraphy | | | | | | | | | | | | |
| UMT094-1096 | MZ | 26.5 | 3.79 | 16.35 | <0.05 | 0.705 | 0.022 | 0.28 | 4.690 | 8.5 | 3.24 | 719 | 0.45 |
| UMT094-1111 | MZ | 32.9 | 4.55 | 15.15 | 0.08 | 0.661 | 0.021 | 0.27 | 5.610 | 8.2 | 4.94 | 841 | 0.31 |
| UMT094-1135 | MZ | 30.7 | 4.25 | 15.15 | 0.05 | 0.728 | 0.018 | 0.31 | 4.990 | 11.6 | 3.79 | 839 | 0.44 |
| UMT094-1165 | MZ | 22.2 | 4.77 | 14.80 | 0.05 | 0.574 | 0.028 | 0.27 | 4.590 | 14.3 | 4.71 | 1020 | 0.48 |
| UMT094-1184 | MZ | 12.0 | 3.22 | 16.85 | 0.06 | 0.233 | 0.017 | 0.11 | 1.970 | 4.6 | 2.99 | 631 | 0.33 |
| UMT094-1213 | BCU | 26.7 | 3.37 | 16.55 | <0.05 | 0.335 | 0.009 | 0.12 | 2.250 | 3.9 | 2.34 | 638 | 0.33 |
| UMT094-1218 | BCU | 30.0 | 4.38 | 12.90 | <0.05 | 0.198 | 0.018 | 0.14 | 2.690 | 6.3 | 6.23 | 883 | 0.32 |
| UMT094-1226 | BCU | 28.1 | 1.69 | 19.10 | <0.05 | 0.158 | 0.011 | 0.43 | 1.305 | 9.1 | 1.79 | 334 | 0.43 |
| UMT094-1228 | BCU | 39.9 | 8.21 | 6.85 | 0.08 | 0.378 | 0.027 | 0.07 | 2.550 | 7.9 | 14.55 | 1650 | 0.39 |
| UMT094-1232 | BCU | 1010 | 8.55 | 6.07 | 0.10 | 0.202 | 0.028 | 0.05 | 1.360 | 9.1 | 15.05 | 1715 | 0.23 |
| UMT094-1233 | MCU | 1350 | 7.61 | 6.71 | 0.12 | 0.226 | 0.033 | 0.12 | 2.050 | 7.9 | 13.25 | 1460 | 0.28 |
| UMT094-1238 | MCU | 812 | 7.58 | 6.58 | 0.10 | 0.327 | 0.030 | 0.17 | 2.980 | 5.9 | 13.85 | 1480 | 0.35 |
| UMT094-1245 | MCU | 351 | 7.14 | 6.41 | 0.07 | 0.156 | 0.020 | 0.20 | 1.425 | 6.1 | 13.75 | 1575 | 0.35 |
| UMT094-1252 | MCU | 456 | 7.85 | 5.56 | 0.08 | 0.335 | 0.026 | 0.14 | 2.470 | 8.2 | 14.60 | 1560 | 0.25 |
| UMT094-1254 | MCU | 675 | 8.52 | 5.12 | 0.10 | 0.330 | 0.028 | 0.11 | 2.060 | 5.8 | 15.80 | 1695 | 0.47 |
| UMT094-1258 | MCU | 928 | 8.14 | 4.86 | 0.10 | 0.246 | 0.025 | 0.08 | 1.480 | 6.9 | 15.55 | 1605 | 0.15 |
| UMT094-1265 | MCU | 392 | 7.47 | 5.02 | 0.08 | 0.363 | 0.028 | 0.15 | 2.260 | 6.1 | 14.70 | 1540 | 0.20 |
| UMT094-1273 | MCU | 931 | 5.14 | 10.20 | 0.07 | 0.357 | 0.025 | 0.45 | 6.750 | 10.2 | 8.40 | 1050 | 0.55 |
| UMT094-1277 | MCU | 565 | 9.05 | 4.87 | 0.11 | 0.255 | 0.031 | 0.08 | 1.220 | 5.7 | 15.55 | 1705 | 0.24 |
| UMT094-1278 | MCU | 242 | 8.38 | 5.11 | 0.08 | 0.187 | 0.023 | 0.08 | 1.240 | 6.6 | 15.15 | 1680 | 0.20 |
| UMT094-1279 | MCU | 369 | 9.43 | 4.09 | 0.09 | 0.259 | 0.016 | 0.19 | 1.495 | 4.0 | 18.10 | 1530 | 0.29 |
| UMT094-1282 | MCU | 592 | 8.31 | 6.40 | 0.08 | 0.186 | 0.029 | 0.05 | 1.815 | 16.2 | 14.45 | 1615 | 0.27 |

Table 3. (Cont.)

| | Analyte | Cu | Fe | Ga | Ge | Hf | In | K | La | Li | Mg | Mn | Mo |
|---|---|---|---|---|---|---|---|---|---|---|---|---|---|
| | Units | ppm | % | ppm | ppm | ppm | ppm | % | ppm | ppm | % | ppm | ppm |
| | LDL | 0.02 | 0.002 | 0.05 | 0.05 | 0.004 | 0.005 | 0.01 | 0.005 | 0.2 | 0.01 | 0.2 | 0.02 |
| Sample | Stratigraphy | | | | | | | | | | | | |
| UMT094-1285 | MCU | 1880 | 9.52 | 5.39 | 0.12 | 0.445 | 0.037 | 0.10 | 2.870 | 6.2 | 15.10 | 1630 | 0.42 |
| UMT094-1286 | MCU | 1140 | 7.92 | 5.18 | 0.10 | 0.799 | 0.038 | 0.08 | 3.380 | 7.3 | 13.40 | 1345 | 0.24 |
| UMT094-1288 | MCU | 1220 | 5.68 | 8.26 | 0.09 | 1.33 | 0.033 | 0.03 | 6.260 | 10.5 | 8.73 | 1225 | 0.27 |
| UMT094-1289 | MCU | 1150 | 5.22 | 8.89 | 0.10 | 1.505 | 0.038 | 0.14 | 6.910 | 14.2 | 8.11 | 1080 | 0.30 |
| UMT094-1291A | MCU | 1430 | 4.86 | 7.38 | 0.09 | 0.720 | 0.038 | 0.07 | 3.530 | 10.1 | 8.57 | 987 | 0.23 |
| UMT094-1291B | MCU | 1360 | 9.67 | 4.23 | 0.12 | 0.276 | 0.020 | 0.03 | 0.880 | 2.7 | 17.05 | 1110 | 0.21 |
| UMT094-1292A | FCU | 2680 | 2.56 | 17.55 | 0.12 | 0.095 | 0.022 | 0.41 | 0.774 | 6.1 | 0.70 | 232 | 0.34 |
| UMT094-1292B | FCU | 40.9 | 1.77 | 17.75 | <0.05 | 0.102 | <0.005 | 0.25 | 0.717 | 4.1 | 2.37 | 370 | 0.31 |
| UMT094-1294 | FCU | 26.6 | 1.18 | 18.70 | <0.05 | 0.092 | 0.005 | 0.23 | 0.677 | 3.5 | 1.17 | 208 | 0.35 |
| UMT094-1296 | FCU | 710 | 3.31 | 15.70 | 0.05 | 0.147 | 0.014 | 0.17 | 1.425 | 3.7 | 4.59 | 618 | 0.34 |
| UMT094-1300 | FCU | 79.8 | 3.16 | 14.85 | 0.07 | 0.156 | 0.010 | 0.13 | 1.380 | 3.7 | 5.16 | 645 | 0.31 |
| UMT094-1308 | FCU | 45.1 | 1.60 | 18.70 | 0.12 | 0.107 | 0.008 | 0.02 | 0.686 | 3.5 | 1.75 | 312 | 0.28 |
| UMT094-1311 | FCU | 1150 | 5.37 | 13.40 | 0.09 | 0.314 | 0.028 | 0.23 | 3.720 | 4.7 | 7.01 | 921 | 0.40 |
| UMT094-1319 | FCU | 516 | 7.36 | 8.15 | 0.06 | 0.293 | 0.022 | 0.12 | 2.240 | 4.6 | 12.00 | 1485 | 0.24 |
| UMT094-1325A | FCU | 706 | 8.60 | 6.32 | 0.08 | 0.342 | 0.031 | 0.09 | 1.850 | 3.4 | 13.15 | 1615 | 0.25 |
| UMT094-1325B | FCU | 88.1 | 5.39 | 10.50 | 0.05 | 0.175 | 0.017 | 0.11 | 2.000 | 2.9 | 8.42 | 1130 | 0.29 |
| UMT094-1326A | FCU | 281 | 7.92 | 6.98 | 0.07 | 0.405 | 0.030 | 0.07 | 2.240 | 7.9 | 12.65 | 1525 | 0.30 |
| UMT094-1326B | FCU | 1180 | 8.67 | 5.32 | 0.08 | 0.100 | 0.023 | 0.02 | 0.450 | 2.6 | 14.60 | 1650 | 0.29 |
| UMT094-1327 | FCU | 238 | 7.60 | 7.39 | 0.06 | 0.289 | 0.026 | 0.09 | 2.420 | 3.7 | 12.65 | 1540 | 0.22 |
| UMT094-1329 | FCU | 439 | 8.60 | 5.51 | 0.08 | 0.200 | 0.029 | 0.04 | 0.970 | 3.4 | 15.35 | 1705 | 0.28 |
| UMT094-1332 | FCU | 572 | 7.50 | 6.38 | 0.07 | 0.234 | 0.020 | 0.09 | 1.920 | 4.1 | 12.65 | 1480 | 0.23 |
| UMT094-1334 * | UG2HW | 546 | 6.79 | 7.28 | 0.27 | 14.85 | 0.106 | 0.01 | 6.140 | 1.3 | 13.40 | 1110 | 0.32 |

Table 3. (Cont.)

| | Analyte | Cu | Fe | Ga | Ge | Hf | In | K | La | Li | Mg | Mn | Mo |
|---|---|---|---|---|---|---|---|---|---|---|---|---|---|
| | Units | ppm | % | ppm | ppm | ppm | ppm | % | ppm | ppm | % | ppm | ppm |
| | LDL | 0.02 | 0.002 | 0.05 | 0.05 | 0.004 | 0.005 | 0.01 | 0.005 | 0.2 | 0.01 | 0.2 | 0.02 |
| Sample | Stratigraphy | | | | | | | | | | | | |
| UMT094-1335 | UG2HW | 1680 | 6.30 | 8.07 | 0.11 | 1.735 | 0.052 | 0.07 | 4.190 | 5.9 | 9.84 | 986 | 0.27 |
| UMT094-1336A | UG2HW | 753 | 7.34 | 7.17 | 0.08 | 0.131 | 0.021 | 0.09 | 0.867 | 4.6 | 12.50 | 1215 | 0.30 |
| UMT094-1336B | UG2HW | 957 | 8.28 | 7.90 | 0.09 | 0.147 | 0.024 | 0.12 | 1.050 | 5.7 | 13.35 | 1360 | 0.20 |
| UMT094-1337 | UG2HW | 1680 | 9.81 | 7.56 | 0.10 | 0.194 | 0.037 | 0.05 | 1.060 | 2.8 | 13.75 | 1650 | 0.25 |
| UMT094-1339 | UG2HW | 277 | 8.93 | 6.15 | 0.07 | 0.256 | 0.030 | 0.06 | 1.295 | 4.1 | 14.75 | 1720 | 0.15 |
| UMT094-1340 | UG2HW | 354 | 7.84 | 6.82 | 0.07 | 0.211 | 0.024 | 0.08 | 1.215 | 4.7 | 13.20 | 1525 | 0.19 |
| UMT094-1343 | UG2HW | 143.5 | 8.01 | 7.35 | 0.08 | 0.179 | 0.025 | 0.06 | 1.135 | 3.6 | 13.75 | 1590 | 0.18 |
| UMT094-1351 | UG2HW | 241 | 8.69 | 6.19 | 0.09 | 0.224 | 0.019 | 0.06 | 1.390 | 5.5 | 15.00 | 1580 | 0.25 |
| UMT094-1359 | FAZ | 695 | 10.25 | 5.70 | 0.09 | 0.272 | 0.031 | 0.11 | 2.140 | 7.5 | 16.25 | 1640 | 0.18 |
| UMT094-1365 | UG2FW | 542 | 8.14 | 4.08 | 0.08 | 0.608 | 0.025 | 0.01 | 2.890 | 4.0 | 16.50 | 1225 | 0.19 |
| UMT094-1366 | FAZ | 834 | 7.80 | 14.55 | 0.08 | 1.20 | 0.055 | 0.05 | 4.450 | 6.6 | 10.30 | 1575 | 0.37 |
| UMT094-1376 | FAZ | 908 | 4.22 | 9.25 | 0.07 | 0.880 | 0.035 | 0.22 | 3.530 | 17.0 | 9.14 | 1150 | 0.32 |
| UMT094-1384 | UG2FW | 496 | 6.73 | 11.00 | 0.06 | 0.916 | 0.039 | 0.10 | 2.890 | 8.4 | 14.75 | 1040 | 0.12 |
| UMT094-1386 | FAZ | 772 | 7.13 | 12.95 | 0.09 | 1.14 | 0.052 | 0.04 | 3.690 | 4.8 | 13.35 | 932 | 0.23 |
| UMT094-1402 | UG2FW | 514 | 6.84 | 9.91 | 0.09 | 1.21 | 0.036 | 0.14 | 3.420 | 3.4 | 11.75 | 876 | 0.21 |
| UMT094-1405 | FAZ | 1030 | 5.09 | 8.54 | 0.06 | 0.850 | 0.065 | 0.05 | 4.500 | 2.2 | 19.50 | 447 | 0.11 |
| UMT094-1410 * | FW2A | 2740 | 5.51 | 10.20 | 0.09 | 3.39 | 0.105 | <0.01 | 14.20 | 1.2 | 7.07 | 1085 | 0.42 |
| UMT094-1412 | FW2A | 205 | 5.06 | 8.37 | 0.07 | 0.228 | 0.048 | <0.01 | 3.630 | 0.9 | 13.70 | 1705 | 0.12 |
| UMT094-1421 | FW2A | 89.1 | 2.22 | 9.72 | <0.05 | 0.478 | 0.072 | <0.01 | 3.450 | 11.3 | 17.00 | 582 | 0.14 |
| UMT094-1424 | FW2A | 2230 | 2.65 | 11.45 | 0.05 | 0.127 | 0.040 | <0.01 | 1.080 | 0.4 | 14.25 | 438 | 0.10 |
| UMT094-1436 | FW2A | 163 | 2.83 | 10.00 | <0.05 | 0.367 | 0.023 | <0.01 | 2.110 | 1.2 | 17.00 | 1410 | 0.11 |
| UMT094-1454 * | FW2A | 390 | 5.71 | 2.34 | 0.18 | 3.11 | 0.044 | <0.01 | 1.075 | 0.3 | >25.0 | 1660 | 0.18 |

Table 3. (Cont.)

| | Analyte | Cu | Fe | Ga | Ge | Hf | In | K | La | Li | Mg | Mn | Mo |
|---|---|---|---|---|---|---|---|---|---|---|---|---|---|
| | Units | ppm | % | ppm | ppm | ppm | ppm | % | ppm | ppm | % | ppm | ppm |
| | LDL | 0.02 | 0.002 | 0.05 | 0.05 | 0.004 | 0.005 | 0.01 | 0.005 | 0.2 | 0.01 | 0.2 | 0.02 |
| Sample | Stratigraphy | | | | | | | | | | | | |
| UMT094-1457 | FW2A | 40.3 | 3.42 | 19.05 | 0.05 | 0.748 | 0.014 | <0.01 | 20.30 | 6.7 | 6.76 | 1690 | 0.37 |
| UMT094-1461 * | FW2A | 30.2 | 5.87 | 0.99 | 0.24 | 3.80 | 0.114 | <0.01 | 0.210 | 3.1 | 24.10 | 1660 | 0.34 |
| UMT094-1463 * | FW2A | 27.2 | 24.1 | 9.26 | 0.22 | 0.388 | 0.190 | 0.01 | 0.278 | 0.2 | 17.05 | 1045 | 0.20 |
| UMT094-1466 * | FW2A | 9.21 | 8.35 | 6.25 | 0.10 | 0.085 | 0.168 | <0.01 | 0.207 | 0.3 | 20.80 | 920 | 0.11 |
| UMT094-1479 | FW2A | 547 | 4.88 | 9.21 | <0.05 | 0.153 | 0.105 | <0.01 | 1.365 | 0.6 | 11.95 | 2740 | 0.10 |
| UMT094-1494 | TVL - DS | 234 | 3.61 | 2.99 | 0.06 | 0.696 | 0.226 | <0.01 | 5.500 | 6.9 | 14.05 | 1405 | 0.07 |
| UMT094-1537 | TVL - DS | 21.4 | 0.95 | 1.37 | <0.05 | 0.571 | 0.041 | <0.01 | 6.070 | 5.5 | 12.00 | 743 | 0.20 |
| UMT094-1573 | TVL - DS | 62.5 | 1.59 | 2.17 | <0.05 | 0.734 | 0.055 | <0.01 | 6.060 | 2.8 | 11.85 | 784 | 0.13 |
| UMT094-1601 | TVL - DS | 33.3 | 0.71 | 0.95 | 0.05 | 0.481 | 0.022 | <0.01 | 7.220 | 3.8 | 12.05 | 573 | 0.15 |
| LUD001 | TVL - Shale | 17.8 | 5.97 | 35.10 | 0.16 | 3.66 | 0.070 | 2.60 | 21.80 | 58.8 | 0.60 | 248 | 0.38 |
| LUD002 | TVL - Shale | 12.9 | 5.65 | 34.40 | 0.15 | 3.95 | 0.075 | 2.55 | 33.20 | 55.4 | 0.59 | 243 | 1.29 |
| LUD003 | TVL | 3.87 | 2.41 | 8.20 | 0.09 | 1.060 | 0.023 | 0.80 | 11.40 | 33.9 | 8.13 | 586 | 0.18 |
| LUD004 | TVL - Qtz | 7.54 | 1.32 | 3.97 | <0.05 | 0.381 | 0.011 | 0.61 | 3.200 | 3.8 | 1.87 | 297 | 0.33 |
| LUD005 | TVL - Shale | 7270 | 5.50 | 22.40 | 0.20 | 4.03 | 0.066 | 0.98 | 24.30 | 84.7 | 4.05 | 321 | 0.58 |
| LUD006 | TVL - DS | 1.30 | 0.63 | 1.09 | <0.05 | 0.132 | 0.013 | 0.03 | 2.480 | 10.6 | 12.75 | 1405 | 0.09 |
| LUD007 | TVL | 1.53 | 5.44 | 18.40 | 0.14 | 2.58 | 0.047 | 1.77 | 32.30 | 73.1 | 4.72 | 1700 | 0.38 |
| LUD008 | TVL - Qtz | 10.5 | 0.66 | 0.30 | <0.05 | 0.013 | <0.005 | 0.02 | 0.247 | 1.2 | 1.99 | 308 | 0.69 |
| LUD009 | TVL - Shale | 1.63 | 7.63 | 28.30 | 0.15 | 3.780 | 0.080 | 2.42 | 34.60 | 81.3 | 1.99 | 532 | 0.44 |
| LUD010A | TVL - Qtz | 5.60 | 0.34 | 0.12 | <0.05 | 0.010 | <0.005 | <0.01 | 0.070 | 1.3 | 1.49 | 506 | 0.60 |
| LUD010B | TVL - DS | 2.41 | 0.71 | 0.30 | <0.05 | 0.098 | <0.005 | <0.01 | 0.715 | 3.8 | 12.35 | 3730 | 0.14 |
| LUD011 | TVL - DS | 1.91 | 0.31 | 0.39 | 0.16 | 0.016 | <0.005 | 0.02 | 0.529 | 2.3 | 9.76 | 1900 | 0.18 |

Notes: Re not shown (consistently at or below LDL). Stratigraphy Codes: MZ = Main Zone, BCU = Bastard Cyclic Unit, MCU = Merensky Cyclic Unit, FCU = Footwall Cyclic Unit, UG2CU = Upper Group 2 Cyclic Unit, FAZ = Footwall Assimilation Zone, FW2A = Calc-silicate footwall, TVL = Transvaal, DS = Dolostone, Qtz = quartzite. Average RSD of standards for ME-MS61L: 4.372
* Sample was for mineral identification, was non-representative and excluded from geochemical interpretation.

Table 3. (Cont.)

| | Analyte | Na | Nb | Ni | P | Pb | Rb | S | Sb | Sc | Se | Sn | Sr |
|---|---|---|---|---|---|---|---|---|---|---|---|---|---|
| | Units | % | ppm | ppm | % | ppm | ppm | % | ppm | ppm | ppm | ppm | ppm |
| | LDL | 0.001 | 0.005 | 0.08 | 0.001 | 0.01 | 0.02 | 0.01 | 0.02 | 0.01 | 0.2 | 0.02 | 0.02 |
| Sample | Stratigraphy | | | | | | | | | | | | |
| UMT094-1096 | MZ | 1.590 | 1.38 | 151.5 | 0.008 | 2.75 | 3.32 | <0.01 | 0.07 | 11.8 | <0.2 | 0.36 | 269 |
| UMT094-1111 | MZ | 1.430 | 0.965 | 197.5 | 0.007 | 2.08 | 4.38 | <0.01 | 0.06 | 17.2 | <0.2 | 0.29 | 242 |
| UMT094-1135 | MZ | 1.690 | 2.08 | 177 | 0.004 | 2.60 | 10.15 | <0.01 | 0.19 | 14.45 | <0.2 | 0.37 | 259 |
| UMT094-1165 | MZ | 1.445 | 0.927 | 204 | 0.007 | 20.1 | 7.73 | <0.01 | 0.23 | 15.25 | <0.2 | 0.28 | 252 |
| UMT094-1184 | MZ | 1.405 | 0.242 | 134 | 0.004 | 1.53 | 0.19 | <0.01 | 0.03 | 11.55 | <0.2 | 0.13 | 287 |
| UMT094-1213 | BCU | 1.675 | 0.614 | 122 | 0.009 | 1.90 | 1.11 | <0.01 | 0.07 | 9.48 | <0.2 | 0.18 | 293 |
| UMT094-1218 | BCU | 1.120 | 0.199 | 276 | 0.005 | 1.52 | 2.65 | 0.02 | 0.05 | 12.85 | <0.2 | 0.16 | 239 |
| UMT094-1226 | BCU | 1.510 | 0.201 | 91.8 | 0.004 | 2.31 | 2.09 | <0.01 | 0.14 | 4.73 | <0.2 | 0.20 | 305 |
| UMT094-1228 | BCU | 0.447 | 0.400 | 581 | 0.005 | 2.44 | 2.07 | <0.01 | 0.10 | 28.7 | <0.2 | 0.24 | 61.6 |
| UMT094-1232 | BCU | 0.326 | 0.095 | 2460 | 0.002 | 2.68 | 1.84 | 0.41 | 0.22 | 31.7 | 2.4 | 0.30 | 55.5 |
| UMT094-1233 | MCU | 0.475 | 0.130 | 3440 | 0.002 | 4.60 | 5.30 | 0.62 | 0.09 | 25.0 | 3.6 | 0.30 | 113 |
| UMT094-1238 | MCU | 0.442 | 0.374 | 1800 | 0.005 | 2.88 | 8.26 | 0.33 | 0.06 | 27.5 | 1.5 | 0.24 | 65.5 |
| UMT094-1245 | MCU | 0.430 | 0.125 | 862 | 0.002 | 2.29 | 10.2 | 0.05 | 0.05 | 24.0 | 0.3 | 0.16 | 78.9 |
| UMT094-1252 | MCU | 0.352 | 0.351 | 1300 | 0.003 | 2.08 | 6.14 | 0.22 | 0.08 | 27.3 | 0.7 | 0.25 | 44.6 |
| UMT094-1254 | MCU | 0.245 | 0.403 | 1800 | 0.003 | 4.65 | 6.52 | 0.33 | 0.11 | 28.5 | 1.6 | 0.41 | 25.3 |
| UMT094-1258 | MCU | 0.213 | 0.215 | 2180 | 0.002 | 3.03 | 4.12 | 0.44 | 0.08 | 27.6 | 2.0 | 0.27 | 27.8 |
| UMT094-1265 | MCU | 0.254 | 0.330 | 1265 | 0.004 | 3.36 | 8.60 | 0.17 | 0.13 | 29.1 | 0.5 | 0.27 | 34.1 |
| UMT094-1273 | MCU | 1.230 | 0.981 | 1680 | 0.041 | 7.61 | 23.5 | 0.41 | 0.16 | 21.5 | 2.4 | 0.47 | 192 |
| UMT094-1277 | MCU | 0.194 | 0.204 | 1695 | 0.002 | 5.08 | 3.59 | 0.33 | 0.11 | 30.7 | 1.2 | 0.32 | 25.2 |
| UMT094-1278 | MCU | 0.274 | 0.092 | 770 | 0.001 | 7.72 | 4.43 | 0.07 | 0.05 | 29.0 | 0.3 | 0.16 | 45.1 |
| UMT094-1279 | MCU | 0.082 | 0.460 | 1965 | 0.003 | 49.8 | 7.95 | 0.25 | 0.09 | 17.05 | 0.8 | 0.36 | 27.8 |
| UMT094-1282 | MCU | 0.400 | 0.274 | 1620 | 0.004 | 4.22 | 3.64 | 0.16 | 0.06 | 26.6 | 1.0 | 0.26 | 62.1 |

Table 3. (Cont.)

| | Analyte | Na | Nb | Ni | P | Pb | Rb | S | Sb | Sc | Se | Sn | Sr |
|---|---|---|---|---|---|---|---|---|---|---|---|---|---|
| | Units | % | ppm | ppm | % | ppm | ppm | % | ppm | ppm | ppm | ppm | ppm |
| | LDL | 0.001 | 0.005 | 0.08 | 0.001 | 0.01 | 0.02 | 0.01 | 0.02 | 0.01 | 0.2 | 0.02 | 0.02 |
| Sample | Stratigraphy | | | | | | | | | | | | |
| UMT094-1285 | MCU | 0.256 | 0.918 | 3940 | 0.012 | 9.95 | 6.56 | 0.94 | 0.11 | 25.8 | 4.2 | 0.52 | 31.8 |
| UMT094-1286 | MCU | 0.219 | 0.186 | 2750 | 0.004 | 9.74 | 3.40 | 0.62 | 0.11 | 29.4 | 2.2 | 0.62 | 45.8 |
| UMT094-1288 | MCU | 0.304 | 0.454 | 2150 | 0.010 | 5.52 | 1.65 | 0.60 | 0.12 | 42.8 | 2.4 | 0.56 | 116.5 |
| UMT094-1289 | MCU | 0.422 | 0.695 | 2300 | 0.009 | 20.8 | 6.63 | 0.39 | 0.19 | 36.5 | 2.9 | 0.63 | 186.5 |
| UMT094-1291A | MCU | 0.514 | 0.275 | 2120 | 0.002 | 7.66 | 2.68 | 0.50 | 0.06 | 38.5 | 2.0 | 0.49 | 118 |
| UMT094-1291B | MCU | 0.167 | 0.123 | 3570 | 0.003 | 3.64 | 1.46 | 0.57 | 0.04 | 9.58 | 2.1 | 0.27 | 71.7 |
| UMT094-1292A | FCU | 1.515 | 0.163 | 3880 | 0.002 | 11.75 | 4.08 | 1.09 | 0.07 | 2.17 | 4.2 | 0.47 | 499 |
| UMT094-1292B | FCU | 1.505 | 0.178 | 111 | 0.002 | 2.64 | 1.16 | 0.01 | 0.09 | 4.3 | <0.2 | 0.12 | 405 |
| UMT094-1294 | FCU | 1.640 | 0.216 | 66.1 | 0.002 | 2.04 | 1.12 | <0.01 | 0.14 | 2.8 | <0.2 | 0.14 | 416 |
| UMT094-1296 | FCU | 1.325 | 0.208 | 1030 | 0.002 | 4.14 | 1.68 | 0.24 | 0.07 | 9.0 | 1.0 | 0.16 | 368 |
| UMT094-1300 | FCU | 1.275 | 0.220 | 236 | 0.003 | 1.32 | 1.12 | 0.03 | 0.04 | 10.55 | <0.2 | 0.13 | 330 |
| UMT094-1308 | FCU | 1.535 | 0.228 | 115 | 0.003 | 1.22 | 0.11 | 0.01 | 0.04 | 4.64 | <0.2 | 0.13 | 398 |
| UMT094-1311 | FCU | 1.170 | 0.397 | 1835 | 0.005 | 8.94 | 11.35 | 0.56 | 0.08 | 19.0 | 1.6 | 0.35 | 275 |
| UMT094-1319 | FCU | 0.561 | 0.282 | 1140 | 0.003 | 6.14 | 5.81 | 0.20 | 0.29 | 27.9 | 0.5 | 0.29 | 118.5 |
| UMT094-1325A | FCU | 0.384 | 0.474 | 1745 | 0.007 | 6.84 | 5.08 | 0.34 | 0.07 | 28.1 | 1.2 | 0.30 | 78.9 |
| UMT094-1325B | FCU | 0.912 | 0.179 | 437 | 0.005 | 1.48 | 2.01 | 0.02 | 0.05 | 19.35 | <0.2 | 0.15 | 209 |
| UMT094-1326A | FCU | 0.370 | 0.423 | 991 | 0.009 | 3.36 | 4.50 | 0.08 | 0.06 | 30.2 | <0.2 | 0.25 | 62.9 |
| UMT094-1326B | FCU | 0.246 | 0.069 | 2030 | <0.001 | 3.81 | 0.51 | 0.49 | 0.05 | 29.0 | 1.9 | 0.21 | 52.6 |
| UMT094-1327 | FCU | 0.529 | 0.279 | 729 | 0.004 | 2.20 | 2.75 | 0.07 | 0.06 | 28.1 | <0.2 | 0.17 | 105.5 |
| UMT094-1329 | FCU | 0.287 | 0.171 | 1000 | 0.002 | 2.36 | 1.12 | 0.18 | 0.04 | 28.7 | 0.4 | 0.16 | 52.7 |
| UMT094-1332 | FCU | 0.479 | 0.258 | 1320 | 0.003 | 3.30 | 2.75 | 0.28 | 0.05 | 27.6 | 0.7 | 0.16 | 96.0 |
| UMT094-1334 * | UG2HW | 0.034 | 1.315 | 893 | 0.002 | 12.05 | 0.65 | 0.31 | 0.07 | 27.8 | 1.1 | 3.27 | 13.3 |

Table 3. (Cont.)

| | Analyte | Na | Nb | Ni | P | Pb | Rb | S | Sb | Sc | Se | Sn | Sr |
|---|---|---|---|---|---|---|---|---|---|---|---|---|---|
| | Units | % | ppm | ppm | % | ppm | ppm | % | ppm | ppm | ppm | ppm | ppm |
| | LDL | 0.001 | 0.005 | 0.08 | 0.001 | 0.01 | 0.02 | 0.01 | 0.02 | 0.01 | 0.2 | 0.02 | 0.02 |
| Sample | Stratigraphy | | | | | | | | | | | | |
| UMT094-1335 | UG2HW | 0.228 | 0.350 | 2100 | 0.005 | 12.0 | 3.87 | 1.21 | 0.09 | 24.5 | 2.0 | 0.88 | 74.2 |
| UMT094-1336A | UG2HW | 0.701 | 0.091 | 1385 | 0.001 | 4.23 | 3.46 | 0.31 | 0.05 | 18.5 | 0.9 | 0.15 | 156.5 |
| UMT094-1336B | UG2HW | 0.512 | 0.116 | 1700 | 0.003 | 6.37 | 4.17 | 0.45 | 0.06 | 20.8 | 1.2 | 0.25 | 126 |
| UMT094-1337 | UG2HW | 0.328 | 0.180 | 2820 | 0.002 | 8.88 | 1.62 | 0.90 | 0.05 | 27.6 | 2.5 | 0.34 | 62.2 |
| UMT094-1339 | UG2HW | 0.235 | 0.268 | 823 | 0.006 | 3.50 | 2.63 | 0.09 | 0.04 | 30.7 | <0.2 | 0.21 | 40.6 |
| UMT094-1340 | UG2HW | 0.378 | 0.163 | 787 | 0.001 | 3.27 | 3.18 | 0.15 | 0.03 | 26.7 | <0.2 | 0.15 | 72.7 |
| UMT094-1343 | UG2HW | 0.368 | 0.157 | 526 | 0.002 | 2.06 | 1.69 | 0.03 | 0.03 | 23.3 | <0.2 | 0.14 | 81.7 |
| UMT094-1351 | UG2HW | 0.400 | 0.247 | 1105 | 0.003 | 1.94 | 1.63 | 0.07 | 0.05 | 20.4 | <0.2 | 0.13 | 97.4 |
| UMT094-1359 | FAZ | 0.360 | 0.299 | 1810 | 0.005 | 6.34 | 3.29 | 0.35 | 0.06 | 19.5 | 0.4 | 0.31 | 97.2 |
| UMT094-1365 | UG2FW | 0.090 | 0.534 | 858 | 0.004 | 4.90 | 0.54 | 0.54 | 0.09 | 9.42 | 0.3 | 0.44 | 33.1 |
| UMT094-1366 | FAZ | 0.229 | 0.541 | 961 | 0.007 | 11.45 | 2.33 | 0.40 | 0.27 | 21.6 | 0.3 | 0.79 | 50.5 |
| UMT094-1376 | FAZ | 0.268 | 0.858 | 1205 | 0.015 | 8.42 | 13.95 | 0.24 | 0.57 | 30.0 | 0.8 | 0.45 | 112.5 |
| UMT094-1384 | UG2FW | 0.343 | 0.389 | 573 | 0.005 | 4.91 | 3.05 | 0.42 | 0.17 | 14.25 | 0.6 | 0.41 | 116.5 |
| UMT094-1386 | FAZ | 0.193 | 0.747 | 1090 | 0.014 | 8.72 | 2.07 | 0.90 | 0.27 | 11.4 | 1.0 | 0.91 | 60.4 |
| UMT094-1402 | UG2FW | 0.154 | 0.365 | 764 | 0.003 | 3.80 | 12.8 | 0.46 | 0.18 | 15.2 | 0.3 | 0.60 | 37.0 |
| UMT094-1405 | FAZ | 0.026 | 1.00 | 787 | 0.002 | 7.63 | 3.98 | 0.39 | 0.24 | 20.9 | 0.4 | 1.56 | 25.8 |
| UMT094-1410 * | FW2A | 0.068 | 2.35 | 1445 | 0.067 | 15.5 | 0.28 | 0.77 | 0.13 | 26.3 | 1.2 | 2.10 | 33.3 |
| UMT094-1412 | FW2A | 0.010 | 0.606 | 807 | 0.002 | 7.04 | 0.10 | 0.17 | 0.23 | 4.2 | 0.6 | 0.85 | 2.65 |
| UMT094-1421 | FW2A | 0.007 | 1.195 | 381 | 0.001 | 6.55 | 0.11 | 0.07 | 1.25 | 6.12 | 0.2 | 2.97 | 8.00 |
| UMT094-1424 | FW2A | 0.008 | 0.132 | 707 | 0.003 | 73.8 | 0.04 | 0.68 | 0.37 | 3.29 | 1.2 | 0.83 | 1.81 |
| UMT094-1436 | FW2A | 0.006 | 0.905 | 224 | <0.001 | 12.35 | 0.10 | 0.07 | 0.38 | 6.95 | <0.2 | 0.27 | 5.47 |
| UMT094-1454 * | FW2A | 0.002 | 0.119 | 1000 | 0.001 | 1.81 | 0.06 | 0.72 | 1.90 | 5.46 | 0.4 | 1.60 | 4.44 |

Table 3. (Cont.)

| | Analyte | Na | Nb | Ni | P | Pb | Rb | S | Sb | Sc | Se | Sn | Sr |
|---|---|---|---|---|---|---|---|---|---|---|---|---|---|
| | Units | % | ppm | ppm | % | ppm | ppm | % | ppm | ppm | ppm | ppm | ppm |
| | LDL | 0.001 | 0.005 | 0.08 | 0.001 | 0.01 | 0.02 | 0.01 | 0.02 | 0.01 | 0.2 | 0.02 | 0.02 |
| Sample | Stratigraphy | | | | | | | | | | | | |
| UMT094-1457 | FW2A | 0.002 | 0.055 | 414 | 0.001 | 1.47 | 0.07 | 0.56 | 0.24 | 1.52 | <0.2 | 0.61 | 143.5 |
| UMT094-1461 * | FW2A | 0.005 | 71.8 | 798 | 0.005 | 5.63 | 0.78 | 1.33 | 0.77 | 5.68 | 0.9 | 1.23 | 30.4 |
| UMT094-1463 * | FW2A | 0.003 | 2.06 | 70.3 | <0.001 | 14.05 | 2.78 | 0.06 | 1.04 | 4.14 | 0.5 | 9.12 | 4.39 |
| UMT094-1466 * | FW2A | 0.004 | 1.50 | 186.5 | 0.018 | 1.70 | 0.18 | 0.08 | 1.71 | 2.19 | <0.2 | 2.25 | 14.55 |
| UMT094-1479 | FW2A | 0.008 | 3.19 | 171.5 | 0.007 | 8.71 | 0.10 | 0.80 | 0.59 | 2.53 | 0.6 | 0.64 | 16.85 |
| UMT094-1494 | TVL - DS | 0.010 | 0.496 | 23.0 | 0.007 | 3.00 | 0.25 | 1.49 | 0.16 | 2.32 | 0.6 | 1.03 | 80.2 |
| UMT094-1537 | TVL - DS | 0.003 | 0.473 | 11.5 | 0.002 | 3.49 | 0.27 | 0.10 | 0.11 | 1.90 | <0.2 | 0.53 | 66.8 |
| UMT094-1573 | TVL - DS | 0.001 | 0.722 | 65.5 | 0.002 | 3.71 | 0.12 | 0.15 | 0.65 | 2.20 | 0.2 | 1.51 | 65.7 |
| UMT094-1601 | TVL - DS | 0.002 | 0.568 | 9.97 | 0.005 | 3.67 | 0.28 | 0.11 | 0.13 | 2.62 | 0.2 | 0.47 | 115 |
| LUD001 | TVL - Shale | 0.553 | 7.85 | 46.5 | 0.038 | 22.5 | 142 | <0.01 | 3.70 | 21.0 | <0.2 | 4.37 | 105.5 |
| LUD002 | TVL - Shale | 0.529 | 8.47 | 43.4 | 0.055 | 24.5 | 141 | <0.01 | 3.51 | 19.0 | <0.2 | 4.54 | 102.5 |
| LUD003 | TVL | 0.027 | 3.48 | 29.5 | 0.043 | 2.53 | 43.6 | <0.01 | 0.56 | 7.37 | <0.2 | 1.24 | 21.3 |
| LUD004 | TVL - Qtz | 0.030 | 1.205 | 5.14 | 0.024 | 2.28 | 37.3 | <0.01 | 0.39 | 3.16 | <0.2 | 0.66 | 8.69 |
| LUD005 | TVL - Shale | 0.267 | 6.90 | 11.75 | 0.132 | 5.21 | 55.4 | 0.09 | 0.69 | 27.6 | 0.5 | 2.05 | 16.3 |
| LUD006 | TVL - DS | 0.011 | 0.388 | 7.23 | 0.027 | 1.07 | 1.47 | <0.01 | 0.05 | 1.03 | 0.2 | 0.12 | 33.9 |
| LUD007 | TVL | 0.386 | 9.03 | 72.5 | 0.057 | 4.90 | 89.5 | <0.01 | 1.52 | 13.15 | <0.2 | 3.43 | 46.2 |
| LUD008 | TVL - Qtz | 0.013 | 0.031 | 5.04 | 0.004 | 0.74 | 0.63 | 0.03 | 0.15 | 0.09 | <0.2 | 0.16 | 10.25 |
| LUD009 | TVL - Shale | 0.591 | 10.55 | 138.5 | 0.050 | 8.73 | 125 | <0.01 | 1.62 | 21.9 | <0.2 | 4.76 | 106 |
| LUD010A | TVL - Qtz | 0.002 | 0.049 | 3.77 | <0.001 | 0.35 | 0.18 | <0.01 | 0.10 | 0.05 | <0.2 | 0.17 | 7.39 |
| LUD010B | TVL - DS | 0.008 | 0.058 | 2.62 | <0.001 | 0.77 | 0.25 | <0.01 | 0.04 | 0.19 | 0.2 | 0.05 | 51.5 |
| LUD011 | TVL - DS | 0.006 | 0.039 | 3.69 | 0.001 | 0.61 | 0.80 | 0.01 | 0.08 | 0.19 | <0.2 | 0.08 | 11.95 |

Notes: Re not shown (consistently at or below LDL). Stratigraphy Codes: MZ = Main Zone, BCU = Bastard Cyclic Unit, MCU = Merensky Cyclic Unit, FCU = Footwall Cyclic Unit, UG2CU = Upper Group 2 Cyclic Unit, FAZ = Footwall Assimilation Zone, FW2A = Calc-silicate footwall, TVL = Transvaal, DS = Dolostone, Qtz = quartzite. Average RSD of standards for ME-MS61L: 4.372
* Sample was for mineral identification, was non-representative and excluded from geochemical interpretation.

Table 3. (Cont.)

| | Analyte | Ta | Te | Th | Ti | Tl | U | V | W | Y | Zn | Zr |
|---|---|---|---|---|---|---|---|---|---|---|---|---|
| | Units | ppm | ppm | ppm | % | ppm | ppm | ppm | ppm | ppm | ppm | ppm |
| | LDL | 0.01 | 0.04 | 0.004 | 0.001 | 0.004 | 0.01 | 0.1 | 0.008 | 0.01 | 0.2 | 0.1 |
| Sample | Stratigraphy | | | | | | | | | | | |
| UMT094-1096 | MZ | 0.10 | <0.04 | 0.869 | 0.126 | 0.049 | 0.30 | 89.3 | 0.118 | 4.46 | 46.0 | 25.0 |
| UMT094-1111 | MZ | 0.08 | <0.04 | 0.784 | 0.146 | 0.035 | 0.20 | 109.5 | 0.256 | 6.55 | 53.4 | 23.4 |
| UMT094-1135 | MZ | 0.15 | <0.04 | 1.375 | 0.173 | 0.099 | 0.45 | 101.5 | 0.142 | 5.95 | 55.6 | 28.0 |
| UMT094-1165 | MZ | 0.06 | <0.04 | 0.626 | 0.122 | 0.078 | 0.18 | 102.5 | 0.241 | 5.07 | 91.9 | 20.2 |
| UMT094-1184 | MZ | 0.02 | <0.04 | 0.197 | 0.074 | 0.010 | 0.06 | 81.1 | 0.029 | 2.52 | 40.4 | 8.3 |
| UMT094-1213 | BCU | 0.05 | <0.04 | 0.313 | 0.089 | 0.043 | 0.11 | 73.9 | 0.058 | 3.06 | 40.9 | 12.1 |
| UMT094-1218 | BCU | 0.02 | <0.04 | 0.225 | 0.081 | 0.027 | 0.07 | 75.4 | 0.029 | 3.14 | 52.3 | 7.0 |
| UMT094-1226 | BCU | 0.01 | <0.04 | 0.077 | 0.051 | 0.107 | 0.03 | 33.1 | 0.092 | 1.36 | 25.6 | 5.2 |
| UMT094-1228 | BCU | 0.03 | <0.04 | 0.392 | 0.138 | 0.018 | 0.14 | 125.5 | 0.070 | 5.65 | 94.2 | 13.4 |
| UMT094-1232 | BCU | <0.01 | 0.58 | 0.059 | 0.130 | 0.072 | 0.02 | 118.5 | 0.022 | 5.09 | 81.8 | 6.0 |
| UMT094-1233 | MCU | 0.01 | 2.88 | 0.152 | 0.096 | 0.095 | 0.03 | 102.5 | 0.030 | 3.91 | 75.7 | 7.3 |
| UMT094-1238 | MCU | 0.03 | 0.80 | 0.913 | 0.120 | 0.052 | 0.09 | 117.0 | 0.035 | 5.02 | 79.3 | 11.1 |
| UMT094-1245 | MCU | 0.01 | 0.13 | 0.116 | 0.080 | 0.044 | 0.03 | 101.5 | 0.025 | 2.85 | 73.1 | 5.3 |
| UMT094-1252 | MCU | 0.02 | 0.22 | 0.662 | 0.122 | 0.037 | 0.12 | 110.0 | 0.047 | 4.79 | 82.1 | 10.2 |
| UMT094-1254 | MCU | 0.03 | 0.35 | 0.827 | 0.112 | 0.061 | 0.19 | 119.0 | 0.245 | 4.70 | 94.9 | 11.6 |
| UMT094-1258 | MCU | 0.01 | 0.44 | 0.190 | 0.096 | 0.040 | 0.04 | 111.5 | 0.045 | 3.59 | 87.0 | 7.9 |
| UMT094-1265 | MCU | 0.02 | 0.18 | 0.559 | 0.111 | 0.056 | 0.14 | 109.0 | 0.143 | 4.85 | 80.2 | 11.6 |
| UMT094-1273 | MCU | 0.07 | 1.61 | 1.275 | 0.097 | 0.110 | 0.33 | 84.1 | 0.296 | 5.00 | 57.2 | 12.3 |
| UMT094-1277 | MCU | 0.02 | 0.28 | 0.213 | 0.110 | 0.054 | 0.05 | 114.5 | 0.262 | 4.85 | 96.1 | 8.1 |
| UMT094-1278 | MCU | 0.01 | 0.04 | 0.082 | 0.095 | 0.055 | 0.03 | 108.0 | 0.197 | 4.03 | 88.4 | 5.7 |
| UMT094-1279 | MCU | 0.04 | 0.33 | 0.512 | 0.067 | 0.136 | 0.10 | 79.2 | 0.440 | 2.13 | 92.5 | 9.5 |
| UMT094-1282 | MCU | 0.02 | 0.14 | 0.418 | 0.108 | 0.074 | 0.08 | 133.0 | 0.184 | 3.49 | 91.7 | 6.7 |

Table 3. (Cont.)

| | Analyte | Ta | Te | Th | Ti | Tl | U | V | W | Y | Zn | Zr |
|---|---|---|---|---|---|---|---|---|---|---|---|---|
| | Units | ppm | ppm | ppm | % | ppm | ppm | ppm | ppm | ppm | ppm | ppm |
| | LDL | 0.01 | 0.04 | 0.004 | 0.001 | 0.004 | 0.01 | 0.1 | 0.008 | 0.01 | 0.2 | 0.1 |
| Sample | Stratigraphy | | | | | | | | | | | |
| UMT094-1285 | MCU | 0.06 | 1.04 | 0.881 | 0.136 | 0.104 | 0.25 | 125.0 | 0.140 | 4.53 | 96.2 | 15.9 |
| UMT094-1286 | MCU | 0.02 | 0.35 | 0.237 | 0.166 | 0.060 | 0.06 | 127.0 | 0.041 | 9.93 | 68.4 | 24.7 |
| UMT094-1288 | MCU | 0.06 | 0.36 | 0.664 | 0.217 | 0.120 | 0.16 | 191.0 | 0.048 | 11.35 | 57.7 | 46.8 |
| UMT094-1289 | MCU | 0.05 | 0.40 | 0.601 | 0.215 | 0.140 | 0.14 | 159.0 | 0.135 | 12.00 | 47.3 | 47.9 |
| UMT094-1291A | MCU | 0.02 | 0.31 | 0.197 | 0.168 | 0.098 | 0.06 | 151.0 | 0.048 | 8.61 | 35.1 | 21.0 |
| UMT094-1291B | MCU | 0.02 | 0.49 | 0.169 | 0.057 | 0.061 | 0.02 | 51.1 | 0.024 | 2.61 | 78.3 | 7.9 |
| UMT094-1292A | FCU | 0.01 | 1.02 | 0.081 | 0.025 | 0.409 | 0.02 | 15.5 | 0.029 | 0.65 | 20.1 | 3.3 |
| UMT094-1292B | FCU | 0.02 | <0.04 | 0.075 | 0.034 | 0.137 | 0.02 | 25.9 | 0.046 | 0.78 | 26.3 | 4.1 |
| UMT094-1294 | FCU | 0.01 | <0.04 | 0.063 | 0.028 | 0.106 | 0.02 | 18.8 | 0.047 | 0.62 | 17.2 | 3.6 |
| UMT094-1296 | FCU | 0.01 | 0.08 | 0.114 | 0.047 | 0.085 | 0.04 | 41.8 | 0.038 | 1.34 | 38.2 | 5.4 |
| UMT094-1300 | FCU | 0.02 | <0.04 | 0.113 | 0.053 | 0.037 | 0.04 | 51.7 | 0.027 | 1.51 | 38.4 | 5.7 |
| UMT094-1308 | FCU | 0.01 | <0.04 | 0.081 | 0.031 | 0.013 | 0.03 | 26.9 | 0.041 | 0.71 | 22.2 | 4.0 |
| UMT094-1311 | FCU | 0.03 | 0.32 | 0.384 | 0.101 | 0.086 | 0.10 | 120.5 | 0.074 | 2.95 | 71.1 | 11.5 |
| UMT094-1319 | FCU | 0.02 | 0.30 | 0.239 | 0.097 | 0.048 | 0.07 | 120.5 | 0.109 | 3.53 | 88.3 | 9.6 |
| UMT094-1325A | FCU | 0.03 | 0.32 | 0.472 | 0.105 | 0.041 | 0.13 | 114.0 | 0.113 | 3.98 | 93.4 | 13.0 |
| UMT094-1325B | FCU | 0.01 | <0.04 | 0.144 | 0.086 | 0.013 | 0.04 | 93.2 | 0.030 | 3.06 | 66.9 | 6.4 |
| UMT094-1326A | FCU | 0.03 | 0.13 | 0.498 | 0.114 | 0.036 | 0.13 | 128.5 | 0.063 | 4.40 | 92.7 | 13.4 |
| UMT094-1326B | FCU | 0.01 | 0.37 | 0.043 | 0.076 | 0.009 | 0.01 | 104.5 | 0.017 | 2.07 | 91.4 | 3.3 |
| UMT094-1327 | FCU | 0.02 | 0.04 | 0.330 | 0.102 | 0.019 | 0.08 | 117.5 | 0.036 | 3.80 | 88.5 | 10.3 |
| UMT094-1329 | FCU | 0.01 | 0.07 | 0.131 | 0.091 | 0.013 | 0.04 | 103.0 | 0.031 | 2.89 | 93.8 | 5.9 |
| UMT094-1332 | FCU | 0.02 | 0.15 | 0.217 | 0.094 | 0.028 | 0.06 | 98.5 | 0.032 | 3.59 | 84.1 | 7.7 |
| UMT094-1334 * | UG2HW | 0.19 | 0.08 | 2.470 | 0.380 | 0.012 | 0.21 | 69.8 | 0.131 | 26.1 | 182.5 | 394 |

Table 3. (Cont.)

| Sample | Analyte | Ta | Te | Th | Ti | Tl | U | V | W | Y | Zn | Zr |
|---|---|---|---|---|---|---|---|---|---|---|---|---|
| | Units | ppm | ppm | ppm | % | ppm | ppm | ppm | ppm | ppm | ppm | ppm |
| | LDL | 0.01 | 0.04 | 0.004 | 0.001 | 0.004 | 0.01 | 0.1 | 0.008 | 0.01 | 0.2 | 0.1 |
| Sample | Stratigraphy | | | | | | | | | | | |
| UMT094-1335 | UG2HW | 0.04 | 0.55 | 0.330 | 0.208 | 0.079 | 0.07 | 88.5 | 0.043 | 10.05 | 69.7 | 48.3 |
| UMT094-1336A | UG2HW | 0.01 | 0.16 | 0.052 | 0.057 | 0.026 | 0.01 | 68.0 | 0.022 | 2.28 | 80.0 | 3.5 |
| UMT094-1336B | UG2HW | 0.01 | 0.39 | 0.096 | 0.066 | 0.043 | 0.03 | 74.8 | 0.026 | 2.19 | 86.3 | 4.4 |
| UMT094-1337 | UG2HW | 0.01 | 0.49 | 0.111 | 0.116 | 0.033 | 0.04 | 160.5 | 0.026 | 3.25 | 116.5 | 6.0 |
| UMT094-1339 | UG2HW | 0.02 | 0.08 | 0.233 | 0.123 | 0.031 | 0.06 | 144.0 | 0.029 | 4.11 | 110.5 | 8.5 |
| UMT094-1340 | UG2HW | 0.01 | 0.06 | 0.112 | 0.100 | 0.023 | 0.03 | 121.5 | 0.020 | 3.35 | 92.1 | 6.8 |
| UMT094-1343 | UG2HW | 0.01 | <0.04 | 0.122 | 0.104 | 0.016 | 0.03 | 130.5 | 0.021 | 3.11 | 103.5 | 6.1 |
| UMT094-1351 | UG2HW | 0.02 | <0.04 | 0.218 | 0.081 | 0.016 | 0.05 | 95.8 | 0.038 | 2.98 | 105.5 | 7.8 |
| UMT094-1359 | FAZ | 0.02 | 0.08 | 0.264 | 0.096 | 0.064 | 0.07 | 122.0 | 0.050 | 4.45 | 105.5 | 9.1 |
| UMT094-1365 | UG2FW | 0.06 | 0.04 | 0.467 | 0.099 | 0.036 | 0.11 | 64.8 | 0.031 | 3.75 | 55.5 | 25.8 |
| UMT094-1366 | FAZ | 0.06 | 0.19 | 0.557 | 0.219 | 0.154 | 0.12 | 233.0 | 0.101 | 7.62 | 164.0 | 40.0 |
| UMT094-1376 | FAZ | 0.05 | 0.34 | 0.727 | 0.168 | 0.291 | 0.21 | 111.5 | 0.218 | 7.75 | 46.1 | 21.0 |
| UMT094-1384 | UG2FW | 0.04 | 0.23 | 0.276 | 0.132 | 0.083 | 0.07 | 74.2 | 0.074 | 5.57 | 155 | 25.0 |
| UMT094-1386 | FAZ | 0.08 | 0.09 | 0.771 | 0.177 | 0.059 | 0.14 | 88.5 | 0.113 | 7.12 | 129.5 | 35.8 |
| UMT094-1402 | UG2FW | 0.04 | 0.05 | 0.296 | 0.191 | 0.140 | 0.08 | 114.5 | 0.096 | 8.29 | 110.5 | 33.5 |
| UMT094-1405 | FAZ | 0.07 | 0.11 | 0.691 | 0.152 | 0.110 | 0.13 | 55.7 | 0.148 | 6.16 | 31.2 | 24.9 |
| UMT094-1410 * | FW2A | 0.20 | 0.20 | 3.110 | 0.402 | 0.162 | 0.74 | 145 | 0.241 | 20.5 | 27.9 | 95.4 |
| UMT094-1412 | FW2A | 0.08 | 0.11 | 1.525 | 0.072 | 0.032 | 0.16 | 6.8 | 0.111 | 13.25 | 68.3 | 7.6 |
| UMT094-1421 | FW2A | 0.18 | 0.06 | 2.220 | 0.060 | 0.045 | 0.40 | 3.0 | 0.284 | 10.45 | 130.0 | 8.7 |
| UMT094-1424 | FW2A | 0.02 | 0.58 | 0.233 | 0.080 | 0.474 | 0.05 | 10.0 | 0.171 | 9.10 | 183.5 | 3.4 |
| UMT094-1436 | FW2A | 0.13 | <0.04 | 1.575 | 0.067 | 0.021 | 0.15 | 4.0 | 0.384 | 6.60 | 96.2 | 8.4 |
| UMT094-1454 * | FW2A | 0.04 | 0.10 | 0.247 | 0.089 | 0.072 | 0.05 | 3.3 | 0.845 | 1.80 | 97.8 | 125.5 |

Table 3. (Cont.)

| | Analyte | Ta | Te | Th | Ti | Tl | U | V | W | Y | Zn | Zr |
|---|---|---|---|---|---|---|---|---|---|---|---|---|
| | Units | ppm | ppm | ppm | % | ppm | ppm | ppm | ppm | ppm | ppm | ppm |
| | LDL | 0.01 | 0.04 | 0.004 | 0.001 | 0.004 | 0.01 | 0.1 | 0.008 | 0.01 | 0.2 | 0.1 |
| Sample | Stratigraphy | | | | | | | | | | | |
| UMT094-1457 | FW2A | <0.01 | <0.04 | 0.015 | 0.132 | 0.192 | 0.02 | 9.4 | 0.135 | 4.92 | 410.0 | 17.1 |
| UMT094-1461 * | FW2A | 2.19 | 0.06 | 4.460 | 0.373 | 0.050 | 11.65 | 0.5 | 5.87 | 3.65 | 49.9 | 123 |
| UMT094-1463 * | FW2A | 0.18 | <0.04 | 0.653 | 0.076 | 0.044 | 2.59 | 4.0 | 0.734 | 3.77 | 178.5 | 9.6 |
| UMT094-1466 * | FW2A | 0.09 | <0.04 | 0.239 | 0.059 | 0.029 | 0.97 | 6.4 | 0.86 | 2.57 | 840.0 | 1.1 |
| UMT094-1479 | FW2A | 0.16 | 0.08 | 1.375 | 0.054 | 0.117 | 0.52 | 8.2 | 0.075 | 5.53 | 87.6 | 4.2 |
| UMT094-1494 | TVL - DS | 0.22 | 0.06 | 1.660 | 0.067 | 0.056 | 0.03 | 8.7 | 0.08 | 3.41 | 40.8 | 21.9 |
| UMT094-1537 | TVL - DS | 0.16 | <0.04 | 0.350 | 0.049 | 0.007 | 0.02 | 4.6 | 0.019 | 4.08 | 28.2 | 19.7 |
| UMT094-1573 | TVL - DS | 0.08 | <0.04 | 0.290 | 0.091 | 0.010 | 0.01 | 12.9 | 0.02 | 4.43 | 30.1 | 13.4 |
| UMT094-1601 | TVL - DS | 0.07 | <0.04 | 0.824 | 0.041 | 0.016 | 0.05 | 3.0 | 0.019 | 4.59 | 159.0 | 16.5 |
| LUD001 | TVL - Shale | 0.83 | <0.04 | 17.60 | 0.215 | 0.838 | 5.52 | 151.5 | 2.70 | 14.2 | 72.6 | 135 |
| LUD002 | TVL - Shale | 0.88 | <0.04 | 18.40 | 0.227 | 0.854 | 6.10 | 148.5 | 2.97 | 17.05 | 72.2 | 130 |
| LUD003 | TVL | 0.33 | <0.04 | 5.630 | 0.113 | 0.131 | 1.17 | 41.2 | 1.15 | 7.69 | 14.4 | 38.5 |
| LUD004 | TVL - Qtz | 0.12 | <0.04 | 2.160 | 0.044 | 0.145 | 0.63 | 23.1 | 0.314 | 2.21 | 2.1 | 13.7 |
| LUD005 | TVL - Shale | 0.43 | <0.04 | 2.960 | 0.933 | 0.209 | 6.94 | 330 | 1.92 | 24.5 | 87.9 | 164 |
| LUD006 | TVL - DS | 0.04 | <0.04 | 0.556 | 0.014 | 0.006 | 0.57 | 8.4 | 0.225 | 3.24 | 9.2 | 4.6 |
| LUD007 | TVL | 0.88 | <0.04 | 13.25 | 0.264 | 0.473 | 2.94 | 86.3 | 2.91 | 16.55 | 72.6 | 95.7 |
| LUD008 | TVL - Qtz | <0.01 | <0.04 | 0.046 | 0.001 | 0.013 | 0.35 | 2.8 | 0.027 | 0.27 | 4.6 | 0.7 |
| LUD009 | TVL - Shale | 0.95 | 0.08 | 17.75 | 0.348 | 0.713 | 4.33 | 139.5 | 3.65 | 21.9 | 97.7 | 130 |
| LUD010A | TVL - Qtz | <0.01 | <0.04 | 0.145 | 0.001 | 0.005 | 0.03 | 0.6 | 0.034 | 0.23 | 0.9 | 0.4 |
| LUD010B | TVL - DS | <0.01 | <0.04 | 1.185 | 0.001 | 0.004 | 0.23 | 2.4 | 0.095 | 1.22 | 3.7 | 1.8 |
| LUD011 | TVL - DS | <0.01 | <0.04 | 0.094 | 0.001 | 0.017 | 0.04 | 1.3 | 0.073 | 0.31 | 1.1 | 0.6 |

Notes: Re not shown (consistently at or below LDL). Stratigraphy Codes: MZ = Main Zone, BCU = Bastard Cyclic Unit, MCU = Merensky Cyclic Unit, FCU = Footwall Cyclic Unit, UG2CU = Upper Group 2 Cyclic Unit, FAZ = Footwall Assimilation Zone, FW2A = Calc-silicate footwall, TVL = Transvaal, DS = Dolostone, Qtz = quartzite. Average RSD of standards for ME-MS61L: 4.372
* Sample was for mineral identification, was non-representative and excluded from geochemical interpretation.

Table 4. Ivanplats UMT094 Assay data

| Sample start | Stratigraphy | 4PGE ppb | Ni ppm | Cu ppm | Pt ppb | Pd ppb | Au ppb | Cr ppm | Rh ppb | S ppm |
|---|---|---|---|---|---|---|---|---|---|---|
| 1215.3 | BCU | 5 | 174 | 58 | 3 | 1 | 1 | 250 | <LDL | 300 |
| 1216.3 | BCU | 4 | 250 | 54 | 2 | 1 | 1 | 470 | <LDL | 350 |
| 1217.3 | BCU | 5 | 346 | 44 | 3 | 1 | 1 | 720 | <LDL | 250 |
| 1218.3 | BCU | 5 | 258 | 30 | 3 | 1 | 1 | 470 | <LDL | 200 |
| 1219.34 | BCU | 5 | 228 | 22 | 3 | 1 | 1 | 400 | <LDL | 200 |
| 1220.34 | BCU | 6 | 220 | 24 | 4 | 1 | 1 | 410 | <LDL | 150 |
| 1221.08 | BCU | 5 | 262 | 24 | 3 | 1 | 1 | 450 | <LDL | 200 |
| 1221.84 | BCU | 7 | 314 | 56 | 4 | 2 | 1 | 590 | <LDL | 850 |
| 1222.8 | BCU | 4 | 204 | 38 | 2 | 1 | 1 | 370 | <LDL | 450 |
| 1223.64 | BCU | 3 | 52 | 18 | 1 | 1 | 1 | 70 | <LDL | 800 |
| 1224.3 | BCU | 3 | 38 | 12 | 1 | 1 | 1 | 50 | <LDL | 150 |
| 1224.9 | BCU | 17 | 208 | 24 | 9 | 7 | 1 | 390 | <LDL | 150 |
| 1225.96 | BCU | 12 | 254 | 22 | 6 | 4 | 2 | 510 | <LDL | 200 |
| 1227.01 | BCU | 17 | 130 | 16 | 13 | 3 | 1 | 180 | <LDL | 150 |
| 1227.87 | BCU | 8 | 500 | 72 | 3 | 2 | 2 | 1430 | 1 | 600 |
| 1228.87 | BCU | 293 | 1770 | 746 | 79 | 90 | 118 | 1500 | 6 | 4950 |
| 1229.87 | BCU | 130 | 964 | 298 | 40 | 46 | 41 | 1750 | 3 | 1500 |
| 1230.83 | BCU | 790 | 2640 | 1360 | 259 | 209 | 311 | 1720 | 11 | 6850 |
| 1231.83 | BCU | 1019 | 1990 | 884 | 400 | 234 | 372 | 1870 | 13 | 3800 |
| 1232.54 | BCU | 1859 | 2740 | 1290 | 1010 | 459 | 358 | 2340 | 32 | 6000 |
| 1233.26 | BCU | 5803 | 5250 | 3040 | 2620 | 2360 | 737 | 2010 | 86 | 13300 |
| 1234.26 | BCU | 2707 | 2790 | 1470 | 1260 | 1060 | 345 | 2080 | 42 | 6450 |
| 1235.26 | BCU | 1212 | 2010 | 886 | 570 | 472 | 141 | 1970 | 29 | 4300 |
| 1236.26 | BCU | 1277 | 1920 | 868 | 601 | 487 | 157 | 1650 | 32 | 4100 |
| 1237.26 | BCU | 2007 | 2260 | 1080 | 827 | 622 | 524 | 2010 | 34 | 4950 |
| 1238.26 | BCU | 1770 | 2800 | 1220 | 844 | 631 | 256 | 1900 | 39 | 6450 |
| 1239.26 | MCU | 301 | 1060 | 364 | 151 | 57 | 83 | 1790 | 10 | 1500 |
| 1240.26 | MCU | 257 | 1010 | 288 | 132 | 46 | 73 | 2110 | 6 | 1100 |
| 1241.26 | MCU | 278 | 1010 | 310 | 140 | 67 | 62 | 2000 | 9 | 1150 |
| 1242.26 | MCU | 561 | 1320 | 460 | 257 | 197 | 95 | 2320 | 12 | 2150 |
| 1243.23 | MCU | 592 | 1230 | 490 | 242 | 159 | 184 | 2080 | 7 | 1900 |
| 1244.23 | MCU | 452 | 1120 | 404 | 211 | 144 | 91 | 1530 | 6 | 1450 |
| 1245.23 | MCU | 1455 | 1950 | 890 | 697 | 550 | 190 | 1870 | 18 | 4500 |
| 1246.23 | MCU | 631 | 1290 | 448 | 287 | 208 | 122 | 1800 | 14 | 2200 |
| 1247.23 | MCU | 553 | 1230 | 398 | 261 | 176 | 105 | 2040 | 11 | 2100 |
| 1247.83 | MCU | 663 | 1220 | 414 | 320 | 225 | 104 | 2010 | 14 | 2150 |
| 1248.49 | MCU | 703 | 1200 | 436 | 333 | 227 | 132 | 1910 | 11 | 1950 |
| 1249.49 | MCU | 595 | 1120 | 382 | 294 | 197 | 92 | 1660 | 12 | 2700 |
| 1250.49 | MCU | 423 | 1110 | 344 | 223 | 107 | 84 | 1680 | 9 | 1700 |
| 1251.08 | MCU | 429 | 1040 | 344 | 220 | 120 | 79 | 1620 | 10 | 1700 |
| 1251.73 | MCU | 12 | 36 | 24 | 5 | 3 | 3 | 40 | 1 | 100 |

Table 4. (Cont.)

| Sample start | Stratigraphy | 4PGE ppb | Ni ppm | Cu ppm | Pt ppb | Pd ppb | Au ppb | Cr ppm | Rh ppb | S ppm |
|---|---|---|---|---|---|---|---|---|---|---|
| 1252.05 | MCU | 578 | 1140 | 438 | 311 | 133 | 122 | 1390 | 12 | 2250 |
| 1253.05 | MCU | 7172 | 2910 | 1480 | 4030 | 2320 | 456 | 23500 | 366 | 7000 |
| 1254.1 | MCU | 3184 | 1640 | 660 | 1560 | 1300 | 193 | 2360 | 131 | 3400 |
| 1254.95 | MCU | 1842 | 1460 | 562 | 848 | 795 | 135 | 2400 | 64 | 2600 |
| 1255.95 | MCU | 2010 | 1780 | 780 | 853 | 902 | 201 | 2250 | 54 | 3750 |
| 1256.99 | MCU | 2803 | 2090 | 972 | 1270 | 1230 | 231 | 2070 | 72 | 4500 |
| 1257.82 | MCU | 3341 | 2550 | 1080 | 1450 | 1620 | 157 | 2190 | 114 | 5800 |
| 1258.64 | MCU | 2784 | 2150 | 916 | 1340 | 1210 | 152 | 2730 | 82 | 4700 |
| 1259.64 | MCU | 3694 | 2360 | 1080 | 1680 | 1690 | 201 | 2550 | 123 | 5450 |
| 1260.64 | MCU | 2882 | 1980 | 876 | 1350 | 1260 | 192 | 2500 | 80 | 4250 |
| 1261.58 | MCU | 3710 | 1950 | 858 | 1860 | 1590 | 154 | 2550 | 106 | 4300 |
| 1262.58 | MCU | 3862 | 2120 | 920 | 1790 | 1740 | 211 | 2600 | 121 | 4350 |
| 1263.58 | MCU | 5045 | 2470 | 1140 | 2310 | 2160 | 431 | 2200 | 144 | 5500 |
| 1264.58 | MCU | 3289 | 1770 | 702 | 1560 | 1450 | 184 | 2550 | 95 | 3400 |
| 1265.58 | MCU | 1841 | 1280 | 420 | 871 | 835 | 83 | 2400 | 52 | 2050 |
| 1266.58 | MCU | 4336 | 2470 | 990 | 1920 | 1990 | 299 | 2480 | 127 | 3950 |
| 1267.58 | MCU | 6415 | 2830 | 1410 | 2920 | 2980 | 334 | 2570 | 181 | 5600 |
| 1268.58 | MCU | 8630 | 3700 | 1850 | 3970 | 4030 | 408 | 2450 | 222 | 8300 |
| 1269.58 | MCU | 6856 | 2640 | 1350 | 3070 | 3290 | 309 | 1900 | 187 | 7100 |
| 1270.58 | MCU | 5411 | 2610 | 1360 | 2340 | 2630 | 298 | 1790 | 143 | 5850 |
| 1271.58 | MCU | 4732 | 2420 | 1150 | 1990 | 2340 | 271 | 1980 | 131 | 5850 |
| 1272.58 | MCU | 4143 | 2220 | 1040 | 1790 | 2060 | 178 | 1900 | 115 | 5450 |
| 1273.51 | MCU | 7366 | 1630 | 938 | 5650 | 1510 | 144 | 1050 | 62 | 4450 |
| 1273.89 | MCU | 2879 | 1700 | 750 | 1360 | 1260 | 204 | 2340 | 55 | 3800 |
| 1274.28 | MCU | 12907 | 6730 | 4450 | 4900 | 6370 | 1320 | 1160 | 317 | 20200 |
| 1275.16 | MCU | 4514 | 2820 | 1360 | 1960 | 2200 | 234 | 1970 | 120 | 7250 |
| 1275.79 | MCU | 2418 | 1710 | 780 | 1110 | 1100 | 147 | 1720 | 61 | 3950 |
| 1276.82 | MCU | 1816 | 1490 | 514 | 749 | 914 | 113 | 2160 | 40 | 3250 |
| 1277.66 | MCU | 2333 | 1870 | 744 | 1040 | 1060 | 182 | 2070 | 51 | 4400 |
| 1278.38 | MCU | 1760 | 1380 | 670 | 867 | 782 | 68 | 2490 | 43 | 2750 |
| 1279.52 | MCU | 1305 | 2490 | 654 | 488 | 660 | 115 | 3440 | 42 | 14900 |
| 1280.5 | MCU | 2181 | 2730 | 1420 | 1010 | 917 | 199 | 23400 | 55 | 5250 |
| 1281.5 | MCU | 2311 | 2330 | 1270 | 1100 | 992 | 145 | 10100 | 74 | 4050 |
| 1282.5 | MCU | 4026 | 2980 | 1630 | 1850 | 1780 | 311 | 15700 | 85 | 6750 |
| 1283.5 | MCU | 3852 | 3410 | 1870 | 1680 | 1780 | 311 | 4000 | 81 | 9250 |
| 1284.5 | MCU | 3115 | 3190 | 1690 | 1210 | 1510 | 321 | 3440 | 74 | 6100 |
| 1285.5 | MCU | 1950 | 2350 | 1150 | 846 | 864 | 189 | 4590 | 51 | 5150 |
| 1286.5 | MCU | 2479 | 2580 | 1460 | 1140 | 1090 | 195 | 5450 | 54 | 6300 |
| 1287.5 | MCU | 2138 | 2750 | 970 | 998 | 962 | 100 | 1170 | 78 | 4600 |
| 1288.5 | MCU | 1435 | 2040 | 1100 | 626 | 634 | 136 | 4870 | 39 | 6000 |
| 1289.5 | MCU | 2016 | 2340 | 1690 | 818 | 952 | 192 | 4570 | 54 | 6050 |

Table 4. (Cont.)

| Sample start | Stratigraphy | 4PGE ppb | Ni ppm | Cu ppm | Pt ppb | Pd ppb | Au ppb | Cr ppm | Rh ppb | S ppm |
|---|---|---|---|---|---|---|---|---|---|---|
| 1290.69 | MCU | 2109 | 2160 | 1420 | 863 | 1000 | 203 | 2060 | 43 | 5200 |
| 1291.35 | MCU | 2482 | 2650 | 1490 | 1030 | 1200 | 189 | 3850 | 63 | 6800 |
| 1291.96 | FCU | 346 | 646 | 452 | 165 | 133 | 48 | 230 | <LDL | 1700 |
| 1292.96 | FCU | 487 | 552 | 360 | 247 | 197 | 43 | 410 | <LDL | 1400 |
| 1293.96 | FCU | 118 | 96 | 62 | 85 | 30 | 3 | 360 | <LDL | 150 |
| 1294.72 | FCU | 776 | 992 | 544 | 389 | 330 | 57 | 2730 | <LDL | 3150 |
| 1295.79 | FCU | 612 | 978 | 752 | 276 | 286 | 50 | 580 | <LDL | 2550 |
| 1296.69 | FCU | 302 | 426 | 268 | 115 | 94 | 13 | 1250 | 80 | 1100 |
| 1297.69 | FCU | 1504 | 992 | 486 | 734 | 568 | 60 | 830 | 142 | 2700 |
| 1298.69 | FCU | 690 | 1240 | 864 | 319 | 310 | 61 | 1390 | <LDL | 3800 |
| 1299.69 | FCU | 1150 | 1640 | 1280 | 542 | 528 | 80 | 2210 | <LDL | 5050 |
| 1300.69 | FCU | 234 | 446 | 224 | 130 | 88 | 16 | 1200 | <LDL | 1000 |
| 1301.69 | FCU | 481 | 666 | 398 | 227 | 216 | 38 | 1260 | <LDL | 1650 |
| 1302.72 | FCU | 617 | 1050 | 846 | 275 | 296 | 46 | 770 | <LDL | 3750 |
| 1303.72 | FCU | 538 | 826 | 550 | 249 | 240 | 49 | 1120 | <LDL | 2550 |
| 1304.72 | FCU | 555 | 534 | 268 | 276 | 240 | 39 | 1200 | <LDL | 1400 |
| 1305.57 | FCU | 428 | 424 | 292 | 226 | 176 | 26 | 330 | <LDL | 1250 |
| 1306.57 | FCU | 104 | 234 | 130 | 53 | 42 | 9 | 230 | <LDL | 750 |
| 1307.57 | FCU | 139 | 146 | 84 | 83 | 49 | 7 | 240 | <LDL | 400 |
| 1308.39 | FCU | 572 | 720 | 362 | 387 | 156 | 29 | 2970 | <LDL | 1650 |
| 1309.39 | FCU | 214 | 688 | 310 | 126 | 72 | 16 | 2800 | <LDL | 1350 |
| 1310.39 | FCU | 821 | 1400 | 978 | 347 | 389 | 85 | 3020 | <LDL | 4200 |
| 1311.39 | FCU | 149 | 468 | 146 | 72 | 66 | 11 | 1660 | <LDL | 650 |
| 1312.39 | FCU | 1152 | 1820 | 1360 | 535 | 481 | 136 | 2350 | <LDL | 6800 |
| 1313.39 | FCU | 755 | 1310 | 1060 | 336 | 338 | 81 | 2010 | <LDL | 4550 |
| 1314.39 | FCU | 444 | 824 | 482 | 173 | 119 | 152 | 1350 | <LDL | 2300 |
| 1315 | FCU | 176 | 522 | 290 | 77 | 52 | 47 | 1140 | <LDL | 1350 |
| 1315.61 | FCU | 367 | 758 | 332 | 176 | 138 | 53 | 2270 | <LDL | 1600 |
| 1316.61 | FCU | 821 | 1890 | 970 | 367 | 233 | 221 | 2280 | <LDL | 6550 |
| 1317.61 | FCU | 437 | 956 | 358 | 250 | 130 | 57 | 2700 | <LDL | 1600 |
| 1318.33 | FCU | 722 | 2030 | 1120 | 302 | 219 | 201 | 3360 | <LDL | 5400 |
| 1319.33 | FCU | 840 | 1020 | 568 | 416 | 306 | 118 | 2390 | <LDL | 2400 |
| 1320.33 | FCU | 1056 | 1110 | 664 | 522 | 432 | 102 | 2260 | <LDL | 2800 |
| 1321.4 | FCU | 1238 | 1590 | 808 | 617 | 464 | 157 | 1940 | <LDL | 4250 |
| 1322.4 | FCU | 2196 | 1610 | 710 | 1100 | 780 | 273 | 2860 | 43 | 4050 |
| 1323.4 | FCU | 1383 | 1100 | 472 | 730 | 545 | 108 | 2040 | <LDL | 2450 |
| 1324.4 | FCU | 235 | 550 | 134 | 110 | 106 | 19 | 2300 | <LDL | 650 |
| 1325 | FCU | 737 | 724 | 332 | 386 | 299 | 52 | 1060 | <LDL | 1450 |
| 1325.58 | FCU | 806 | 952 | 362 | 425 | 323 | 58 | 2260 | <LDL | 1500 |
| 1326.5 | FCU | 1213 | 1530 | 738 | 581 | 564 | 68 | 2940 | <LDL | 3650 |
| 1327.5 | FCU | 822 | 1100 | 490 | 366 | 404 | 52 | 3360 | <LDL | 2400 |

Table 4. (Cont.)

| Sample start | Stratigraphy | 4PGE ppb | Ni ppm | Cu ppm | Pt ppb | Pd ppb | Au ppb | Cr ppm | Rh ppb | S ppm |
|---|---|---|---|---|---|---|---|---|---|---|
| 1328.5 | FCU | 1394 | 2020 | 1460 | 617 | 681 | 96 | 3410 | <LDL | 8550 |
| 1329.5 | FCU | 1234 | 2180 | 1170 | 559 | 615 | 60 | 3510 | <LDL | 8050 |
| 1330.5 | FCU | 1322 | 2100 | 1240 | 570 | 636 | 116 | 2870 | <LDL | 6750 |
| 1331.5 | FCU | 800 | 1680 | 960 | 354 | 391 | 55 | 2480 | <LDL | 5350 |
| 1332.5 | FCU | 834 | 2040 | 1180 | 308 | 456 | 70 | 2500 | <LDL | 6250 |
| 1333.28 | FCU | 1318 | 2190 | 2130 | 483 | 722 | 113 | 540 | <LDL | 14000 |
| 1334.28 | UG2CU | 941 | 1660 | 1860 | 337 | 493 | 111 | 140 | <LDL | 9500 |
| 1334.95 | UG2CU | 649 | 1290 | 1420 | 207 | 307 | 135 | 1280 | <LDL | 12900 |
| 1335.64 | UG2CU | 2601 | 2100 | 1330 | 1090 | 1200 | 277 | 3610 | 34 | 9150 |
| 1336.64 | UG2CU | 6348 | 2210 | 1290 | 3450 | 2590 | 224 | 4640 | 84 | 8200 |
| 1337.64 | UG2CU | 4248 | 2090 | 1240 | 2320 | 1700 | 111 | 19700 | 117 | 6800 |
| 1338.58 | UG2CU | 933 | 1370 | 766 | 419 | 473 | 41 | 8160 | <LDL | 4150 |
| 1339.58 | UG2CU | 462 | 1060 | 504 | 193 | 245 | 24 | 7210 | <LDL | 2850 |
| 1340.58 | UG2CU | 751 | 1450 | 830 | 309 | 396 | 46 | 8940 | <LDL | 4700 |
| 1341.58 | UG2CU | 629 | 1720 | 1070 | 234 | 352 | 43 | 8880 | <LDL | 6100 |
| 1342.58 | UG2CU | 714 | 1740 | 998 | 237 | 435 | 42 | 10300 | <LDL | 6700 |
| 1343.58 | UG2CU | 309 | 962 | 448 | 131 | 161 | 17 | 7970 | <LDL | 2850 |
| 1344.5 | UG2CU | 965 | 1550 | 966 | 368 | 526 | 71 | 7450 | <LDL | 5750 |
| 1345.5 | UG2CU | 1109 | 1700 | 998 | 439 | 591 | 79 | 10100 | <LDL | 5850 |
| 1346.5 | UG2CU | 1080 | 1700 | 948 | 467 | 564 | 49 | 13400 | <LDL | 5100 |
| 1347.5 | UG2CU | 764 | 1600 | 934 | 300 | 425 | 39 | 7140 | <LDL | 5400 |
| 1348.2 | UG2CU | 312 | 908 | 394 | 143 | 156 | 13 | 6360 | <LDL | 2100 |
| 1348.85 | UG2CU | 435 | 1470 | 544 | 142 | 267 | 26 | 5220 | <LDL | 4150 |
| 1349.85 | UG2CU | 612 | 1850 | 750 | 192 | 383 | 37 | 6530 | <LDL | 5100 |
| 1350.74 | UG2CU | 738 | 1550 | 496 | 280 | 408 | 50 | 5800 | <LDL | 3200 |
| 1351.74 | UG2CU | 65 | 1050 | 130 | 27 | 34 | 4 | 4650 | <LDL | 950 |
| 1352.74 | UG2CU | 175 | 1620 | 378 | 54 | 108 | 13 | 4920 | <LDL | 2900 |
| 1353.74 | UG2CU | 178 | 1790 | 380 | 56 | 110 | 12 | 4310 | <LDL | 2700 |
| 1354.74 | UG2CU | 159 | 1620 | 278 | 46 | 102 | 11 | 4080 | <LDL | 2200 |
| 1355.74 | UG2CU | 409 | 2010 | 522 | 97 | 285 | 27 | 4940 | <LDL | 4300 |
| 1356.74 | UG2CU | 169 | 1650 | 298 | 46 | 113 | 10 | 5200 | <LDL | 2250 |
| 1357.74 | UG2CU | 583 | 1870 | 426 | 168 | 389 | 26 | 19300 | <LDL | 3050 |
| 1358.41 | UG2CU | 306 | 2040 | 734 | 74 | 214 | 18 | 4820 | <LDL | 5100 |
| 1359.1 | UG2CU | 444 | 1960 | 918 | 126 | 280 | 38 | 4900 | <LDL | 6550 |
| 1360.1 | UG2CU | 526 | 1580 | 570 | 182 | 318 | 26 | 26700 | <LDL | 3550 |
| 1361.1 | UG2CU | 653 | 2100 | 1060 | 147 | 466 | 40 | 5230 | <LDL | 6250 |
| 1362.1 | UG2CU | 586 | 1810 | 666 | 166 | 387 | 33 | 7920 | <LDL | 4750 |
| 1363.17 | UG2CU | 662 | 1760 | 914 | 179 | 446 | 37 | 7200 | <LDL | 6300 |
| 1364.17 | UG2CU | 1122 | 1960 | 1040 | 381 | 701 | 40 | 94900 | <LDL | 8200 |
| 1365.17 | UG2CU | 1013 | 1130 | 654 | 511 | 477 | 25 | 65500 | <LDL | 5900 |
| 1366.17 | UG2CU | 1052 | 1050 | 718 | 513 | 504 | 35 | 37600 | <LDL | 6900 |

Table 4. (Cont.)

| Sample start | Stratigraphy | 4PGE ppb | Ni ppm | Cu ppm | Pt ppb | Pd ppb | Au ppb | Cr ppm | Rh ppb | S ppm |
|---|---|---|---|---|---|---|---|---|---|---|
| 1367.17 | UG2CU | 798 | 1070 | 772 | 353 | 420 | 25 | 26400 | <LDL | 9750 |
| 1367.86 | UG2CU | 446 | 846 | 546 | 170 | 253 | 23 | 590 | <LDL | 7400 |
| 1368.22 | UG2CU | 1495 | 886 | 646 | 826 | 647 | 22 | 63000 | <LDL | 6150 |
| 1369.03 | UG2CU | 1555 | 1100 | 938 | 849 | 678 | 28 | 71600 | <LDL | 8900 |
| 1369.9 | FAZ | 198 | 686 | 422 | 68 | 118 | 12 | 3090 | <LDL | 7750 |
| 1370.9 | FAZ | 220 | 828 | 400 | 66 | 141 | 13 | 1550 | <LDL | 6100 |
| 1371.9 | FAZ | 338 | 988 | 570 | 117 | 202 | 19 | 1760 | <LDL | 7700 |
| 1372.9 | FAZ | 188 | 788 | 500 | 56 | 119 | 13 | 980 | <LDL | 4500 |
| 1373.9 | FAZ | 221 | 796 | 370 | 78 | 130 | 13 | 780 | <LDL | 5500 |
| 1374.84 | FAZ | 468 | 946 | 652 | 181 | 264 | 23 | 920 | <LDL | 7300 |
| 1375.81 | FAZ | 775 | 1000 | 788 | 270 | 462 | 43 | 940 | <LDL | 7750 |
| 1376.81 | FAZ | 137 | 532 | 304 | 43 | 75 | 19 | 550 | <LDL | 2850 |
| 1377.51 | FAZ | 165 | 672 | 428 | 40 | 109 | 16 | 690 | <LDL | 6300 |
| 1378.23 | FAZ | 249 | 708 | 250 | 98 | 118 | 33 | 480 | <LDL | 5750 |
| 1378.87 | FAZ | 258 | 726 | 660 | 78 | 151 | 29 | 550 | <LDL | 5450 |
| 1379.58 | FAZ | 177 | 594 | 498 | 54 | 103 | 20 | 420 | <LDL | 4550 |
| 1380.65 | FAZ | 692 | 770 | 514 | 82 | 592 | 18 | 260 | <LDL | 5600 |
| 1381 | FAZ | 233 | 746 | 460 | 64 | 154 | 15 | 200 | <LDL | 6200 |
| 1381.65 | FAZ | 530 | 1060 | 888 | 186 | 317 | 27 | 410 | <LDL | 12500 |
| 1382.65 | FAZ | 140 | 570 | 386 | 31 | 93 | 16 | 220 | <LDL | 4900 |
| 1383.65 | FAZ | 162 | 504 | 426 | 35 | 100 | 27 | 250 | <LDL | 4050 |
| 1384.65 | FAZ | 273 | 770 | 708 | 55 | 145 | 73 | 220 | <LDL | 8050 |
| 1385.65 | FAZ | 696 | 1220 | 944 | 259 | 400 | 37 | 250 | <LDL | 13200 |
| 1386.65 | FAZ | 641 | 980 | 802 | 283 | 315 | 43 | 70 | <LDL | 10200 |
| 1387.65 | FAZ | 264 | 794 | 746 | 70 | 165 | 29 | 50 | <LDL | 9150 |
| 1388.65 | FAZ | 112 | 554 | 402 | 28 | 73 | 11 | 70 | <LDL | 5900 |
| 1389.65 | FAZ | 343 | 780 | 712 | 114 | 183 | 46 | 60 | <LDL | 6800 |
| 1390.65 | FAZ | 273 | 588 | 498 | 103 | 151 | 19 | 70 | <LDL | 5300 |
| 1391.65 | FAZ | 312 | 700 | 568 | 96 | 191 | 25 | 60 | <LDL | 6600 |
| 1392.65 | FAZ | 209 | 606 | 444 | 51 | 138 | 20 | 80 | <LDL | 6950 |
| 1393.65 | FAZ | 90 | 436 | 282 | 26 | 60 | 4 | 50 | <LDL | 4600 |
| 1394.65 | FAZ | 156 | 636 | 554 | 39 | 105 | 12 | 20 | <LDL | 7600 |
| 1395.65 | FAZ | 94 | 498 | 350 | 17 | 68 | 9 | 80 | <LDL | 4550 |
| 1396.65 | FAZ | 171 | 640 | 516 | 46 | 107 | 18 | 110 | <LDL | 5600 |
| 1397.65 | FAZ | 385 | 798 | 648 | 138 | 220 | 27 | 1900 | <LDL | 6000 |
| 1398.6 | FAZ | 719 | 1050 | 990 | 261 | 387 | 71 | 970 | <LDL | 10300 |
| 1399.6 | FAZ | 436 | 716 | 682 | 169 | 244 | 23 | 13000 | <LDL | 5800 |
| 1400.6 | FAZ | 773 | 1060 | 756 | 456 | 290 | 27 | 9770 | <LDL | 8000 |
| 1401.6 | FAZ | 955 | 1120 | 756 | 459 | 429 | 67 | 15200 | <LDL | 8850 |
| 1402.6 | FAZ | 695 | 1010 | 684 | 218 | 437 | 40 | 8930 | <LDL | 11000 |
| 1403.22 | FAZ | 1059 | 1730 | 1340 | 406 | 565 | 88 | 2730 | <LDL | 8200 |

Table 4. (Cont.)

| Sample start | Stratigraphy | 4PGE ppb | Ni ppm | Cu ppm | Pt ppb | Pd ppb | Au ppb | Cr ppm | Rh ppb | S ppm |
|---|---|---|---|---|---|---|---|---|---|---|
| 1403.84 | FAZ | 1751 | 1750 | 1350 | 687 | 908 | 156 | 2970 | <LDL | 8250 |
| 1404.95 | FAZ | 532 | 1050 | 1050 | 105 | 255 | 40 | 60 | 132 | 11800 |
| 1405.95 | CS | 420 | 878 | 786 | 152 | 250 | 18 | 40 | <LDL | 13100 |
| 1406.95 | CS | 174 | 646 | 874 | 46 | 110 | 18 | 40 | <LDL | 11000 |
| 1407.95 | CS | 225 | 708 | 720 | 60 | 154 | 11 | 130 | <LDL | 6350 |
| 1408.84 | CS | 281 | 952 | 1180 | 68 | 189 | 24 | 50 | <LDL | 5000 |
| 1409.84 | CS | 186 | 644 | 748 | 51 | 128 | 7 | 90 | <LDL | 5600 |
| 1410.84 | CS | 167 | 496 | 840 | 26 | 66 | 75 | 40 | <LDL | 3850 |
| 1411.84 | CS | 132 | 602 | 690 | 32 | 93 | 7 | 30 | <LDL | 3650 |
| 1412.84 | CS | 99 | 492 | 570 | 26 | 70 | 3 | 30 | <LDL | 1400 |
| 1414 | CS | 95 | 472 | 480 | 26 | 66 | 3 | 50 | <LDL | 1300 |
| 1415 | CS | 120 | 518 | 500 | 32 | 84 | 4 | 30 | <LDL | 1800 |
| 1416 | CS | 67 | 294 | 568 | 18 | 45 | 4 | 30 | <LDL | 1950 |
| 1417 | CS | 90 | 308 | 414 | 25 | 61 | 4 | 30 | <LDL | 1250 |
| 1418 | CS | 54 | 196 | 100 | 14 | 37 | 3 | 10 | <LDL | 600 |
| 1419 | CS | 132 | 390 | 134 | 42 | 84 | 6 | 30 | <LDL | 1550 |
| 1420 | CS | 14 | 58 | 22 | 3 | 7 | 4 | 10 | <LDL | 250 |
| 1421 | CS | 128 | 514 | 330 | 35 | 90 | 3 | 20 | <LDL | 1450 |
| 1422 | CS | 115 | 442 | 452 | 32 | 81 | 2 | 40 | <LDL | 1350 |
| 1423 | CS | 65 | 396 | 76 | 18 | 42 | 5 | 30 | <LDL | 1000 |
| 1424 | CS | 261 | 472 | 682 | 66 | 174 | 21 | 20 | <LDL | 3400 |
| 1425 | CS | 193 | 378 | 356 | 54 | 135 | 4 | 20 | <LDL | 1350 |
| 1425.86 | CS | 97 | 398 | 382 | 28 | 64 | 5 | 30 | <LDL | 1450 |
| 1426.86 | CS | 89 | 372 | 330 | 23 | 62 | 4 | 40 | <LDL | 1450 |
| 1427.86 | CS | 28 | 136 | 110 | 7 | 18 | 3 | 50 | <LDL | 1000 |
| 1428.79 | CS | 3 | 24 | 22 | 1 | 1 | 1 | 10 | <LDL | 200 |
| 1429.79 | CS | 39 | 32 | 46 | 1 | 1 | 1 | 10 | 36 | 500 |
| 1430.6 | CS | 34 | 366 | 284 | 8 | 21 | 5 | 20 | <LDL | 1400 |
| 1431.87 | CS | 187 | 502 | 1010 | 60 | 112 | 15 | 20 | <LDL | 2550 |
| 1432.87 | CS | 22 | 416 | 26 | 6 | 13 | 3 | 20 | <LDL | 650 |
| 1433.87 | CS | 79 | 392 | 288 | 23 | 52 | 4 | 20 | <LDL | 1000 |
| 1434.87 | CS | 456 | 660 | 614 | 202 | 247 | 7 | 20 | <LDL | 1650 |
| 1435.87 | CS | 425 | 440 | 556 | 211 | 206 | 8 | 20 | <LDL | 1700 |
| 1436.87 | CS | 12 | 248 | 172 | 4 | 5 | 3 | 20 | <LDL | 750 |
| 1437.75 | CS | 28 | 264 | 60 | 7 | 18 | 3 | 20 | <LDL | 800 |
| 1438.75 | CS | 32 | 118 | 222 | 8 | 18 | 6 | 10 | <LDL | 650 |
| 1439.75 | CS | 115 | 344 | 428 | 30 | 80 | 5 | 20 | <LDL | 1200 |
| 1440.75 | CS | 20 | 124 | 176 | 6 | 12 | 2 | 10 | <LDL | 550 |
| 1441.75 | CS | 60 | 262 | 358 | 17 | 40 | 3 | 20 | <LDL | 900 |
| 1442.75 | CS | 38 | 196 | 106 | 9 | 26 | 3 | 20 | <LDL | 600 |
| 1443.75 | CS | 69 | 260 | 222 | 19 | 47 | 3 | 30 | <LDL | 800 |

Table 4. (Cont.)

| Sample start | Stratigraphy | 4PGE ppb | Ni ppm | Cu ppm | Pt ppb | Pd ppb | Au ppb | Cr ppm | Rh ppb | S ppm |
|---|---|---|---|---|---|---|---|---|---|---|
| 1444.75 | CS | 117 | 378 | 496 | 35 | 78 | 4 | 30 | <LDL | 1400 |
| 1445.75 | CS | 87 | 368 | 542 | 30 | 50 | 7 | 40 | <LDL | 3400 |
| 1446.75 | CS | 122 | 414 | 704 | 27 | 77 | 18 | 40 | <LDL | 2500 |
| 1447.75 | CS | 54 | 116 | 158 | 13 | 27 | 14 | 50 | <LDL | 1150 |
| 1448.75 | CS | 226 | 302 | 248 | 84 | 116 | 26 | 40 | <LDL | 3800 |
| 1449.91 | CS | 487 | 566 | 566 | 185 | 248 | 54 | 50 | <LDL | 4300 |
| 1450.91 | CS | 137 | 644 | 892 | 34 | 84 | 19 | 40 | <LDL | 7000 |
| 1451.91 | CS | 286 | 732 | 426 | 77 | 188 | 21 | 20 | <LDL | 5800 |
| 1452.73 | CS | 270 | 782 | 1070 | 108 | 149 | 13 | 20 | <LDL | 9050 |
| 1453.71 | CS | 261 | 1340 | 986 | 95 | 148 | 18 | 10 | <LDL | 11800 |
| 1454.71 | CS | 116 | 690 | 342 | 29 | 71 | 16 | 10 | <LDL | 7650 |
| 1455.71 | CS | 84 | 766 | 550 | 22 | 55 | 7 | 10 | <LDL | 6200 |
| 1456.71 | CS | 118 | 474 | 114 | 39 | 66 | 13 | 10 | <LDL | 5650 |
| 1457.71 | CS | 51 | 348 | 324 | 12 | 34 | 5 | 10 | <LDL | 5000 |
| 1458.71 | CS | 617 | 870 | 1070 | 279 | 245 | 93 | 10 | <LDL | 8900 |
| 1459.71 | CS | 487 | 1200 | 346 | 195 | 251 | 41 | 40 | <LDL | 14500 |
| 1460.71 | CS | 304 | 740 | 192 | 93 | 168 | 43 | 10 | <LDL | 11300 |
| 1461.85 | CS | 467 | 804 | 616 | 208 | 234 | 25 | 10 | <LDL | 8650 |
| 1462.85 | CS | 126 | 324 | 472 | 50 | 68 | 8 | 10 | <LDL | 9500 |
| 1463.85 | CS | 220 | 276 | 246 | 86 | 123 | 11 | 10 | <LDL | 6900 |
| 1464.85 | CS | 436 | 424 | 132 | 296 | 121 | 19 | 10 | <LDL | 6200 |
| 1465.85 | CS | 178 | 142 | 16 | 112 | 50 | 16 | 20 | <LDL | 550 |
| 1466.85 | CS | 157 | 160 | 12 | 63 | 81 | 13 | 30 | <LDL | 550 |
| 1467.7 | CS | 87 | 96 | 4 | 66 | 16 | 5 | 20 | <LDL | 200 |
| 1468.48 | CS | 10 | 44 | 8 | 6 | 2 | 2 | 10 | <LDL | 1050 |
| 1469.48 | CS | 7 | 40 | 16 | 3 | 1 | 3 | 10 | <LDL | 350 |
| 1470.48 | CS | 6 | 38 | 26 | 3 | 1 | 2 | 10 | <LDL | 400 |
| 1471.48 | CS | 4 | 10 | 10 | 2 | 1 | 1 | 10 | <LDL | 600 |
| 1472.48 | CS | 3 | 4 | 2 | 1 | 1 | 1 | 10 | <LDL | 700 |
| 1473.48 | CS | 3 | 4 | 2 | 1 | 1 | 1 | 10 | <LDL | 650 |
| 1474.4 | CS | 3 | 4 | 2 | 1 | 1 | 1 | 10 | <LDL | 650 |
| 1475.4 | CS | 3 | 8 | 2 | 1 | 1 | 1 | 10 | <LDL | 750 |
| 1476.4 | CS | 3 | 14 | 4 | 1 | 1 | 1 | 10 | <LDL | 900 |

Notes: Samples are continuous from start to start of next sample. 4PGE = Pt+Pd+Au+Rh. Stratigraphy Codes: BCU= Bastard Cyclic Unit, MCU = Merensky Cyclic Unit, QFV = Quartz Feldspar Vein, FCU = Footwall Cyclic Unit, UG2CU = Upper Group 2 Cyclic Unit, FAZ = Footwall Assimilation Zone, Cs = Calc-silicate footwall

Table 5. Pt, Pd and Au Data for UMT094 and De Hoop farm (ALS method PGM-MS23L and PGM-ICP27)

| | Analyte | Au | Pt | Pd | Au | Pt | Pd |
|---|---|---|---|---|---|---|---|
| | Units | ppb | ppb | ppb | ppm | ppm | ppm |
| | LDL | 1 | 0.1 | 0.2 | 0.01 | 0.01 | 0.01 |
| Sample | Stratigraphy | | | | | | |
| UMT094-1096 | MZ | 1 | 1.7 | 0.8 | | | |
| UMT094-1111 | MZ | 2 | 0.9 | 0.8 | | | |
| UMT094-1135 | MZ | 1 | 2.4 | 1.1 | | | |
| UMT094-1165 | MZ | 2 | 2.7 | 1.1 | | | |
| UMT094-1184 | MZ | 1 | 1.9 | 1.1 | | | |
| UMT094-1213 | BCU | 2 | 16.6 | 1.4 | | | |
| UMT094-1218 | BCU | 2 | 2.9 | 2.1 | | | |
| UMT094-1226 | BCU | 2 | 2.4 | 0.5 | | | |
| UMT094-1228 | BCU | 2 | 1.7 | 0.8 | | | |
| UMT094-1232 | BCU | 290 | 603 | 323 | | | |
| UMT094-1233 | MCU | 598 | >1000 | >1000 | 1.23 | 1.46 | 1.27 |
| UMT094-1238 | MCU | 229 | 538 | 217 | | | |
| UMT094-1245 | MCU | 52 | 90.3 | 26.9 | | | |
| UMT094-1252 | MCU | 126 | 326 | 119 | | | |
| UMT094-1254 | MCU | 213 | >1000 | >1000 | 0.18 | 1.44 | 1.18 |
| UMT094-1258 | MCU | 144 | >1000 | >1000 | 0.14 | 1.25 | 1.10 |
| UMT094-1265 | MCU | 78 | 630 | 664 | | | |
| UMT094-1273 | MCU | 111 | >1000 | >1000 | NSS | NSS | NSS |
| UMT094-1277 | MCU | 115 | >1000 | >1000 | 0.14 | 1.06 | 1.08 |
| UMT094-1278 | MCU | 52 | 134 | 70.3 | | | |
| UMT094-1279 | MCU | 65 | 448 | 398 | | | |
| UMT094-1282 | MCU | 40 | 287 | 311 | | | |
| UMT094-1285 | MCU | 294 | >1000 | >1000 | 0.36 | 1.76 | 2.03 |
| UMT094-1286 | MCU | 155 | 956 | 946 | | | |
| UMT094-1288 | MCU | 139 | 699 | 615 | | | |
| UMT094-1289 | MCU | 130 | >1000 | >1000 | 0.17 | 0.93 | 1.03 |
| UMT094-1291A | MCU | 188 | 969 | >1000 | 0.20 | 0.91 | 1.06 |
| UMT094-1291B | MCU | 190 | 979 | 944 | | | |
| UMT094-1292A | FCU | 347 | 877 | 769 | | | |
| UMT094-1292B | FCU | 2 | 113.5 | 39.5 | | | |
| UMT094-1294 | FCU | 2 | 47.3 | 6.7 | | | |
| UMT094-1296 | FCU | 20 | 46.4 | 63.4 | | | |
| UMT094-1300 | FCU | 4 | 65.3 | 29.1 | | | |

Table 5. (Cont.)

| | Analyte | Au | Pt | Pd | Au | Pt | Pd |
|---|---|---|---|---|---|---|---|
| | Units | ppb | ppb | ppb | ppm | ppm | ppm |
| | LDL | 1 | 0.1 | 0.2 | 0.01 | 0.01 | 0.01 |
| Sample | Stratigraphy | | | | | | |
| UMT094-1308 | FCU | 4 | 36.6 | 20.2 | | | |
| UMT094-1311 | FCU | 102 | 581 | 657 | | | |
| UMT094-1319 | FCU | 110 | 488 | 432 | | | |
| UMT094-1325A | FCU | 143 | >1000 | 910 | 0.13 | 1.06 | 0.86 |
| UMT094-1325B | FCU | 11 | 55.7 | 36.6 | | | |
| UMT094-1326A | FCU | 63 | 483 | 313 | | | |
| UMT094-1326B | FCU | 97 | >1000 | 921 | 0.10 | 1.29 | 0.92 |
| UMT094-1327 | FCU | 12 | 115.5 | 173.5 | | | |
| UMT094-1329 | FCU | 25 | 312 | 263 | | | |
| UMT094-1332 | FCU | 63 | 290 | 354 | | | |
| UMT094-1334 * | UG2HW | 37 | 44.2 | 100.5 | | | |
| UMT094-1335 | UG2HW | 380 | 724 | 854 | | | |
| UMT094-1336A | UG2HW | 137 | 513 | 529 | | | |
| UMT094-1336B | UG2HW | 207 | >1000 | >1000 | 0.25 | 1.57 | 1.57 |
| UMT094-1337 | UG2HW | 240 | >1000 | >1000 | 0.19 | 3.17 | 2.11 |
| UMT094-1339 | UG2HW | 30 | 250 | 203 | | | |
| UMT094-1340 | UG2HW | 22 | 137.5 | 149.5 | | | |
| UMT094-1343 | UG2HW | 6 | 22.4 | 19.7 | | | |
| UMT094-1351 | UG2HW | 12 | 58.4 | 71.4 | | | |
| UMT094-1359 | FAZ | 18 | 79.2 | 159.5 | | | |
| UMT094-1365 | UG2FW | 16 | 173.5 | 194 | | | |
| UMT094-1366 | FAZ | 51 | 654 | 742 | | | |
| UMT094-1376 | FAZ | 24 | 460 | 612 | | | |
| UMT094-1384 | UG2FW | 63 | 96.3 | 198.5 | | | |
| UMT094-1386 | FAZ | 25 | 890 | 337 | | | |
| UMT094-1402 | UG2FW | 18 | 203 | 307 | | | |
| UMT094-1405 | FAZ | 36 | 76.6 | 210 | | | |
| UMT094-1410 * | FW2A | 12 | 100.5 | 281 | | | |
| UMT094-1412 | FW2A | 6 | 47.0 | 140 | | | |
| UMT094-1421 | FW2A | 5 | 28.8 | 89.0 | | | |
| UMT094-1424 | FW2A | 56 | 209 | 479 | | | |
| UMT094-1436 | FW2A | 5 | 6.1 | 16.9 | | | |
| UMT094-1454 * | FW2A | 24 | 27.9 | 88.8 | | | |

Table 5. (Cont.)

| | Analyte | Au | Pt | Pd | Au | Pt | Pd |
|---|---|---|---|---|---|---|---|
| | Units | ppb | ppb | ppb | ppm | ppm | ppm |
| | LDL | 1 | 0.1 | 0.2 | 0.01 | 0.01 | 0.01 |
| Sample | Stratigraphy | | | | | | |
| UMT094-1457 | FW2A | 5 | 13.2 | 38.9 | | | |
| UMT094-1461 * | FW2A | 95 | 109 | 278 | | | |
| UMT094-1463 * | FW2A | 4 | 16.6 | 1.0 | | | |
| UMT094-1466 * | FW2A | 18 | 227 | 49.7 | | | |
| UMT094-1479 | FW2A | 7 | 5.7 | 12 | | | |
| UMT094-1494 | TVL - DS | 3 | 1.9 | 1.1 | | | |
| UMT094-1537 | TVL – DS | 3 | 1.1 | 0.8 | | | |
| UMT094-1573 | TVL – DS | 4 | 2.3 | 2.3 | | | |
| UMT094-1601 | TVL – DS | 3 | 0.3 | 0.3 | | | |
| LUD001 | TVL – Shale | 4 | 2.4 | 2.2 | | | |
| LUD002 | TVL – Shale | 3 | 2.3 | 2.4 | | | |
| LUD003 | TVL | 2 | 0.2 | 0.4 | | | |
| LUD004 | TVL – Qtz | 1 | 0.2 | <0.2 | | | |
| LUD005 | TVL – Shale | 10 | 0.1 | <0.2 | | | |
| LUD006 | TVL – DS | 2 | 0.2 | 0.3 | | | |
| LUD007 | TVL | 1 | 1.1 | 0.7 | | | |
| LUD008 | TVL – Qtz | 2 | 0.1 | 0.2 | | | |
| LUD009 | TVL – Shale | 2 | 3.1 | 2.7 | | | |
| LUD010A | TVL – Qtz | 2 | <0.1 | <0.2 | | | |
| LUD010B | TVL – DS | 2 | 0.1 | 0.2 | | | |
| LUD011 | TVL – DS | 2 | 0.1 | <0.2 | | | |

Stratigraphy Codes: MZ =Main Zone, BCU= Bastard Cyclic Unit, MCU = Merensky Cyclic Unit, FCU = Footwall Cyclic Unit, UG2CU = Upper Group 2 Cyclic Unit, FAZ = Footwall Assimilation Zone, FW2A = Calc-silicate footwall, TVL = Transvaal, DS = Dolostone, Qtz = quartzite
NSS = Not sufficient sample
* Sample was for mineral identification, was non-representative and excluded from geochemical interpretation.

Table 6. Major and Trace Element Data for ATS139 and UMT 365 (ALS Method ME-MS61L)

| | | Analyte | Ag | Al | As | Ba | Be | Bi | Ca | Cd | Ce | Co |
|---|---|---|---|---|---|---|---|---|---|---|---|---|
| | | Units | ppm | % | ppm | ppm | ppm | ppm | % | ppm | ppm | ppm |
| | | LDL | 0.002 | 0.01 | 0.05 | 1 | 0.02 | 0.005 | 0.01 | 0.005 | 0.01 | 0.005 |
| Sample | Lithology | Stratigraphy | | | | | | | | | | |
| 139-0081 | GRV | MZ | 0.023 | 9.40 | 1.55 | 150 | 0.46 | 0.013 | 7.66 | 0.057 | 7.75 | 41 |
| 139-0111 | PX | MCU | 0.358 | 2.93 | 1.46 | 43 | 0.14 | 0.699 | 2.77 | 0.183 | 6.06 | 123 |
| 139-0113 | APX | MCU | 0.161 | 2.12 | 12.55 | 29 | 0.44 | 0.466 | 2.37 | 0.042 | 13.45 | 141.5 |
| 139-0117 | AS-HF | MCU | 1.830 | 2.41 | 2.19 | 35 | 0.14 | 0.623 | 2.32 | 0.284 | 4.91 | 161.5 |
| 139-0121 | APX | MCU | 0.733 | 2.25 | 1.15 | 10 | 0.08 | 0.773 | 1.93 | 0.278 | 4.61 | 137 |
| 139-0128 | AS | FAZ | 0.499 | 9.72 | 1.26 | 184 | 0.31 | 1.120 | 6.90 | 0.167 | 5.66 | 98.1 |
| 139-0155 | AS-HF | FAZ | 0.170 | 8.01 | 23.6 | 212 | 0.19 | 1.100 | 6.16 | 0.155 | 4.68 | 98.4 |
| 139-0168 | AS-HF | FAZ | 0.568 | 9.16 | 24.7 | 253 | 0.32 | 1.515 | 6.79 | 0.282 | 8.82 | 173.5 |
| 139-0179 | AS-HF | FAZ | 0.059 | 8.91 | 23.7 | 76 | 0.29 | 0.260 | 6.07 | 0.042 | 7.79 | 47.6 |
| 139-0206 | AS-HF | FAZ | 0.245 | 8.78 | 59.4 | 81 | 0.39 | 1.700 | 5.32 | 0.191 | 10.25 | 117.5 |
| 139-0218 | AS-HF | FAZ | 0.051 | 7.12 | 9.05 | 74 | 0.54 | 0.361 | 4.22 | 0.146 | 10.05 | 27.7 |
| 139-0226 | AS-HF | FAZ | 0.112 | 7.27 | 6.55 | 82 | 0.34 | 0.620 | 5.24 | 0.044 | 7.77 | 85.4 |
| 139-0231 | GRV | FAZ | 0.028 | 5.79 | 3.34 | 227 | 9.99 | 0.143 | 0.43 | 0.015 | 25.6 | 2.21 |
| 139-0259 | AS-HF | FAZ | 0.050 | 5.45 | 3.35 | 54 | 0.41 | 1.215 | 4.08 | 0.115 | 4.71 | 87 |
| 139-0270 | AS-HF | FAZ | 0.258 | 8.95 | 9.02 | 98 | 0.92 | 0.437 | 6.03 | 0.147 | 15.8 | 41.1 |
| 139-0275 | HF | FAZ | 0.018 | 11.15 | 68.6 | 2 | 4.66 | 0.364 | 0.04 | <0.005 | 0.20 | 36 |
| 139-0276 | HF | FAZ | 0.025 | 10.30 | 6.45 | 690 | 1.12 | 0.118 | 5.05 | 0.076 | 1.66 | 11.85 |
| 139-0298 | HF | FAZ | 0.004 | 11.60 | 75.7 | 166 | 4.20 | 0.212 | 0.23 | 0.036 | 0.99 | 35.9 |
| 139-0302 | HF | FAZ | 0.086 | 7.33 | 15.85 | 342 | 2.98 | 1.015 | 1.80 | 0.052 | 7.07 | 138.5 |
| 139-0307 | QTZ | TVL | 0.029 | 0.25 | 3.03 | 15 | 0.06 | 0.077 | 0.30 | 0.007 | 1.50 | 2.35 |
| 365-1253 | PX | MCU | 0.252 | 1.40 | 0.25 | 19 | 0.08 | 0.250 | 1.68 | 0.099 | 2.38 | 99.2 |
| 365-1260 | PGPX | MCU | 0.939 | 2.98 | 0.21 | 34 | 0.12 | 0.437 | 4.38 | 0.223 | 7.07 | 181 |
| 365-1283 | APX | MCU | 0.596 | 1.27 | 0.29 | 12 | 0.06 | 0.593 | 1.66 | 0.173 | 1.48 | 119.5 |
| 365-1348 | CS | FAZ | 0.776 | 3.27 | 1.04 | <1 | 0.18 | 2.400 | 11.35 | 1.715 | 8.44 | 80.6 |
| 365-1408 | CS | FAZ | 0.114 | 3.86 | 6.79 | 64 | 0.17 | 0.198 | 10.65 | 0.342 | 10.9 | 42 |
| 365-1429 | CS | FAZ | 1.390 | 5.41 | 3.48 | 1 | 0.10 | 1.250 | 4.64 | 0.181 | 9.47 | 77.2 |

Table 6. (Cont.)

| Sample | Lithology | Stratigraphy | Cr | Cs | Cu | Fe | Ga | Ge | Hf | In | K | La |
|---|---|---|---|---|---|---|---|---|---|---|---|---|
| | | Analyte | Cr | Cs | Cu | Fe | Ga | Ge | Hf | In | K | La |
| | | Units | ppm | ppm | ppm | % | ppm | ppm | ppm | ppm | % | ppm |
| | | LDL | 0.3 | 0.01 | 0.02 | 0.002 | 0.05 | 0.05 | 0.004 | 0.005 | 0.01 | 0.005 |
| 139-0081 | GRV | MZ | 225 | 0.76 | 50.1 | 4.68 | 17.7 | 0.05 | 0.385 | 0.025 | 0.43 | 3.96 |
| 139-0111 | PX | MCU | 1450 | 1.87 | 592 | 8.23 | 5.45 | 0.09 | 0.341 | 0.021 | 0.11 | 3.10 |
| 139-0113 | APX | MCU | 1385 | 1.77 | 712 | 7.99 | 5.81 | 0.09 | 0.728 | 0.032 | 0.15 | 7.20 |
| 139-0117 | AS-HF | MCU | 1475 | 1.09 | 1920 | 9.16 | 4.96 | 0.13 | 0.278 | 0.045 | 0.05 | 2.69 |
| 139-0121 | APX | MCU | 1635 | 1.41 | 1560 | 9.12 | 3.96 | 0.10 | 0.318 | 0.043 | 0.02 | 2.24 |
| 139-0128 | AS | FAZ | 398 | 2.19 | 1080 | 4.59 | 14.2 | 0.07 | 0.222 | 0.028 | 0.53 | 2.85 |
| 139-0155 | AS-HF | FAZ | 398 | 1.21 | 628 | 5.40 | 14.5 | 0.07 | 0.193 | 0.021 | 0.59 | 2.50 |
| 139-0168 | AS-HF | FAZ | 280 | 1.37 | 1030 | 7.05 | 16.45 | 0.10 | 0.377 | 0.021 | 0.43 | 4.73 |
| 139-0179 | AS-HF | FAZ | 341 | 1.00 | 75.3 | 5.59 | 16.6 | <0.05 | 0.506 | 0.011 | 0.26 | 4.21 |
| 139-0206 | AS-HF | FAZ | 398 | 1.27 | 526 | 8.83 | 17.15 | 0.10 | 0.490 | 0.030 | 0.28 | 5.30 |
| 139-0218 | AS-HF | FAZ | 328 | 0.93 | 7.9 | 8.86 | 16.75 | 0.08 | 0.558 | 0.036 | 0.18 | 5.28 |
| 139-0226 | AS-HF | FAZ | 343 | 1.01 | 391 | 9.92 | 19.75 | 0.12 | 0.390 | 0.045 | 0.40 | 4.05 |
| 139-0231 | GRV | FAZ | 19.3 | 0.35 | 302 | 0.32 | 24.2 | 0.07 | 6.30 | 0.026 | 2.49 | 11 |
| 139-0259 | AS-HF | FAZ | 743 | 0.42 | 91.9 | 10.45 | 13.0 | 0.10 | 0.371 | 0.038 | 0.10 | 2.55 |
| 139-0270 | AS-HF | FAZ | 199.5 | 1.26 | 220 | 5.82 | 20.1 | 0.07 | 0.758 | 0.022 | 0.29 | 7.77 |
| 139-0275 | HF | FAZ | 308 | 4.13 | 13.45 | 7.71 | 35.2 | 0.06 | 0.023 | 0.005 | 0.01 | 0.112 |
| 139-0276 | HF | FAZ | 352 | 6.19 | 14.8 | 3.06 | 24.6 | <0.05 | 0.009 | <0.005 | 1.47 | 0.981 |
| 139-0298 | HF | FAZ | 189.5 | 13.75 | 12.7 | 7.48 | 29.5 | 0.07 | 0.122 | <0.005 | 1.79 | 0.487 |
| 139-0302 | HF | FAZ | 485 | 3.45 | 1000 | 17.1 | 19.8 | 0.25 | 0.111 | <0.005 | 2.24 | 3.93 |
| 139-0307 | QTZ | TVL | 42.8 | 0.04 | 22.9 | 0.54 | 0.47 | <0.05 | 0.185 | <0.005 | 0.19 | 0.816 |
| 365-1253 | PX | MCU | 2970 | 0.52 | 573 | 7.60 | 3.94 | 0.07 | 0.230 | 0.019 | 0.05 | 1.18 |
| 365-1260 | PGPX | MCU | >10000 | 0.73 | 2040 | 9.85 | 12.25 | 0.14 | 0.417 | 0.028 | 0.06 | 3.33 |
| 365-1283 | APX | MCU | 2830 | 0.33 | 1400 | 7.91 | 3.64 | 0.09 | 0.151 | 0.025 | 0.03 | 0.701 |
| 365-1348 | CS | FAZ | 26.9 | 0.01 | 1640 | 4.94 | 11.0 | 0.08 | 0.658 | 0.047 | <0.01 | 2.62 |
| 365-1408 | CS | FAZ | 127 | 0.88 | 341 | 5.02 | 8.08 | 0.05 | 0.739 | 0.043 | 0.14 | 5.49 |
| 365-1429 | CS | FAZ | 23.2 | 0.01 | 320 | 4.07 | 19.25 | 0.10 | 0.549 | 0.032 | <0.01 | 3.62 |

Table 6. (Cont.)

| Sample | Lithology | Stratigraphy | Li | Mg | Mn | Mo | Na | Nb | Ni | P | Pb | Rb |
|---|---|---|---|---|---|---|---|---|---|---|---|---|
| | | Analyte | Li | Mg | Mn | Mo | Na | Nb | Ni | P | Pb | Rb |
| | | Units | ppm | % | ppm | ppm | % | ppm | ppm | % | ppm | ppm |
| | | LDL | 0.2 | 0.01 | 0.2 | 0.02 | 0.001 | 0.005 | 0.08 | 0.001 | 0.01 | 0.02 |
| 139-0081 | GRV | MZ | 9.9 | 3.24 | 877 | 0.27 | 1.875 | 0.651 | 148 | 0.014 | 5.95 | 9.93 |
| 139-0111 | PX | MCU | 11.2 | 13.5 | 1490 | 0.58 | 0.342 | 0.984 | 2260 | 0.005 | 8.23 | 7.38 |
| 139-0113 | APX | MCU | 9.8 | 13.15 | 1125 | 0.96 | 0.123 | 1.045 | 2380 | 0.018 | 2.11 | 14.85 |
| 139-0117 | AS-HF | MCU | 13.3 | 13.7 | 1560 | 0.64 | 0.289 | 0.347 | 3800 | 0.007 | 8.39 | 2.40 |
| 139-0121 | APX | MCU | 25.1 | 14.2 | 1480 | 0.40 | 0.100 | 0.520 | 2650 | 0.004 | 12.15 | 2.30 |
| 139-0128 | AS | FAZ | 12.6 | 5.37 | 769 | 0.63 | 1.09 | 0.242 | 1555 | 0.005 | 8.30 | 23.3 |
| 139-0155 | AS-HF | FAZ | 9.0 | 5.03 | 810 | 2.01 | 0.657 | 0.368 | 1330 | 0.005 | 13.4 | 24.3 |
| 139-0168 | AS-HF | FAZ | 7.5 | 3.70 | 733 | 4.93 | 0.848 | 0.659 | 1420 | 0.009 | 10.65 | 18.15 |
| 139-0179 | AS-HF | FAZ | 7.3 | 4.99 | 828 | 2.13 | 1.010 | 0.795 | 233 | 0.006 | 3.06 | 9.62 |
| 139-0206 | AS-HF | FAZ | 2.9 | 4.77 | 868 | 3.50 | 1.055 | 1.17 | 926 | 0.010 | 11.65 | 11.65 |
| 139-0218 | AS-HF | FAZ | 4.3 | 5.00 | 1340 | 1.51 | 1.410 | 2.58 | 14.3 | 0.013 | 6.68 | 5.51 |
| 139-0226 | AS-HF | FAZ | 6.8 | 4.01 | 1300 | 3.25 | 0.969 | 0.622 | 443 | 0.008 | 4.11 | 14.2 |
| 139-0231 | GRV | FAZ | 1.2 | 0.03 | 39.1 | 0.63 | 3.59 | 63.7 | 47 | 0.001 | 21.4 | 95.4 |
| 139-0259 | AS-HF | FAZ | 6.3 | 7.79 | 1690 | 0.32 | 0.852 | 0.519 | 599 | 0.005 | 2.64 | 2.59 |
| 139-0270 | AS-HF | FAZ | 10.5 | 3.57 | 934 | 0.40 | 1.95 | 1.095 | 144.5 | 0.074 | 10.9 | 8.02 |
| 139-0275 | HF | FAZ | 95.1 | 1.79 | 328 | 2.24 | 0.109 | 0.071 | 153.5 | <0.001 | 0.17 | 19.6 |
| 139-0276 | HF | FAZ | 102.5 | 2.16 | 353 | 1.65 | 0.403 | 0.069 | 85.5 | <0.001 | 8.90 | 33 |
| 139-0298 | HF | FAZ | 88 | 1.81 | 521 | 2.15 | 0.427 | 0.557 | 121.5 | 0.002 | 2.31 | 54.2 |
| 139-0302 | HF | FAZ | 20.1 | 2.95 | 686 | 24.8 | 0.301 | 1.06 | 536 | 0.073 | 6.04 | 109.5 |
| 139-0307 | QTZ | TVL | 2.0 | 0.15 | 60.5 | 2.08 | 0.007 | 0.737 | 9.99 | 0.043 | 5.93 | 5.47 |
| 365-1253 | PX | MCU | 4.3 | 17.15 | 1515 | 0.29 | 0.146 | 0.245 | 1450 | 0.003 | 2.33 | 2.45 |
| 365-1260 | PGPX | MCU | 9.3 | 13.55 | 1265 | 0.26 | 0.238 | 0.485 | 4190 | 0.013 | 7.90 | 1.98 |
| 365-1283 | APX | MCU | 3.4 | 16.35 | 1515 | 0.27 | 0.105 | 0.106 | 2520 | 0.001 | 4.69 | 1.57 |
| 365-1348 | CS | FAZ | 0.5 | 13.45 | 457 | 0.11 | 0.013 | 0.931 | 2180 | 0.002 | 261 | 0.05 |
| 365-1408 | CS | FAZ | 15.3 | 12.45 | 940 | 0.19 | 0.108 | 0.97 | 151 | 0.078 | 12.05 | 11.05 |
| 365-1429 | CS | FAZ | 1.2 | 16.85 | 1090 | 0.09 | 0.002 | 2.06 | 2110 | 0.003 | 14.25 | 0.10 |

Table 6. (Cont.)

| | | Analyte | Re | S | Sb | Sc | Se | Sn | Sr | Ta | Te | Th |
|---|---|---|---|---|---|---|---|---|---|---|---|---|
| | | Units | ppm | % | ppm | ppm | ppm | ppm | ppm | ppm | ppm | ppm |
| | | LDL | 0.002 | 0.01 | 0.02 | 0.01 | 0.2 | 0.02 | 0.02 | 0.01 | 0.04 | 0.004 |
| Sample | Lithology | Stratigraphy | | | | | | | | | | |
| 139-0081 | GRV | MZ | <0.002 | 0.15 | 0.83 | 16 | <0.2 | 0.25 | 305 | 0.04 | <0.04 | 0.417 |
| 139-0111 | PX | MCU | 0.007 | 0.67 | 0.23 | 26 | 1.6 | 0.39 | 46.6 | 0.07 | 0.53 | 1.155 |
| 139-0113 | APX | MCU | 0.015 | 0.93 | 0.82 | 29.2 | 2.5 | 0.82 | 12.1 | 0.08 | 0.72 | 1.67 |
| 139-0117 | AS-HF | MCU | 0.009 | 1.23 | 0.22 | 26.7 | 4.3 | 0.35 | 34.1 | 0.02 | 0.64 | 0.342 |
| 139-0121 | APX | MCU | 0.008 | 0.74 | 0.17 | 25 | 2.9 | 0.34 | 9.97 | 0.04 | 0.66 | 0.637 |
| 139-0128 | AS | FAZ | 0.007 | 0.65 | 0.19 | 12 | 2.1 | 0.30 | 314 | 0.02 | 0.24 | 0.284 |
| 139-0155 | AS-HF | FAZ | 0.010 | 1.00 | 0.63 | 9.49 | 3.2 | 0.27 | 198.5 | 0.02 | 0.33 | 0.664 |
| 139-0168 | AS-HF | FAZ | 0.015 | 2.37 | 0.36 | 13.55 | 6.3 | 0.48 | 224 | 0.04 | 0.36 | 0.833 |
| 139-0179 | AS-HF | FAZ | <0.002 | 0.17 | 0.51 | 20.8 | 0.4 | 0.31 | 198 | 0.06 | <0.04 | 0.743 |
| 139-0206 | AS-HF | FAZ | 0.009 | 1.32 | 0.97 | 28.8 | 3.0 | 0.63 | 174.5 | 0.09 | 0.24 | 0.848 |
| 139-0218 | AS-HF | FAZ | <0.002 | 0.40 | 0.44 | 31.7 | <0.2 | 0.72 | 170.5 | 0.19 | <0.04 | 0.806 |
| 139-0226 | AS-HF | FAZ | 0.006 | 2.23 | 0.38 | 20.7 | 6.5 | 0.39 | 168.5 | 0.05 | 0.30 | 0.576 |
| 139-0231 | GRV | FAZ | <0.002 | 0.10 | 0.34 | 0.92 | 0.2 | 3.07 | 31.1 | 5.87 | <0.04 | 36.6 |
| 139-0259 | AS-HF | FAZ | 0.002 | 0.30 | 0.11 | 28 | 0.6 | 0.26 | 133 | 0.04 | 0.10 | 0.539 |
| 139-0270 | AS-HF | FAZ | <0.002 | 0.28 | 0.73 | 20.1 | 0.4 | 0.87 | 264 | 0.11 | <0.04 | 2.67 |
| 139-0275 | HF | FAZ | 0.005 | 0.01 | 1.07 | 4.25 | <0.2 | 0.18 | 4.87 | <0.01 | <0.04 | 0.059 |
| 139-0276 | HF | FAZ | <0.002 | <0.01 | 0.94 | 4.52 | <0.2 | 0.16 | 292 | <0.01 | <0.04 | 0.010 |
| 139-0298 | HF | FAZ | 0.003 | 0.16 | 0.74 | 4 | 0.3 | 0.13 | 38.4 | 0.06 | 0.06 | 0.259 |
| 139-0302 | HF | FAZ | 0.034 | 7.82 | 0.29 | 9.93 | 28.7 | 0.08 | 92.6 | 0.03 | 1.16 | 0.549 |
| 139-0307 | QTZ | TVL | <0.002 | 0.07 | 0.30 | 0.2 | <0.2 | 0.29 | 1.16 | 0.04 | <0.04 | 2.83 |
| 365-1253 | PX | MCU | 0.002 | 0.24 | 0.07 | 24.6 | 0.8 | 0.18 | 16.1 | 0.02 | 0.34 | 0.213 |
| 365-1260 | PGPX | MCU | 0.007 | 0.91 | 0.09 | 20.1 | 3.9 | 0.37 | 37.5 | 0.04 | 0.69 | 0.626 |
| 365-1283 | APX | MCU | 0.005 | 0.67 | 0.06 | 26.5 | 2.2 | 0.30 | 13.85 | 0.01 | 0.60 | 0.092 |
| 365-1348 | CS | FAZ | <0.002 | 0.38 | 0.15 | 6.36 | 2.7 | 2.78 | 7.61 | 0.25 | 0.65 | 2.53 |
| 365-1408 | CS | FAZ | <0.002 | 0.44 | 0.70 | 27.9 | 0.8 | 0.66 | 47.1 | 0.04 | 0.09 | 0.667 |
| 365-1429 | CS | FAZ | 0.002 | 0.29 | 0.82 | 4.5 | 0.8 | 1.43 | 1.07 | 0.25 | 0.47 | 3.43 |

Table 6. (Cont.)

| | | Analyte | Ti | Tl | U | V | W | Y | Zn | Zr |
|---|---|---|---|---|---|---|---|---|---|---|
| | | Units | % | ppm | ppm | ppm | ppm | ppm | ppm | ppm |
| | | LDL | 0.001 | 0.004 | 0.01 | 0.1 | 0.008 | 0.01 | 0.2 | 0.1 |
| Sample | Lithology | Stratigraphy | | | | | | | | |
| 139-0081 | GRV | MZ | 0.144 | 0.098 | 0.12 | 104 | 0.123 | 5.00 | 49.2 | 13.2 |
| 139-0111 | PX | MCU | 0.102 | 0.100 | 0.31 | 245 | 0.446 | 3.00 | 78.0 | 11.0 |
| 139-0113 | APX | MCU | 0.154 | 0.150 | 0.44 | 265 | 0.243 | 6.46 | 51.5 | 29.3 |
| 139-0117 | AS-HF | MCU | 0.101 | 0.081 | 0.10 | 231 | 0.231 | 3.58 | 77.6 | 8.4 |
| 139-0121 | APX | MCU | 0.099 | 0.061 | 0.19 | 213 | 0.133 | 3.15 | 92.3 | 10.2 |
| 139-0128 | AS | FAZ | 0.063 | 0.135 | 0.10 | 139.5 | 0.157 | 2.63 | 43.4 | 7.7 |
| 139-0155 | AS-HF | FAZ | 0.068 | 0.196 | 0.27 | 206 | 0.184 | 2.72 | 42.9 | 6.7 |
| 139-0168 | AS-HF | FAZ | 0.087 | 0.217 | 0.27 | 185 | 0.577 | 3.72 | 47.1 | 12.2 |
| 139-0179 | AS-HF | FAZ | 0.095 | 0.085 | 0.32 | 211 | 0.167 | 3.75 | 36.2 | 19.3 |
| 139-0206 | AS-HF | FAZ | 0.114 | 0.102 | 0.35 | 352 | 0.331 | 4.29 | 52.4 | 16.0 |
| 139-0218 | AS-HF | FAZ | 0.226 | 0.036 | 0.32 | 420 | 0.352 | 5.04 | 90.5 | 19.0 |
| 139-0226 | AS-HF | FAZ | 0.103 | 0.138 | 0.23 | 370 | 0.112 | 4.00 | 74.5 | 11.9 |
| 139-0231 | GRV | FAZ | 0.038 | 0.611 | 30.3 | 1.0 | 0.527 | 88.4 | 7.1 | 93.6 |
| 139-0259 | AS-HF | FAZ | 0.127 | 0.030 | 0.22 | 187.5 | 0.125 | 3.97 | 94.9 | 11.7 |
| 139-0270 | AS-HF | FAZ | 0.086 | 0.089 | 1.37 | 103 | 0.54 | 6.78 | 55.8 | 25.1 |
| 139-0275 | HF | FAZ | 0.041 | 0.142 | 0.03 | 230 | 0.028 | 0.09 | 47.8 | 0.6 |
| 139-0276 | HF | FAZ | 0.015 | 1.27 | 0.02 | 441 | 0.744 | 0.19 | 90.6 | 0.3 |
| 139-0298 | HF | FAZ | 0.049 | 0.919 | 0.22 | 155.5 | 0.199 | 0.33 | 74.2 | 4.0 |
| 139-0302 | HF | FAZ | 0.037 | 1.085 | 0.53 | 338 | 0.291 | 3.69 | 19.2 | 3.6 |
| 139-0307 | QTZ | TVL | 0.022 | 0.043 | 9.38 | 3.0 | 0.128 | 1.76 | 3.4 | 6.6 |
| 365-1253 | PX | MCU | 0.085 | 0.027 | 0.06 | 96.6 | 0.036 | 2.76 | 72.2 | 7.5 |
| 365-1260 | PGPX | MCU | 0.136 | 0.058 | 0.13 | 285 | 0.032 | 4.87 | 147.5 | 14.7 |
| 365-1283 | APX | MCU | 0.072 | 0.040 | 0.02 | 94.5 | 0.026 | 2.41 | 72.7 | 5.1 |
| 365-1348 | CS | FAZ | 0.127 | 0.124 | 0.10 | 23.5 | 0.298 | 8.80 | 111 | 13.2 |
| 365-1408 | CS | FAZ | 0.146 | 0.130 | 0.32 | 112.5 | 0.783 | 7.95 | 135 | 20.2 |
| 365-1429 | CS | FAZ | 0.163 | 0.927 | 0.50 | 21.6 | 0.394 | 11.45 | 139 | 16.0 |

Lithology codes: GRV = Granitic Vein, PX = Pyroxenite, APX = Altered Pyroxenite, AS-HF = Horfelsed shale assimilation, HF = Hornfelsed shale, QTZ = Quartzite, PGPX = Pegmatoidal Pyroxentite, CS = Calc-silicate Stratigraphy Codes: MZ = Main Zone, MCU = Merensky Cyclic Unit, FAZ = Footwall Assimilation Zone, TVL = Transvaal,

Table 7. $\delta^{34}S$ for UMT094

| Sample ID | Type | Depth | wt. % S | $\delta^{34}S$‰ vs VCDT |
|---|---|---|---|---|
| UMT094-1233 | Drill | 1233 | 9.7 | 2.5 |
| UMT094-1233 | Drill | 1233 | 29.3 | 2.8 |
| UMT094-1233 | Drill | 1233 | 33.4 | 2.6 |
| UMT094-1238 | Drill | 1238 | 33.5 | 2.7 |
| UMT094-1245 | Drill | 1245 | 26.4 | 2.4 |
| UMT094-1252 | Drill | 1252 | 24.5 | 2.2 |
| UMT094-1253 | IVP Pulp Whole Rock | 1253 | 0.7 | 2.3 |
| UMT094-1257 | IVP Pulp Whole Rock | 1257 | 0.45 | 2.4 |
| UMT094-1258 | IVP Pulp Whole Rock | 1258 | 0.47 | 1.5 |
| UMT094-1262 | IVP Pulp Whole Rock | 1262 | 0.435 | 2.1 |
| UMT094-1265 | IVP Pulp Whole Rock | 1265 | 0.205 | 3.9 |
| UMT094-1268 | IVP Pulp Whole Rock | 1268 | 0.83 | 3.7 |
| UMT094-1271 | IVP Pulp Whole Rock | 1271 | 0.585 | 2.0 |
| UMT094-1273 | IVP Pulp Whole Rock | 1273 | 0.445 | 2.4 |
| UMT094-1274 | IVP Pulp Whole Rock | 1274 | 2.02 | 3.7 |
| UMT094-1278 | Whole Rock | 1278 | 0.04 | 4.1 |
| UMT094-1282 | Drill | 1282 | 25.8 | 3.4 |
| UMT094-1288 | Drill | 1288 | 25.8 | 3.8 |
| UMT094-1291A | Drill | 1291 | 31.3 | 3.5 |
| UMT094-1291B | Drill | 1291 | 26.7 | 3.3 |
| UMT094-1311 | Drill | 1311 | 23.8 | 3.8 |
| UMT094-1319 | Drill | 1319 | 32.5 | 4.5 |
| UMT094-1329 | Drill | 1329 | 37.8 | 5.0 |
| UMT094-1333 | Drill | 1333 | 31.2 | 6.0 |
| UMT094-1335 | Drill | 1335 | 18.5 | 6.0 |
| UMT094-1336 | Whole Rock | 1336 | 0.3 | 6.6 |
| UMT094-1336 | Drill | 1336 | 33.8 | 5.3 |
| UMT094-1337 | Drill | 1337 | 9.8 | 5.0 |
| UMT094-1365 | Drill | 1365 | 7.4 | 7.9 |
| UMT094-1384 | Drill | 1384 | 38.1 | 8.1 |
| UMT094-1402 | Drill | 1402 | 33.2 | 8.0 |
| UMT094-1410 | Whole Rock | 1410 | 0.1 | 9.1 |
| UMT094-1410 | Drill | 1410 | 16.8 | 1.9 |
| UMT094-1424 | Whole Rock | 1424 | 0.1 | 7.5 |
| UMT094-1454 | Whole Rock | 1454 | 0.7 | 10.0 |
| UMT094-1494 | Whole Rock | 1494 | 0.1 | 8.9 |
| UMT094-1601 | Drill | 1601 | 4.7 | 3.7 |

Notes: IVP pulps were collected from remaining pulps of original assaying. Duplicates were reproducible to 0.2 ‰ $\delta^{34}S$.

# 10. Appendix

Table A1. Summary of thin section mineralogy estimates

| | Mafic | | | | | | | Felsic/Carbonate | | | | Sulphides/Oxides | | | | |
|---|---|---|---|---|---|---|---|---|---|---|---|---|---|---|---|---|
| Sample | Ol | Opx | Cpx | Amp | Bt | Chl | Tlc/WM | Qtz | Pl | Cal/Dol | Anh | Po | Py | Pn | Ccp | Mag |
| 94 - 1096 | 0 | 30 | 15 | 0 | 1 | 0 | 0 | 0 | 55 | 0 | 0 | 0 | 0 | 0 | 0 | 0 |
| 94 - 1233 | 0 | 60 | 20 | 0 | 0 | 0 | 0 | 0 | 20 | 0 | 0 | 0 | 0 | 0 | 0 | 0 |
| 94 - 1252 | 2 | 70 | 15 | 0 | 0 | 0 | 0 | 0 | 10 | 0 | 0 | 1 | 0 | 1 | 1 | 0 |
| 94 - 1256 | 0 | 60 | 30 | 0 | 3 | 0 | 0 | 0 | 5 | 0 | 0 | 1 | 0 | 0 | 1 | 0 |
| 94 - 1260 | 0 | 70 | 8 | 0 | 2 | 0 | 0 | 0 | 10 | 5 | 0 | 3 | 0 | 0 | 2 | 0 |
| 94 - 1285 | 0 | 5 | 57 | 1 | 0 | 0 | 10 | 0 | 16 | 10 | 0 | 1 | 0 | 0 | 0 | 0 |
| 94 - 1291 | 0 | 30 | 0 | 15 | 0 | 40 | 0 | 0 | 5 | 0 | 0 | 0 | 0 | 0 | 10 | 0 |
| 94 - 1292A | 15 | 5 | 15 | 0 | 0 | 0 | 0 | 0 | 60 | 0 | 0 | 0 | 0 | 0 | 0 | 5 |
| 94 - 1333 | 10 | 30 | 0 | 0 | 0 | 0 | 0 | 0 | 0 | 25 | 15 | 3 | 1 | 5 | 1 | 10 |
| 94 - 1359 | 0 | 49 | 0 | 0 | 0 | 0 | 30 | 0 | 7 | 0 | 0 | 2 | 2 | 1 | 2 | 7 |
| 94 - 1390-1 | 0 | 57 | 0 | 0 | 5 | 0 | 30 | 0 | 0 | 0 | 0 | 0 | 0 | 3 | 0 | 5 |
| 94 - 1390-2 | 5 | 54 | 0 | 0 | 0 | 0 | 15 | 0 | 0 | 0 | 0 | 0 | 1 | 5 | 0 | 20 |
| 94 - 1410 | 60 | 0 | 0 | 0 | 0 | 0 | 12 | 0 | 0 | 20 | 0 | 0 | 1 | 1 | 1 | 5 |
| 94 - 1412 | 0 | 0 | 0 | 0 | 0 | 20 | 58 | 0 | 0 | 0 | 0 | 0 | 1 | 1 | 0 | 20 |
| 94 - 1461 | 85 | 0 | 0 | 0 | 0 | 0 | 5 | 0 | 0 | 5 | 0 | 0 | 0 | 0 | 0 | 5 |
| 94 - 1463 | 0 | 0 | 0 | 0 | 0 | 0 | 26 | 0 | 0 | 0 | 0 | 2 | 0 | 0 | 2 | 70 |
| 94 - 1527 | 10 | 0 | 0 | 0 | 0 | 0 | 10 | 0 | 0 | 80 | 0 | 0 | 0 | 0 | 0 | 0 |
| 94 - 1573 | 20 | 0 | 0 | 0 | 0 | 0 | 0 | 0 | 0 | 75 | 0 | 0 | 0 | 1 | 1 | 3 |
| 94 - 1601 | 20 | 0 | 0 | 0 | 0 | 0 | 0 | 0 | 0 | 75 | 0 | 0 | 1 | 0 | 0 | 4 |

Amp = Amphibole, Anh = Anhydrite, Bt = Biotite, Cal/Dol = Calcite/dolomite, Ccp = Chalcopyrite, Chl = Chlorite, Cpx = Clinopyroxene, Mag = Magnetite, Ol = Olivine, Opx = Orthopyroxene, Pl = Plagioclase, Pn = Pentlandite, Po = Pyrrhotite, Py = Pyrite, Tlc/WM = Talc/serpentine/white mica (not distinguished). Letters in sample name denote different samples, numbers denote different thin sections within same sample.